University of Sussex

Observational Constraints on Non-Canonical Inflation

Thesis documented by

Sheng Li

Supervised by Andrew R. Liddle & Antony M. Lewis

Submitted for the degree of Doctor of Philosophy

University of Sussex

Declaration

The work presented in this thesis is the result of a number of collaborations with my supervisor Andrew R. Liddle at the Astronomy Centre of University of Sussex. Some of the work has already been published. Chapter 3 encloses my study which has been published in Journal of Cosmology and AstroPhysics (JCAP) (Li, 2010). From Chapter 4 to Chapter 5, the works are completed in collaboration with Andrew R. Liddle. The work in Chapter 4 has been published in JCAP (Li and Liddle, 2012). Chapter 5 contain the recent works which are available at e-print archive arXiv.org by [arXiv:1311.4664] (Li and Liddle, 2013a).

I hereby declare that this thesis describes my own original work, except where explicitly stated. No part of this work has previously been submitted, either in the same or different form, to this or any other University in connection with a higher degree or qualification.

Signed: _____ Date: _____

UNIVERSITY OF SUSSEX

Sheng Li, Doctor of Philosophy

Observational Constraints on Non-Canonical Inflation

Summary

This work concentrates on theoretical cosmology in the aspect of modelling the inflationary cosmology, and the central work investigates Non-Canonical inflation (NCI) through the K-inflation paradigm. In this work the objective NCI models can be classified to three classes which are summation-separable models, product-separable models and an ansatz for NCI models, respectively. For simplicity of discussion, the application of the methods, and also the generality of the resulting predictions, I studied NCI models which are associated with the single-term polynomial potential $V(\phi) = A\phi^m$.

By means of several methods, which include scalar field redefinition and the asymptotic method, as well as the efficient approximations such as slow-roll approximation, for the first time I formulated and revealed the degeneracy and the correlations for the model parameters, in for instance both the scalar potential and the kinetic energy for different investigated NCI models in the work.

The work also introduces one developed code, namely Kinetic Model (KMC) for the considered NCI models which implements and extends the scope of ModeCode based on the CosmoMC packages from the conventional canonical inflation to the generic NCI models. The results from numerical exploration helps in illustrating the constraints on the model parameters without the limits of slow-roll assumptions, and the generated results present the consistency as well as similar correlations to those derived from theoretical calculations.

Specifically, all investigated NCI models which are driven by a quartic potential $\lambda\phi^4$ present a novel explanation as a viable candidate theory in modelling our universe given the current high precise observational data, such as from Wilkinson Microwave Anisotropy Probe (WMAP) satellite and *Planck* satellite.

Acknowledgements

My first and foremost thanks go to my supervisor, Prof. Andrew R. Liddle who is now working at the Institute for Astronomy, University of Edinburgh, for his directing in the field of cosmology studies, for many fruitful discussions and suggestions, for his encouragement and for his supports of all of my plans over the last four years. Without his guidance and help, this work would not be possible.

I also want to present many thanks to my supervisor Dr. Antony Lewis, for his powerful cosmology software, his useful advice and discussions on my work as well as Dr. David Seery for several useful discussions. Many thanks to the authors of ModeCode for making their code public, and two of them, Richard Easther and Hiranya Peiris, for discussions in relation to the work.

During my years in studying at University of Sussex, I also thank other astronomy members at the astronomy centre, Gemma Anderson, Leon Baruah, Christian Byrnes, Mafalda Dias, Naomi Dubois, Jonathan Frazer, Pete Hurley, Marisa C. March, Donough Regan, Ruth Pearson, William Watson, for the joyful experience during my studies. And thanks to two visitors, Julien Lesgourgues and N. Chandrachani Devi for useful discussion and happy talks in coding. This precious experience will never fade away in my life.

For assistance since my enrolment, Mr Richard Chambers is always the key person who is so patient and nice to give me any kind of inquiries. For the examination of my viva, I also present my gratitude to Prof. Mark Hindmarsh at Sussex and Dr. Eugene Lim from Kings College London. Thanks for their attending and reviewing of my viva in this cold winter.

My thanks should be also addressed to two of my friends, Mr Yang Liu who is studying at Simon Fraser University at Canada, and Miss Yiyang Yang who is studying at Reading University in England, for their kind generosity in financial support from July 2013. Also thanks to my boss Daniel for his offering me a part-time job from July 2013.

My life wouldn't be so smooth without the supports from my dear parents and my sisters. It is never enough to simply show my appreciations to my dear family. But I love you, all of you. Thank you all for the constant understanding and unbiased support such that I have no fear in living and studying beyond of your protection.

Contents

I Introduction **1**

1 Fundamentals of Cosmology **2**

1.1 Friedmann-Lemaître-Robertson-Walker Metric . . . 3

1.1.1 The Space-time Property of the Universe . . . 3

1.1.2 Solution to The Einstein Field Equation . . . 4

1.2 Field theory in Cosmology . . . 5

1.2.1 Action and Euler-Lagrangian Equation . . . 5

1.3 Study Areas in Cosmology . . . 6

1.3.1 Cosmic Microwave Background . . . 6

1.3.2 Baryon Asymmetry and Dark Matter & Dark Energy . . . 9

1.3.3 Inflation Theory . . . 12

2 Objective Models and Methodologies **15**

2.1 Cosmological Perturbations . . . 16

2.2 Modelling Inflationary Cosmology . . . 18

2.2.1 Canonical Inflation . . . 18

2.2.2 Non-Canonical Inflation . . . 19

2.3 Methodology in Constraining Inflation Models . . . 21

2.3.1 Field Redefinition . . . 21

2.3.2 Slow-roll Approximation . . . 22

2.3.3 Evaluation With e-folds N . . . 23

2.4 Connection to Observations . . . 24

2.4.1 The CMB Power Spectrum . . . 24

2.4.2 Model Parameter Estimation . . . 24

2.4.3 Breaking the Model Degeneracy . . . 26

2.4.4 Brief Review: Kinetic Module Companion 27

II Modelling and Constraints on Inflationary Cosmology 29

3 Inhomogeneous Reheating 30

3.1 Introduction 31

3.2 Basic Mechanism 33

3.3 Non-Gaussianity 34

3.4 Discussion 36

3.4.1 Observable Parameters 36

3.4.2 Some Specific Examples 37

3.5 Summary and Outlook 39

4 Analytic and Numerical Study on K-inflation 41

4.1 Introduction 42

4.2 The K-inflation model 43

4.2.1 Background field equations and sound speed 43

4.2.2 Perturbation mode equations 44

4.2.3 Power spectra and observables 45

4.3 Slow-roll predictions 46

4.3.1 General prediction without specifying a potential 46

4.3.2 Predictions for specific models through e-folding N 48

4.4 ModeCode for K-inflation 51

4.4.1 Brief description of ModeCode 52

4.4.2 Modifications needed for K-inflation 53

4.4.3 Comparison tests 53

4.5 Parameter explorations with MCMC 55

4.5.1 Global settings and initial conditions 55

4.5.2 Choice of models 55

4.5.3 Overview of effects from additional kinetic terms 56

4.5.4 Interpretation of MCMC explorations 57

4.6 Conclusions 59

5 Analytic Study on Tachyon and DBI Inflation 61

5.1 Introduction 62

5.2 The Models . . . 64
5.3 The General Systematic Method . . . 65
5.3.1 General formula for the spectral index n_s . . . 65
5.3.2 Predictions for two classes of models . . . 69
5.4 Application of the Systematic Method to Two Models . . . 71
5.4.1 Tachyon models . . . 71
5.4.2 DBI inflation models . . . 73
5.4.3 Comparison to *Planck* constraints . . . 77
5.5 Implementation Methods for Particular Cases . . . 79
5.5.1 Field redefinition in Tachyon models . . . 79
5.5.2 DBI inflation with a quadratic potential . . . 81
5.6 Model Parameter Estimation . . . 86
5.6.1 Sum-separable models . . . 87
5.6.2 Tachyon models . . . 87
5.6.3 DBI models . . . 88
5.7 Conclusions . . . 90

6 Discussion and Conclusions **92**

Bibliography **94**

A Validity of the Slow-roll Approximation for DBI inflation **110**
A.1 Preliminaries . . . 110
A.2 Evaluation of the validity of the slow-roll approximation . . . 111
A.3 Validity for particular scalar potentials . . . 115
A.3.1 Quadratic potential . . . 115
A.3.2 Quartic potential . . . 115
A.4 Summary . . . 116

B $s/2\delta$ for DBI inflation with a quadratic potential **117**

Part I

Introduction

· Chapter 1 ·

Fundamentals of Cosmology

I learned to distrust all physical concepts as the basis for a theory. Instead one should put one's trust in a mathematical scheme, even if the scheme does not appear at first sight to be connected with physics. One should concentrate on getting interesting mathematics.

Paul. A. M. Dirac

This chapter will present the very foundations required in the study of cosmology, starting with the space-time geometry which we will obtain by studying the Einstein gravity and the field equations in the first section, then ending with the field theory by means of which most of the cosmological phenomena and observations can be investigated and interpreted with the scalar fields in the second section. The basic and essential understanding at the frontiers of the modern cosmology, in particular in the era of *Planck*, will be sketched in the third section. The fourth section will briefly introduce a couple of topics in cosmological inflation in such a way as to end the whole chapter and guide to my own research interests and work so far.

1.1 Friedmann-Lemaître-Robertson-Walker Metric

1.1.1 The Space-time Property of the Universe

It is known that our universe has been considered as homogeneous and isotropic on a very large scale.*Homogeneity* means that the universe looks the same at any point, while *isotropy* means that the universe is the same in all directions (Trodden and Carroll, 2004). The recent observations evidenced that the universe also presents a degree of $\mathcal{O}(10^{-5})$ *anisotropy* from the *cosmic microwave background* (CMB) radiation (Weinberg, 2008).

To describe this universe with the properties above, a metric which was introduced by the Russian mathematician Alexander Friedmann in 1922 and, independently by the Belgian astrophysicist Georges Edouard Lemaître in 1927, and later developed and perfected by American Mathematician and Physicist Howard Percy Robertson and British Mathematician Arthur Geoffrey Walker during 1930s, can be formulated as

$$ds^2 = -dt^2 + a^2(t)\left(\frac{dr^2}{1-kr^2} + r^2(d\theta^2 + \sin\theta^2 d\phi^2)\right). \tag{1.1}$$

in the "comoving" coordinates in terms of (t, r, θ, ϕ). One should note that we have omitted the coefficient c^2 which should have appeared in front of the term dt^2. The formula contains a scale factor $a = a(t)$ which evolves with time, and the parameter k which is a constant takes value only from $(-1, 0, 1)$ to represent the curvature of the space. The choice of k depends on the geometry of universe, open, flat or closed respectively. It is usually denoted by FLRW metric (or FRW in some cases) for brevity.

1.1.2 Solution to The Einstein Field Equation

The Einstein field equation is expressed by

$$R_{\mu\nu} - \left(\frac{R}{2} + \Lambda\right) g_{\mu\nu} = 8\pi G T_{\mu\nu}\,, \tag{1.2}$$

where $R_{\mu\nu}$ denotes the *Ricci* tensor which is determined from a chosen metric, R the *Ricci* scalar which is defined by $R = g^{\mu\nu}R_{\mu\nu}$, G Newton's gravitational constant, and $T_{\mu\nu}$ the energy-momentum tensor.

Therefore we can see that the Einstein field equation describes and connects the geometry to the energy-momentum tensor of the universe. It reveals also that the curved space-time is the result of the presence of the matter.

Under the FLRW metric in Eq. (1.1), a homogeneous and isotropic universe can described by the Friedmann equations as the solution to the Einstein's Field Equations,

$$\left(\frac{\dot{a}}{a}\right)^2 = \frac{8\pi G}{3}\rho - \frac{k}{a^2} + \frac{\Lambda}{3}\,, \tag{1.3}$$

$$\frac{\ddot{a}}{a} = -\frac{4\pi G}{3}(\rho + 3p) + \frac{\Lambda}{3}\,. \tag{1.4}$$

where ρ and p are the energy density and the pressure of the universe respectively (in the following we will deploy $\mathrm{M}_{\mathrm{Pl}}^2 = 1/8\pi\mathrm{G}$ for convenience). This means that Friedmann equations connect the geometric properties such as the scale factor and the spatial curvature, to both the energy density ρ and the pressure p of the universe. These equations are the basis of the standard big bang cosmological model including the current ΛCDM model. Also one may derive an equation, according to the Friedmann equations above, as follow

$$\dot{\rho} + 3\frac{\dot{a}}{a}(\rho + p) = 0\,. \tag{1.5}$$

This is the fluid equation or the *continuity equation* for the energy-momentum of a perfect fluid. It represents the conservation law of the energy and momentum.

In above equations, we can define an important quantity, the Hubble parameter H, as

$$H = \frac{\dot{a}}{a}\,. \tag{1.6}$$

This parameter is relevant to the redshift $\delta\lambda/\lambda$ in **Hubble's Law**,

$$\frac{\delta\lambda}{\lambda} = H_0 r\,, \tag{1.7}$$

where λ denotes the wavelength of radiation, r the distance of two nearby comoving observers, and the H_0 here is just present value of H which is called Hubble constant (Lyth and Liddle, 2009).

1.2 Field theory in Cosmology

Cosmology relies on scalar field theory. A scalar field can play many roles in particle physics. From the view in particle physics, those elementary particles have their corresponding field. For example, the recently verified **Higgs** boson corresponds to the *Higgs field* which yields the mass for the particles which interact with it. In cosmology studies, we also apply scalar field theory to derive or reveal the governing physical laws behind the phenomena. During inflation, the scalar field can vary with time, such that it performs as components of cosmic fluid (Lyth and Liddle, 2009). When we study the inflationary model, we are intensively use scalar field to construct our Lagrangian and further investigate its effect on the evolution of universe.

1.2.1 Action and Euler-Lagrangian Equation

This tool in field theory is the *action* from which the fundamental laws of physics can be derived. It has the generic form

$$S = \int L dt = \int L(t, q, \dot{q}) dt \,. \tag{1.8}$$

The quantity L is called the *Lagrangian* which denotes and measures the energy for a considered object, usually in a general coordinates system, for example $(q\,,\,\dot{q})$ for the field q in above Eq. (1.8).

By means of the variational principle, we can derive the equation of motion for the field q,

$$\frac{\partial L}{\partial q} - \frac{\partial}{\partial t}\left(\frac{\partial L}{\partial \dot{q}}\right) = 0 \,. \tag{1.9}$$

In context of cosmology, for a generic space-time we have the action with respect to the general relativity as

$$S = \int d^4x\sqrt{-g}\mathcal{L} \,, \tag{1.10}$$

where $\mathcal{L}$ denotes the *Lagrangian density* of the scalar field denoting with ϕ, and the $\sqrt{-g}$ the determinant of the metric $g_{\mu\nu}$. And the Lagrangian L in Eq. (1.8) is related by the relation for $L = \int d^3x\sqrt{-g}\mathcal{L}$ at this moment. Therefore according to the Eq. (1.9) we can also derive the equation of motion for the scalar field ϕ as

$$\frac{\partial(\sqrt{-g}\mathcal{L})}{\partial\phi} - \frac{\partial}{\partial x^\mu}\left(\frac{\partial(\sqrt{-g}\mathcal{L})}{\partial(\partial_\mu\phi)}\right) = 0 \,. \tag{1.11}$$

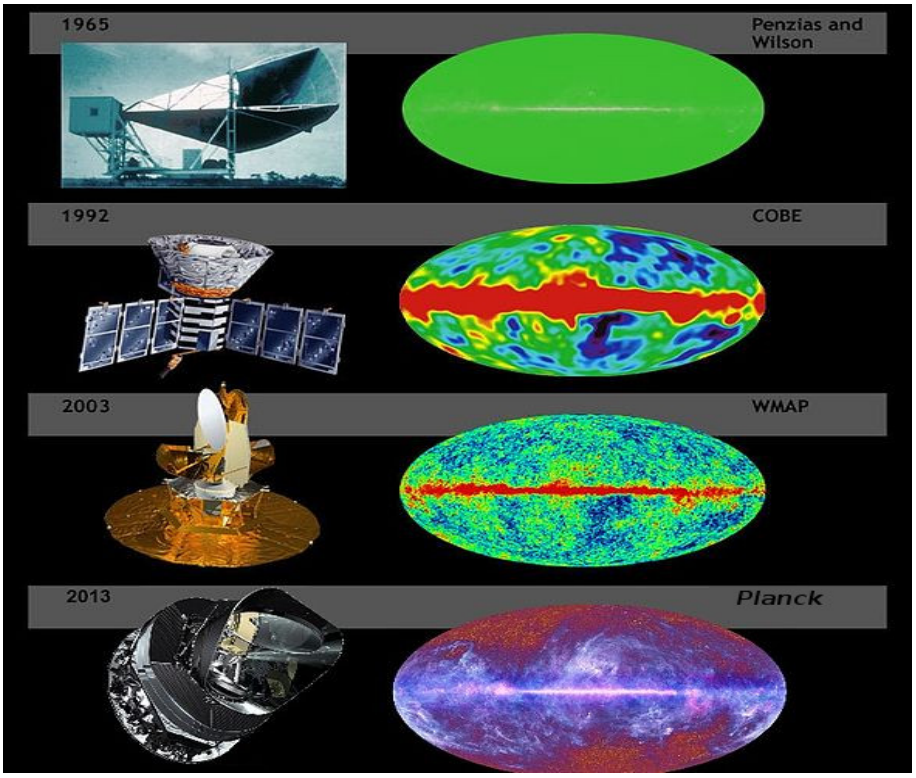

Figure 1.1: The comparison of CMB sky seen by Holmdel Horn Antenna, COBE, WMAP , *Planck*. (Simulation data. Original image courtesy of NASA/JPL-Caltech/ESA).

Equation (1.11) is commonly used in cosmology, for example in the study of inflation models, cosmological perturbations and the analysis of the non-gaussianity of the perturbation. We will present examples by applying it in later chapters.

1.3 Study Areas in Cosmology

1.3.1 Cosmic Microwave Background

The group of images in Figure. 1.1 shows a sketchy history of the research in CMB science from the era of Penzias and Wilson to current *Planck* satellite era. With the development and improvement of instruments, Planck, a satellite which was launched by European Space Agency (ESA) on 14th May 2009, has more capabilities to probe the accurate detail of the CMB sky than its three predecessors such as Holmdel Horn Antenna (in 1965 by Penzias and Wilson), COBE (in 1992 by NASA) and WMAP (in 2003 by NASA). It can be seen from Figure. 1.1 that the more the sensitivity of the observation instrument, the

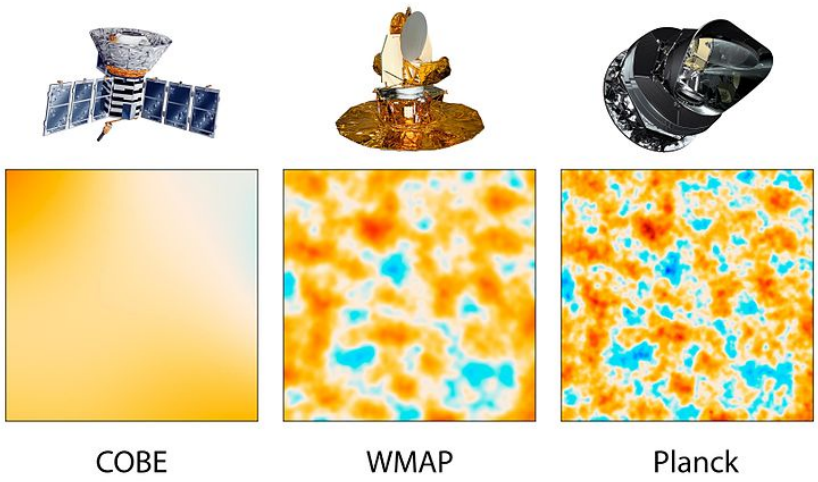

Figure 1.2: Comparison of CMB results from COBE, WMAP and *Planck* (Image courtesy of NASA/JPL-Caltech/ESA).

more precise the CMB sky. This also in turn provides more extensive abilities to pin down or impose constraints on various inflation models.

As we know, the expanding universe can be detectable and evidence is due to the discovery of the 3K Comic Microwave Background (CMB) Radiation by A. Penzias and R. W. Wilson in 1960s. Since then, there have been many other remarkable experiments to detect the CMB sky. During the development of the modern inflationary cosmology, it is worth mentioning three space-based experiments, starting with the Cosmic Background Explorer (COBE) which was the first space-based detector and probed the CMB temperature to 2.73K. It first discovered that the CMB radiation is characterised as blackbody and with small temperature anisotropies at $O(10^{-5})$ (Smoot et al., 1992) (See also the CMB review papers (Hu, 2008; Challinor, 2012). The *Wilkinson Microwave Anisotropy Probe* (WMAP) then improved the map's clarity and sharpness (Hinshaw et al., 2013), and *Planck* (spacecraft) which is expected to extract all information, from CMB has not only confirmed a highly significant detection of both non-Gaussianities which were generated during or after inflation started and anisotropies which are consistent with those in WMAP , also confirmed anomalies around 3σ in the CMB map using a broader frequency range than WMAP (Ade et al., 2013c). Those three missions provide us with powerful tools or "windows" to observe and verify all kinds of the prevailing inflation models which can give successful explanatory to the observations in theory so far. Since the release of the latest *Planck* data in March 2013, we can see that the accuracy of these three missions in Figure 1.2. We are going to work with *Planck*.

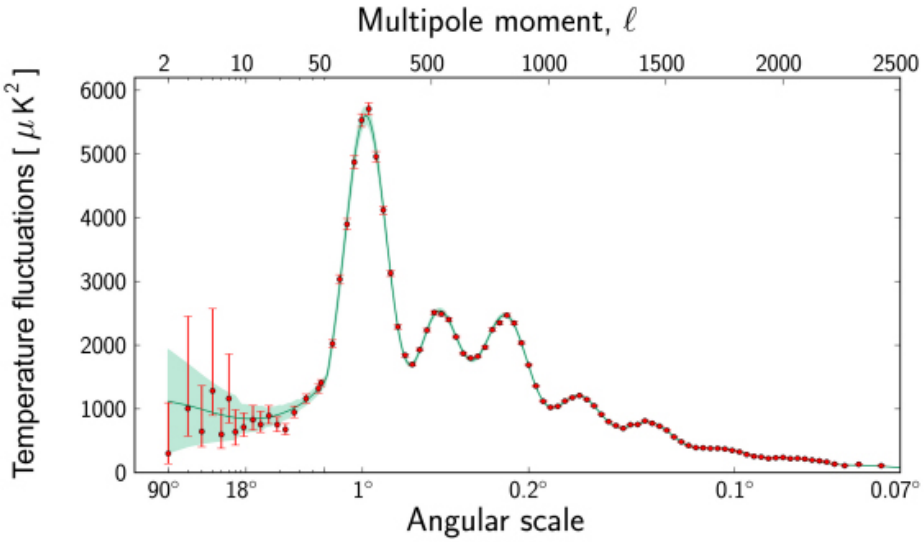

Figure 1.3: Power spectrum of temperature fluctuations in the Cosmic Microwave Background from Planck. In this figure, the red points denotes the value from observational data and the green line the theoretical prediction. Credit: ESA and the Planck Collaboration

CMB Anisotropy

The CMB is assumed and tested to be at a very high level of isotropy and homogeneity. And this isotropy and homogeneity provide us the most information about the history of the CMB, the evolution of the cosmic structures. However, the precise detections for the full CMB sky revealed small scale anisotropies.

This can be measured by (Hu, 2008)

$$\mathbf{\Theta}(\hat{n}) = \int dD\mathbf{\Theta}(\vec{x})\delta(D - D_*)\,, \tag{1.12}$$

with $D = \int dz/H$ is the comoving distance and D_* denotes the distance a CMB photon travels from recombination. In the above equation, $\mathbf{\Theta}(\tilde{\mathbf{x}}) = \Delta T(\vec{x})/T_0$ is the spatial temperature fluctuation at recombination, $\hat{n}, \vec{x}$ the vector denoting the direction of observer. And we can evaluate the expectation value for

$$\langle \Theta(\vec{x})\Theta(\vec{x})\rangle = \int \frac{d^3k}{(2\pi)^3}P(k) = \int d\ln k\Delta_T^2(k)\,. \tag{1.13}$$

Hence we can predict a scale-invariant spectrum if $\Delta_T^2(k) = \text{const} = k^3P(k)/2\pi^2$.

As we can deal the harmonic resonances, we can express this anisotropy by selecting the spherical harmonics, such that we will obtain

$$\Theta_{lm} = 4\pi i^l \int \frac{d^3k}{(2\pi)^3} j_l(kD_*)\mathbf{\Theta}(k)Y_{lm}(k)\,. \tag{1.14}$$

where j_l is the spherical Bessel function, and Y_{lm} the spherical harmonic function. Then according to Eq. (1.13) we can evaluate

$$\langle \Theta^*_{lm} \Theta_{l'm'} \rangle = \delta_{ll'} \delta_{mm'} C_l \,. \tag{1.15}$$

This equation yields an important quantity C_l which takes the form

$$C_l \simeq \frac{2\pi}{l(l+1)} \Delta^2_T(k) \,. \tag{1.16}$$

where k denotes the wavenumber in **Fourier** or momentum space. This equation (1.16) tells us the relation between the CMB anisotropies and the power spectra of the CMB,

$$\Delta^2_T(k) \simeq \frac{l(l+1)}{2\pi} C_l \,. \tag{1.17}$$

in unit of μK^2. And this is called the CMB anisotropic power spectrum in terms of the angular scale (or multipole moment denoted by l), see Figure. 1.3.

In this figure 1.3, there are **THREE** peaks which are important in studies of cosmology. The first peak which is located a $l \sim 200$ tells us the curvature of the universe which is close to flatness, the second peak indicates substantial amounts of dark baryons consistent with nucleosynthesis inferences, and the third peak will measure the physical density of the dark matter. Beyond these three peaks, the damping tail will provide consistency checks of underlying assumptions (Hu, 1995, 2008) (also the online tutorial on (Hu, 2010)).

1.3.2 Baryon Asymmetry and Dark Matter & Dark Energy

Planck's high-precision cosmic microwave background map has allowed scientists to extract the most refined values yet of the Universe's ingredients. The normal matter that makes up stars and galaxies contributes just 4.9% of the Universe's mass/energy inventory. Dark matter, which is detected indirectly by its gravitational influence on nearby matter, occupies 26.8%, while dark energy, a mysterious force thought to be responsible for accelerating the expansion of the Universe, accounts for 68.3%. The "before Planck" figure is based on the WMAP 9-year ("WMAP9") data release presented by Hinshaw et al. (2013).

From the pie-chart in Fig. 1.4 we can see the two largest regions are Dark Energy 68.3% and Dark Matter 26.8%, and the small region about 4.9% is for ordinary matter. These are referred to as the standard model of Big Bang cosmology (symbolised as ΛCDM), since it is the simplest model that provides a reasonably good match to the following observations.

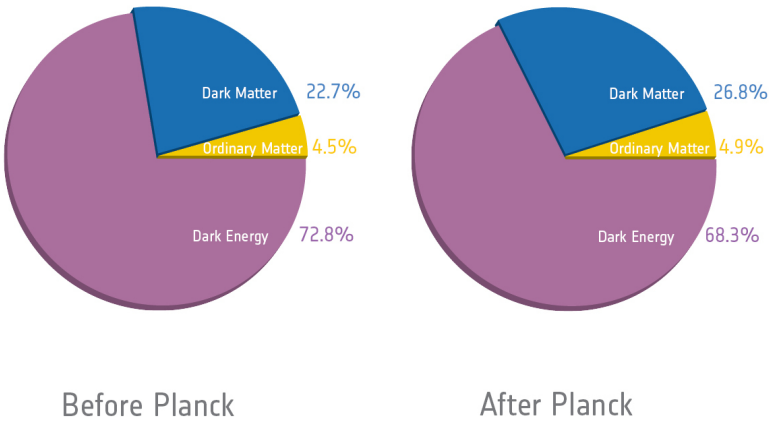

Figure 1.4: The new cosmic recipe from Planck. Credit: ESA and the Planck Collaboration (Planck, 2013b).

Creation of Baryon Asymmetry

The visible universe is asymmetric with an initial excess of baryons over anti-baryons parametrized by $\eta(b) = (n_b - n_{\bar{b}})/s \sim 10^{-10}$ (Dine and Kusenko, 2003; Hertzberg and Karouby, 2013; Boucenna and Morisi, 2013). According to current studies, the origin of the Baryon asymmetry remains unknown in particle physics, although there are several proposed mechanisms. In modern physics research, the asymmetry of baryon also relates broadly to the research of the dark matter (Boucenna and Morisi, 2013).

As for the creation of this asymmetry, one possible mechanism to explain it is the Affleck-Dine mechanism which was first proposed in Affleck and Dine (1985). This mechanism claims the asymmetry occurred when the scalar fields had interactions with each other, and CP violations were also present.

Dark Matter

This matter is not the part of the standard model of particle physics. It accounts for the missing of the mass from the universe by 26.8% according to Figure 1.4 from *Planck*.

One of the proposed candidates for dark matter is commonly accepted as *Weakly Interacting Massive Particles* (WIMPs) because this kind of particle interacts only through gravity and the weak force. With this property we cannot directly detect its existence, unlike the photon which does interact through electromagnetism with others. Hard to detect, but researchers are hoping to produce the WIMPs in laboratory, for example in

LHC. Another candidate but hypothetical particles for the non-baryonic dark matter are known as axions (Peccei and Quinn, 1977b,a), or supersymmetric particles (Davis et al., 1985).

Dark Energy

Like the Dark Matter, Dark Energy hypothetically exists in our universe. Dark energy is inferred from the accelerating expansion of the universe. And since the discovery of the cosmic acceleration through the observation of SN Ia in 1998 (Riess et al., 1998; Perlmutter et al., 1999), this proposed dark energy became the hot pot in cosmology researches. In cosmology community, there are two proposed forms of dark energy. One is the cosmological constant which measures the energy density of the vacuum of space. The constant energy as the part of the Einstein field equation was first introduced by A. Einstein for preserving this theory in explaining a static universe. This was later accepted and studied by the community, although Einstein had abandoned this conceptual energy in 1928. The other is the scalar fields such as quintenssence, for example, discussed in (Zlatev et al., 1999; Steinhardt et al., 1999; Amendola, 2000; Armendariz-Picon et al., 2001; Mukherjee and Banerjee, 2013), or moduli discussed in (Brandenberger, 2006; Greene and Levin, 2007) whose energy can dynamically evolve with time and in space. Besides, as an alternative in accounting for the accelerating expansion, the modified gravity theory has also been studied in articles (Kunz and Sapone, 2007; Exirifard, 2011; Bertschinger and Zukin, 2008; Saltas and Kunz, 2011).

To study and understand how the Universe's expansion rate changes within space-time, we can use the equation of state to quantify this rate,

$$w_{DE} = \frac{p_{DE}}{\rho_{DE}} \,. \tag{1.18}$$

where the subscript $_{DE}$ denotes quantity measuring dark energy. This ratio denotes the relationship for the pressure p, the energy ρ for Dark Energy in the universe. As we will see later section, for the expanding universe we require this ratio $w < -1/3$. Also the equation can present a true cosmological constant which is formulated as $w = -1$, and this value tells us the cosmological constant has the same amount of the energy density but with a negative pressure.

However, the nature of the dark energy remains a speculation. It cannot be detected within the current experiments, due to its rareness, not dense and no interaction through any of the fundamental forces. It has only the gravitational effect of repulsion of two bodies, but still very difficult to be directly detected. There are some experiments for

detecting the dynamic of the expansion as well as resolving this mysterious energy. The most ambitious current project is the *Dark Energy Survey* (DES) Starting in Sept. 2012 and continuing for five years, DES will survey a large swath of the southern sky out to vast distances in order to provide new clues to this most fundamental of questions (Dark Energy Survey, 2012). A forthcoming one is Euclid which is an ESA mission to map the geometry of the dark Universe (Euclid, 2013).

1.3.3 Inflation Theory

To account for the expansion of the universe, apart from the theories mentioned above, we can think about whether exists a short era when the space-time expands extremely rapidly. This is known as cosmic inflation. This theory has its own background in physical cosmology.

Three puzzles in the standard cosmology model

Standard cosmological model (Hot Big Bang model is also used in literature) has successful understandings in many aspects of the universe, but it has three weaknesses and problems which are listed below.

- *Flatness Problem*: This problem can be stated in terms of the density parameter Ω which is defined as,

$$\Omega = \frac{\rho}{\rho_c}\,,\ \rho_c = 3M_{\rm Pl}^2 H^2\,. \tag{1.19}$$

  It points out that the density parameter in (1.19) at the very early universe should be much much close to unity since its present observed value is very close to unity. According to Eq. (1.3), we can write down

$$|1-\Omega| = \frac{|k|}{a^2H^2}\,. \tag{1.20}$$

  So if the universe is observed to be flat, then in the very early universe the density should be also close to unity. If this is not the case, it would have been evolving as (for example see Regan (2011)),

$$\Omega' = \frac{d\Omega}{dN} = -2(1-\epsilon)(1-\Omega)\,,\ \epsilon = -\frac{\dot{H}}{H^2} = \frac{H'}{H}\,. \tag{1.21}$$

  according to Eqs. (1.3 , 1.4). Here we have denoted $' = \frac{d}{dN}$ and $dN = -Hdt$.

- *Horizon Problem*: This points out that the two particles cannot be in contact beyond of their horizon if the universe is homogeneous and isotropic on very large scales. It is a problem because observational data reveals the temperature at the whole sky is the same, to be strictly accurate to one part in one hundred thousand.

  It can be seen from the formula for the co-moving distance

  $$d_{com} = \int_{t_i}^{t_f} \frac{dt}{a(t)} \,. \tag{1.22}$$

  where the speed of light has set to be unity in Planck units $c = k = \hbar = G = 1$, and the time $t_i \ll t_f = t_0$ if we treat the current scale factor $a(t_0) = 1$ at present time. This formula measures the farthest distance one photon can travel. So in the standard big bang scenario, one patch of the universe cannot share the same temperature with another patch which is further apart than one d_{com}.

- *Monopole Relics*: It is also labelled as a problem in combining the standard big bang scenario with particle physics (Ryden, 2002). It points out that Grand Unified Theories (**GUT**) predict the existence of magnetic monopoles of upper bound at about 10^{17}GeV according to Polyakov (1974) and 't Hooft (1974), and other exotic objects should have been created during the GUT phase transition.

  This is GUT monopole problem because current experimental data shows this amount of relics are less than $10^{-16}\text{cm}^{-2}\text{s}^{-1}\text{sr}^{-1}$ according to (Beringer et al., 2012) (and references therein).

Era of Inflation

To solve those three problems remaining in the standard big bang model, the **Inflation Theory** was initially introduced by Guth (1981) in 1981. This is now regarded to be "old inflation". Soon after spotting a flaw in the old version of inflation, the "new inflation" was developed by Linde (1982) also independently by Albrecht and Steinhardt (1982) (See also textbook (Bonometto and Moschella, 2002), or you can check it online here[1]).

The central idea of the inflation theory states that, prior to the big bang stage, the universe experienced a period of exponential expansion during its first few moments. As the result of this very short and swift expansion, one small part of the universe was drastically increased by as much as 60 e-folding number, or equivalently a factor of $\sim 10^{26}$. Consequently, Inflation has been considered as an extension of the Big Bang theory since it

[1] http://web.mit.edu/physics/people/faculty/guth_alan.html

explains the above puzzles so well, while retaining the basic paradigm of a homogeneous expanding universe.

Since we have known that the universe is expanding which means the scale factor $\dot{a} > 0$, and the Hubble parameter in Eq. (1.6), according to the observations, is almost invariant this means $\dot{a}$ must be an increasing function. Therefore the basic idea of inflation can be stated with the Friedmann equation

$$\ddot{a} > 0\,. \tag{1.23}$$

This requirement can be also represented by the relation for the components of the universe, for example,

$$\rho + 3p < 0\,. \tag{1.24}$$

In general we always have a positive energy density ρ, therefore Eq. (1.24) suggests that the accelerating universe should require a negative pressure state, $p < 0$.

Cure for Puzzles

The inflation has its success in solving the mentioned three puzzles in the starting paragraph in this subsection. To see how this is achieved, we can apply Eq. (1.23) to solve the flatness problem. That is, to avoid the drastic deviation of the total energy $\Omega_{\rm tot}$ from unity, we need to have a monotonically increasing function for $aH = \dot{a}$, with cosmic time t. This equivalently states that

$$\frac{d(aH)}{dt} = \frac{d\dot{a}}{dt} = \ddot{a}\,. \tag{1.25}$$

This is the same requirement as for inflation. And we know now inflation indeed predict a spatially-flat universe. Also this spatial property has been supported by several observational data and their combinations, for example the CMB anisotropies. The horizon problem is also resolved provided that the inflation persists for a sufficiently long period, in terms of the e-folds number N around 60 or 70. Whereas the monopole relics problem is never more severe than the horizon problem. It can be solved during inflation because the sufficient amount of inflation, around $N > 23$, can dilute away the monopole relics (Weinberg, 2008).

· Chapter 2 ·

Objective Models and Methodologies

If you disregard the very simplest cases, there is in all of mathematics not a single infinite series whose sum has been rigorously determined. In other words, the most important parts of mathematics stand without a foundation.

Niels Henrik Abel

This chapter will present an overview of the models to be studied as well as the model parameter estimation methodology. My own studies focus on the generation of the primordial density perturbations from inflation. Specifically, the studies involves the modelling of the inflationary universe, and the observational constraints for the various inflation models by using recent data sets, such as *Planck*, WMAP and BAO.

2.1 Cosmological Perturbations

From this section on, we consider the origin of the cosmological perturbation in the scheme of the inflation theory.

According to observations, we find our universe is not perfectly homogeneous. This in turn requires that the scalar field should have fluctuated during inflation. Those fluctuations may seed the formation of the cosmological structures, such as star formation, galaxy and clusters clustering, etc. Therefore to study the evolution of the universe and the formation of the cosmic structures, we consider and compute the relevant quantities in a perturbed universe, rather than the unperturbed metric noted in Eq. (1.1). We will have the perturbed FLRW metric (Lyth and Liddle, 2009) as follows,

$$ds^2 = a(\tau)^2\Big\{-(1+2A)d\tau^2 - B_i d\tau dx^i + [(1+2\psi)\delta_{ij} + 2E_{ij}dx^i dx^j]\Big\}\,. \tag{2.1}$$

where in this metric τ denotes the conformal time. In a linear perturbation, if choosing an appropriate gauge, for example the *conformal Newtonian gauge* we can write down the perturbed evolution equation for the scalar field as (e.g. textbooks by Lyth and Liddle (2009) or Mukhanov et al. (1992)),

$$u_{\rm k}'' + \left(c_{\rm s}^2 k^2 - \frac{z''}{z}\right) u_{\rm k} = 0 \tag{2.2}$$

where $'$ denotes the derivatives with respect to (w.r.t.) the conformal time τ, the $u_{\rm k}$ the Fourier mode of the scalar mode perturbation in momentum space (denoting by k here) [1],

[1] One may find the motion of equation for the curvature perturbation ζ as

$$\ddot{\zeta}_k + 2\frac{\dot{z}}{z}\dot{\zeta}_k + c_{\rm s}^2 k^2 \zeta_k = 0\,,$$

according to (Garriga and Mukhanov, 1999).

and the sound speed $c_{\rm s}^2$ and the variable z are defined via

$$c_{\rm s}^2 = \frac{\partial p/\partial X}{\partial \rho/\partial X} \quad , \quad z^2 \equiv \frac{\rho}{H^2}\frac{a^2}{c_{\rm s}^2}(1+w)\,. \tag{2.3}$$

Instead of the inflaton responsible for the generation of the perturbation, there are alternative mechanisms by which the primordial density perturbation can also be generated, such as *Curvaton* mechanism (Moroi and Takahashi, 2001; Lyth and Wands, 2002; Enqvist and Sloth, 2002) and *Modulated/Inhomogeneous Reheating* scenario (Dvali et al., 2004b,a; Zaldarriaga, 2004; Kofman, 2003; Matarrese and Riotto, 2003; Vernizzi, 2004), also the recent reheating scenario with DBI field discussed (Li, 2010).

General Predictions for Inflation

As is well-known, the universe has an almost scale-invariant power spectrum, and it obeys an almost Gaussian distribution. These properties can be determined by the following relations

$$\mathcal{P}_\zeta = \frac{1}{8\pi^2}\frac{H^2}{c_{\rm s}\epsilon}\Big|_{kc_{\rm s}=aH}\,, \tag{2.4}$$

$$\mathcal{P}_{\rm t} = \frac{2H^2}{\pi^2}\Big|_{k=aH}\,, \tag{2.5}$$

$$n_{\rm s}-1 = \frac{d\ln\mathcal{P}_\zeta}{d\ln {\rm k}}\Big|_{kc_{\rm s}=aH} = -2\epsilon-\eta-s\,, \tag{2.6}$$

$$n_{\rm t} = \frac{d\ln\mathcal{P}_{\rm t}}{d\ln {\rm k}}\Big|_{k=aH} = -2\epsilon \tag{2.7}$$

$$r = \frac{\mathcal{P}_\zeta}{\mathcal{P}_{\rm t}} = 16\epsilon c_{\rm s}\Big|_{kc_{\rm s}=aH}\,. \tag{2.8}$$

according to (Armendariz-Picon et al., 1999; Garriga and Mukhanov, 1999). Among those quantities, $\mathcal{P}_\zeta$ measures the curvature perturbation power spectrum[2], the spectral index $n_{\rm s}$ encodes the small deviation from a scalar-invariant power spectrum, and the tensor-to-scalar ratio r encodes the tensor mode ($\mathcal{P}_{\rm t}$[3]) fraction ($\mathcal{P}_{\rm t}/\mathcal{P}_\zeta$) from inflation. Several observational data tell us that $n_{\rm s}$ is close to one which suggests a scale independent universe. It is also recommended to construct a viable inflationary model of this property together with the low ratio r less than 0.26 if considering the running of the spectral index, or 0.11 without the running of the spectral index (Ade et al., 2013a).

[2]The curvature perturbation $\mathcal{P}_\zeta = k^3/2\pi^2 \times (u_k/z)^2$ can be formulated by gauge invariant Mukhanov-Sasaki variable $u_k = z\zeta$, . Here, we omit the detailed derivations, but readers are suggested to look them in (Garriga and Mukhanov, 1999) and therein.

[3]Tensor perturbation $\mathcal{P}_{\rm t} = 4k^3/M_{\rm Pl}^2\pi^2 \times (v_k/a)^2$ can be also found from the tensor mode $v_{\rm k}'' + \left(k^2 - \ddot{a}/a\right) v_{\rm k} = 0$.

2.2 Modelling Inflationary Cosmology

There has been a fashion in modelling the inflationary models. The reconstruction of models has been discussed in many articles, like the slow-roll hierarchy approach (Liddle et al., 1994; Hoffman and Turner, 2001; Hansen and Kunz, 2002; Kinney, 2002; Easther and Kinney, 2003; Liddle, 2003), and the reconstruction and constraint on the inflation potential (Peiris and Easther, 2006a,b, 2008; Adshead and Easther, 2008; Mortonson et al., 2011).

The types of inflation models can be classified through the number of inflaton fields, which specifies two classes of inflation models, that is *single-field* inflation (SFI) and *multi-field* inflation (MFI). Besides, one may classify inflation models by justifying whether or not the general gravity has a *Minimal Coupling* to the scalar field or the matter Lagrangian (denoting by $\mathcal{L}_m$) in the total action (1.8) for the considering inflation model.

However, in the current work, I adopt an alternative view in determining those models which is to distinguish the kinetic term in their Lagrangian in (1.8), such that we can classify those models as *Canonical* Inflation models (CI) and *Non-Canonical* Inflation models (NCI), respectively.

2.2.1 Canonical Inflation

Canonical inflation (CI) has been studied very well both in theoretical aspect and in numerical aspect.

Single Field Inflation

Single field inflation (SFI) involves a single scalar field which can drive the evolution of the inflation, as well as providing the observationally required density perturbations. We can express the Lagrangian for this type of inflation models as

$$\mathcal{L} = \frac{\dot{\phi}^2}{2} - V(\phi)\,. \tag{2.9}$$

There are a broad range of theoretical models including Chaotic inflation (Linde, 1983), Extended inflation (La and Steinhardt, 1989), Natural inflation (Freese et al., 1990), Hybrid inflation (Linde, 1991), Eternal inflation (Vilenkin, 1983; Linde, 1986), Warm inflation (Moss, 1985; Berera and Fang, 1995), K-inflation (Armendariz-Picon et al., 1999), Ghost

inflation (Arkani-Hamed et al., 2004), Hilltop inflation (Boubekeur and Lyth, 2005) and also the models inspired from string theory (Quevedo, 2002; Kachru et al., 2003), such as Tachyon models (Sen, 2002b,a), Dirac-Born-Infield inflation (Silverstein and Tong, 2004; Alishahiha et al., 2004).

And in recent years, cosmologists are considering the cosmological effects from higher derivatives in the kinetic energy in the Lagrangian, such as Galileon inflation (Burrage et al., 2011a) also called G-inflation in articles (Kobayashi et al., 2010, 2011), etc.

Multi-Field Inflation

However, there is no strong evidence that cosmic inflation should be driven by a sole field. And the hypothetical isocurvature perturbation requires two or more scalar field to exist. It is easy to extend the single field inflation models, mathematically, to involve more than one scalar field in its Lagrangian, then

$$\mathcal{L} = \sum_{i}^{N} \frac{\dot{\phi}_i^2}{2} - V(\phi_i)\,. \tag{2.10}$$

This kind of model for example could involve two scalar fields double inflation (Silk and Turner, 1987; Adams and Freese, 1991) (also known as two-field inflation by Garcia-Bellido and Wands (1996)), Assisted inflation (Liddle et al., 1998), or more fields including N-flation (Dimopoulos et al., 2008) and multi-field inflation (Mukhanov and Steinhardt, 1998).

There may be overlap amonst those models mentioned above. For example, the wider range of interaction potentials possible in multiple field models leads to possibilities such as hybrid inflation (Mukhanov and Steinhardt, 1998).

2.2.2 Non-Canonical Inflation

Non-Canonical Inflation (NCI) models are, as mentioned in the previous section in this chapter, characterised by the kinetic energy which has a non-standard form of the kinetic term $X = \partial_\mu\phi\partial^\mu\phi/2$. We consider the following generic form of the Lagrangian for the scalar field ϕ

$$\mathcal{L} = p(X, \phi)\,, \tag{2.11}$$

where p denotes the pressure of the universe. In detail then, if viewing this generic Lagrangian (2.11) in its Taylor expansion, it contains higher order, other than linear order $n = 1$, in power law of X^n.

The CI models have some difficulties to fit the observations. For example and first, the potential associated to these models has to be tuned to be very flat. And the latest constraint on inflation suggested that a concave potential is favoured by the *Planck* data (Ade et al., 2013b). Second, the CI models cannot genuinely provide a big enough non-Gaussianity of order $\mathcal{O}(1)$ to fit the observation data, such as *Planck* (Ade et al., 2013d).

NCI models have a well-defined string theory background. In the following subsections, before providing the predictions from NCI inflation, it is necessary that we review several NCI models. The thesis work is based on this type of inflation models.

K-inflation

K-inflation was proposed by Armendariz-Picon et al. (1999). In this proposal the Lagrangian of the inflation model takes the general form as stated in Eq. (2.11), where the function for $p = p(X, \phi)$ has arbitrary form which makes this class of model very general. Its perturbation later was calculated in article (Garriga and Mukhanov, 1999).

Tachyon Model

String theory applied to the inflation scenario is an attractive source in providing an explanation of cosmic inflation. Also around 2000, A. Sen and some other authors proposed the Tachyon mechanism to interpret the inflation (Sen, 2002b,a). The Lagrangian for this model is,

$$\mathcal{L} = -V(\phi)\sqrt{1 - 2fX}\,. \tag{2.12}$$

here, the free parameter is f which typically takes a constant value, while ϕ is the tachyon field.

Dirac-Born-Infield Inflation

Dirac-Born-Infield Inflation (Silverstein and Tong, 2004; Alishahiha et al., 2004) was inspired also by string theory, particularly the brane world (Bachas, 1996; Douglas et al., 1997). This type of inflation is a subset of k-inflation, proposing the Lagrangian as,

$$\mathcal{L} = -\frac{\sqrt{1 - 2f(\phi)X}}{f(\phi)} - V(\phi)\,. \tag{2.13}$$

where the warp factor is expressed by the function $f(\phi)$, but now a ϕ the distance between two colliding branes. The warp factor f can take the form λ_s/ϕ^4 where the free parameter λ_s denotes the strength of string coupling.

2.3 Methodology in Constraining Inflation Models

In purpose of constraining inflation models, there are potentially two different approaches. For one hand, the theoretical approach is to derive the relation between the three quantities in Eqs. (2.4, 2.6, 2.8), in the manner of either analytic derivation or approximation by applying some appropriate assumption, such as the slow-roll approximation. On the other hand, numerical simulation can make advances by fully exploring the model parameter spaces, especially with the interface to sources of the observational data, such as *CosmoMC* (which stands for *Cosmological MonteCarlo*) simulation with interfacing to WMAP , *Planck* and other observational data.

2.3.1 Field Redefinition

A field redefinition can simplify not only the given Lagrangian, but also the calculation of observables. The field redefinition can performed as follows. Given a Lagrangian

$$\mathcal{L} = f(\phi)X - V(\phi)\,, \tag{2.14}$$

we can redefine the scalar field ϕ to φ by scaling

$$\varphi = \int \sqrt{f(\phi)}d\phi\,. \tag{2.15}$$

The potential will be transformed via $\phi = \phi(\varphi)$ in principle. The transformed scalar potential can be regarded as a reshaped or renormalised potential. As a result of this field redefinition, we can have the Lagrangian after field redefinition

$$\mathcal{L} = \tilde{X} - \tilde{V}(\varphi)\,. \tag{2.16}$$

The new form of Lagrangian will have at least the following advantages. For the first, the derivation of the equation of motion from the new form of Lagrangian is more easy and less laborious than the original form of Lagrangian. This is evident by referring to the Euler-Lagrangian equation in which we can see there is one term $\partial\mathcal{L}/\partial\phi$ which will evaluate all terms of a given Lagrangian, and a mixed partial derivative in $\partial(\partial\mathcal{L}/\partial(\partial\phi))$ which will double the job for obtaining mix-derivation for all terms of Lagrangian. Also, the derivation will become a boring technical job in other cases where an inflation model has a complicated form of Lagrangian (we will see a few examples in later chapters in this work).

If we can eliminate all the field association from all the kinetic terms X, the derivation of the Euler-Lagrangian equation will be quite easy. For the second, as pointed out in this example, the new form potential of $\tilde{V}(\varphi)$ can directly show us the information about the potential driven inflation. Instead the potential in the old form of the Lagrangian is not straightforward in showing us the information due to the coupling $f(\phi)$ which likely has a strong impact on the motion of field along its scalar potential. For the third, after the field redefinition, we can also quite easily to find out the underlying rules for the degeneracy between the model parameters in the kinetic energy $f(\phi)X$ and the scalar potential energy $V(\phi)$.

2.3.2 Slow-roll Approximation

According to the condition $\ddot{a} > 0$ in Eq. (1.23) for an effective inflation, we know the $|\dot{H}| \ll H^2$ will start the inflationary stage. Otherwise, if $|\dot{H}|$ is close or not sufficiently less than H^2, the inflation will not be effective to interpret our observational universe.

To see how to apply this assumption, let's work out the observables for an example of CI model with the Lagrangian,

$$\mathcal{L} = \frac{\dot{\phi}^2}{2} - V\,. \tag{2.17}$$

The slow-roll assumption suggests the following two relations

$$\epsilon = -\frac{\dot{H}}{H^2} \ll 1\,, \tag{2.18}$$

and that we can approximate the equation of motion for the scalar field ϕ,

$$3H\dot{\phi} \simeq -V'(\phi)\,. \tag{2.19}$$

Here $'$ is the derivative w.r.t. field ϕ. The slow-roll assumption also suggests that the motion of the field ϕ does not vary rapidly, such that we will obtain $|V'| \ll V$ according to Eqs. (2.18) and 2.19). This may imply that inflation could evolve along a flat potential $V(\phi)$. Subject to the validity of the approximation in (2.19), we can also work out another relation denoted by parameter η_V,

$$\eta_V = \frac{V''}{V}\,. \tag{2.20}$$

This quantity also satisfy $\eta_V \ll 1$. In respect to their slowly varying property we can regard these quantities as slow varying parameters. And in analogy to η_V we can define

other two slow varying parameters η, s as[4],

$$\eta = \frac{\dot{\epsilon}}{H\epsilon}\,, \tag{2.21}$$

$$s = \frac{\dot{c_{\rm s}}}{Hc_{\rm s}}\,. \tag{2.22}$$

The parameter η is clearly defined through the varying of ϵ, while s defined through the varying of the sound speed $c_{\rm s}$. Together with Eq. (2.18) these three parameters will be intensively used in the theoretical analysis of inflationary observables.

It is a fact that the single-field canonical inflation model is the simplest viable inflation model. We can now evaluate the observables of interest such as the power spectrum $\mathcal{P}_\zeta$ and its tilt $n_{\rm s}$, as well as the tensor-to-scalar ratio r listed in the previous chapter/section. They are[5]

$$\mathcal{P}_\zeta = \left(\frac{H}{\dot{\phi}}\right)^2 (\delta\phi)^2 = \frac{H^2}{8\pi^2\epsilon}\,, \tag{2.23}$$

$$n_{\rm s} - 1 = -2\epsilon - \eta\,, \tag{2.24}$$

$$r = 16\epsilon\,. \tag{2.25}$$

There is no contribution from $c_{\rm s}$ due to the constant sound speed $c_{\rm s} = 1$ in canonical inflation models.

2.3.3 Evaluation With e-folds N

Although we can present all relevant observables in terms of these three parameters mentioned above, we can seek a bit more depth by reformulating them in terms of e-folding numbers, in short e-folds, N. The advantage of this expression of the observables will show us quantitative understanding since we know how much observable inflation is required.

To make this task possible, we need to re-derive our equation of motion for the scalar field w.r.t. e-folds N. For the canonical inflation model (2.17), according to the relation for $dN = -Hdt$ we can demonstrate this as follows,

$$\phi_{NN} + (\epsilon - 3)\phi_N + \frac{V'}{H^2} = 0\,. \tag{2.26}$$

Now we denote the subscript $_N$ to be the derivative w.r.t. the e-folds N, and $'$ w.r.t. the scalar field. So, one can obtain the final results for these three slow varying parameters, ϵ, η, s, in terms of the e-folds N under slow-roll calculation.

[4]The quantity η_V is measured in respect to the scalar potential, while η denotes the time derivative in terms of Hdt. Through this work, we are using the later convention.

[5]The detail derivations are ignored in this introductory section.

Apart from giving the detailed predictions, for example $\epsilon(N)$, however, it is not difficult to conclude that, within the slow-roll regime, the first term in Eq. (2.26) is less than the second term such that we can obtain the observables with a high accuracy, for this simplest canonical model. We can infer that even under the slow-roll assumption, the resulting observables will be of a high accuracy level giving reliable predictions and fitting the data.

In this introductory chapter, it may be not a good idea to dive into the detailed investigations on how to derive the observables in terms of e-folds N, but they are enlisted as one of the major tasks of this work.

2.4 Connection to Observations

2.4.1 The CMB Power Spectrum

The graph Fig. 1.3 in the previous chapter shows the temperature fluctuations in the Cosmic Microwave Background detected by the *Planck*Satellite at different angular scales on the sky. This curve is known as the power spectrum. The largest angular scales, starting at angles of ninety degrees, are shown on the left side of the graph, whereas smaller and smaller scales are shown towards the right. For comparison, the diameter of the full Moon in the sky measures about half a degree. The multipole moments corresponding to the various angular scales are indicated at the top of the graph (Planck, 2013a). The solid line denotes the prediction from the cosmological model which best fits the *Planck* data.

2.4.2 Model Parameter Estimation

This topic is the crucial role of CMB experiments in constraining the inflationary cosmology as well as specific inflation models. It is a challenging task for model parameter estimation in cosmology, because this is classified as an inverse problem in the studies of science. In cosmology, we only know the properties of the CMB power spectrum, and there may be several inflation models which can give the right explanation for these background properties. The complexity of the CMB curve in Fig. 1.3 prevents us from approximating its form in terms of various parameters. But still there were several attempts to carry on this challenge, for example the theoretical approach in parameter estimation can be found

such as in (Liddle et al., 1994; Knox, 1995). Also the studies in (Jungman et al., 1996b,a) extended this interest enthusiastically.

However, in most cases this approach will encounter the impossible challenge to obtain the very detailed predictions for the model parameters, we can adopt the automated and more reliable numerical exploration, providing the astrophysical datasets.

In terms of these empirical parameters below, for example in (Mortonson et al., 2011),

$$\theta_{\rm emp} = \{A_{\rm s}, n_{\rm s}, \alpha_{\rm s}, ...; r, n_{\rm t}, ...; f_{\rm NL}, ...\}\,, \tag{2.27}$$

where the parameter $A_{\rm s}$ is the curvature fluctuation amplitude [6], $n_{\rm s}$ the scalar spectral index, $\alpha_{\rm s} = d\ln n_{\rm s}/d\ln {\rm k}$ is the running of the scalar spectral index, r the tensor-to-scalar ratio, $n_{\rm t}$ the tensor spectral index, and $f_{\rm NL}$ parametrizes non-Gaussianity [7], we can propose the first approach to constrain the inflation models.

We can also specify the inflation models, for example in studies of CI models, in terms of several free parameters for the scalar potentials (Lesgourgues and Valkenburg, 2007; Mortonson et al., 2011),

$$\theta_{\rm V} = \{V_0, V_1, V_2, ..., V_{\rm n}; \theta_{\rm rh}\}\,, \tag{2.28}$$

where the V_i parametrize the potential as polynomial form of $V(\phi) = V_0 + V_1\phi + V_2\phi^2 + ... + V_{\rm n}\phi^n$, while $\theta_{\rm rh}$ parametrizes the post-inflationary reheating phase, or as (Lesgourgues et al., 2008),

$$\theta_{\rm H} = \{H_1, H_2, ..., H_{\rm n}\}\,. \tag{2.29}$$

where the $H_{\rm i}$ parametrize the Hubble parameter in terms of a single scalar field, as polynomial form of $H(\phi) = H_0 + H_1\phi + H_2\phi^2 + ... + H_{\rm n}\phi^n$.

The current research will focus on the kinetic energy which plays a key role in determining the inflation. Therefore in constraining various NCI models, we will add extra parameters to either of above, making $\theta_{\rm KMC}$ as,

$$\theta_{\rm KMC} = \{K_{\rm i=1,...,n}, V_{\rm j=1,...,m}; \theta_{\rm rh}\}\,. \tag{2.30}$$

where the extra sets $K_{\rm i}$ parametrize the kinetic term, for example $K(X) = K_1 + K_2X + K_3X^2 + ... + K_{\rm n+1}X^n$ where $X = \dot{\phi}^2/2$ is the linear kinetic energy, in the considering NCI models, to replace the empirical inflationary parameter spaces $\theta_{\rm emp}$.

[6] This variable can be seen from the parameterisation $\mathcal{P}_\zeta(k) = A_s(k_0)\,(k/k_0)^{n_{\rm s}-1+(\alpha_s \ln k/k_0)/2+...}$

[7] We use the following formula to denote the nonlinear parameter of perturbation, $\zeta = \zeta_g - 3/5 f_{\rm NL}\zeta_g^2$ where the quantity ζ_g denotes the gaussian perturbation. More details can be found in (Komatsu and Spergel, 2001)

2.4.3 Breaking the Model Degeneracy

Since the map of the observables to the parameters in inflation model is not unique, there arises another challenge which is known as the degeneracy of the inflationary models in the current and the future research in cosmology. Both the theoretical analysis and the experimental constraints are involved in the studies. The model degeneracy can be explained in CMB curve in Fig. 1.3. It is given there may be identical power spectra offered in inflation models, but there is no hint about the model parameters or parameter spaces behind, if we only look at the CMB spectra alone (Tegmark et al., 1998).

From the viewpoint of constraining inflationary models, the degeneracy problem means that there will be probably a wide range of parameters for either or both of the scalar potential and the kinetic energy. This in turn tells us that both classes — the CI models and NCI models — are affected.

We can detect the model degeneracy through two different approaches. The first one is reconstructing the inflation models within the absence of any distinguishing observables, for example with the Monte Carlo method interfacing with existing datasets. For the degeneracy problem in CI models the reader can be referred to (Hamann et al., 2007; Urrestilla et al., 2008), and for curvaton model (Gordon and Malik, 2004), also the recent studies in respect to NCI models in (Huey and Lidsey, 2002; Easson and Powell, 2011, 2013). This significant degeneracy problem may be alleviated by combining different datasets, as well as using the advanced detectors, such as the latest one *Planck* and the forthcoming Euclid .

The current research community are using this approach so far, as there is no strong evidence for the new physics in particle physics. However, the is another possibility that modelling the inflationary universe or simulating the CMB spectra with extra observables may be significant for the understanding of the universe. The science community, especially the particle physics as well as the cosmologists, have been expecting to encounter new physics, because of the predictions from the Standard Model in particle physics, and especially the discovery of the Higgs Boson. This alternative may become the direction of future research in physics, although there is currently no new physics found after the discovery of Higgs Boson. The research operated in AMS and *A Toroidal LHC Apparatus* (ATLAS) as well as *Compact Muon Solenoid* (CMS) on *Large Hadron Collider* (LHC) in *European Organization for Nuclear Research* (known as CERN), may find new physics in the future, then in turn we can expect to efficiently break the model parameter degeneracy

problem.

2.4.4 Brief Review: Kinetic Module Companion

Cosmological simulations for the modelling of the inflationary universe and its constraint are typically using Markov Chain Monte Carlo (MCMC) analysis (Christensen and Meyer, 2000; Christensen et al., 2001; Knox et al., 2001; Lewis and Bridle, 2002; Kosowsky et al., 2002; Verde et al., 2003; Dunkley et al., 2005) and Bayesian Model selection (Parkinson et al., 2006; Liddle et al., 2006; Bridges et al., 2006; Gordon and Trotta, 2007; Feroz et al., 2009). Based on the public code ModeCode (Mortonson et al., 2011) which is the plug-in for CAMB and CosmoMC (Lewis et al., 2000; Lewis and Bridle, 2002), the implemented solving system named as *Kinetic Module Companion* (KMC) can compute the power spectrum $\mathcal{P}_\zeta$ and investigate the model parameter spaces for the extended $\theta_{\rm KMC}$ for the Non-Canonical inflation models.

Profile of Kinetic Module Companion

KMC is a solving system with MCMC simulation interface, which implements ModeCode and extends it to study Non-Canonical inflation model given its Lagrangian. The K-Function Modules in KMC are listed as following.

The following modules are deployed and applied in our numerical exploration.

- KAS: The Pure Algebraic Solver Module;
  It provides all the necessary functions and subroutines used by later modules.
- KFC: The Kinetic Functions Configuration Module;
  It contains ordinary differential equation (ODE) solvers (at the moment of documenting there are three solvers deployed). This module also configures the kinetic energy for Non-Canonical Lagrangian, and returns kinetic relevant values such as the derivatives for kinetic, the sound speed, the small varying parameters. Values are stored in one array.
- KHE: The Hessenberg Eigenvalue Module;
  It converts the matrix obtained from KMS to a standard Hessenberg form, then obtains the Eigenvalue, and sorts the solutions by descending order, etc.
- KMS: The Matrix Solver Module;
  This constructs the Matrices by solving two-variables-higher-order equations (this

step can be completed with other tools, such as Matlab), so this module stores the matrices which are used for KHE. It then solves the ($\phi_{,N}$, H^2) for background equation, also solves the H^2 for perturbation equation given $\phi_{,N}$ [8].

- KPV: The Physical Validity Module;
  Verifies all possible background solution pairs ($\phi_{,N}$, H^2), and H^2 providing $\phi_{,N}$, then Determine the physical one for CAMB and later calculations.

  This module was ONLY used in (Li and Liddle, 2012), but no longer used since the introduction of 3D-solver in KMC while investigating the Tachyon inflation and DBI inflation.

- KSM: The Kinetic Settings Module;
  Settings of the kinetic and potential forms, other parameters and constants used by KFC and whole system.

The experimental function modules are,

- KAI: The Artificial Investigator Module;
  It contains a few sub-systems. For example, one of them is algebraic solver which will determine the root of polynomial function. The key one is the learning system. It aims to learn and exclude the initial condition (for CAMB) or the randomly generated parameters (from MCMC) some of which are used in ODE solver, before either KMS or KFC breaks. This happens because we cannot have a convenience way to freely vary their prior spaces due to the unpredictable correlation of model parameters.

- KCIR: The Conjugate Invert Reconstruction Module;
  It is aimed to inversely reconstruct the inflation potential with conjugate momentum.

I plan to document KMC in detail and make numerical codes public.

[8] The 3D solver was updated in March 2012, and it is proved that this 3D solver can perform stable and accurate calculations in NCI models, for example in (Li and Liddle, 2012)

Part II

Modelling and Constraints on Inflationary Cosmology

· Chapter 3 ·

Inhomogeneous Reheating

We ascribe beauty to that which is simple; which has no superfluous parts; which exactly answers its end; which stands related to all things; which is the mean of many extremes.

Ralph Waldo Emerson

We discuss a new mechanism which can be responsible for the origin of the primordial perturbation in inflationary models, the inhomogeneous DBI reheating scenario. Light DBI fields fluctuate during inflation, and finally create the density perturbations through modulation of the inflation decay rate. In this note, we investigate the curvature perturbation and its non-Gaussianity from this new mechanism. Presenting generalized expressions for them, we show that the curvature perturbation not only depends on the particular process of decay but is also dependent on the sound speed $c_{\rm s}$ from the DBI action. More interestingly we find that the non-Gaussianity parameter $f_{\rm NL}$ is independent of $c_{\rm s}$. As an application we exemplify some decay processes which give a viable and detectable non-Gaussianity. Finally we find a possible connection between our model and the DBI-Curvaton mechanism.

3.1 Introduction

To account for the density perturbation which seeds the structure of the observed universe, the inflationary paradigm (Kolb and Turner, 1993) is a promising candidate. In this picture, the universe went through an accelerated expansion in the very early period. This scenario predicts that the inflaton field ϕ rolls downs its potential with quantum fluctuations superimposed which lead to density perturbations. However it is important to investigate alternatives to this simple scenario.

Recently more and more evidence from observations of cosmic microwave background (CMB) anisotropies favors that the primordial density fluctuations (PDF) are almost Gaussian, Scale invariant, and adiabatic (Spergel et al., 2007; Komatsu et al., 2011). And, according to many works (Lyth and Wands, 2002; Moroi and Takahashi, 2001; Dimopoulos and Lyth, 2004; Lyth et al., 2003; Lyth, 2005; Lyth and Rodriguez, 2005; Dvali et al., 2004a; Kofman, 2003; Dvali et al., 2004b; Zaldarriaga, 2004; Matarrese and Riotto, 2003; Suyama and Yamaguchi, 2008; Battefeld, 2008; Ichikawa et al., 2008), light scalar fields merit attention to investigate their role as candidates for explaining the origin of the PDF. Such light scalar fields generally exist in extensions of the standard model of particle physics, which motivates some alternatives. One is the curvaton scenario (Lyth and Wands, 2002; Moroi and Takahashi, 2001; Enqvist and Sloth, 2002; Dimopoulos and Lyth, 2004;

Lyth et al., 2003; Lyth, 2005; Lyth and Rodriguez, 2005), in which the final curvature perturbations are produced from an initial isocurvature perturbation associated with the quantum fluctuations of a light scalar field other than the inflaton, the curvaton, whose energy density is negligible during inflation. The curvaton isocurvature perturbations are transformed into adiabatic ones when the curvaton decays into radiation well after the end of inflation. Another is the inhomogeneous/modulated reheating scenario (Dvali et al., 2004b,a; Zaldarriaga, 2004; Kofman, 2003; Matarrese and Riotto, 2003; Vernizzi, 2004). This supposes that the decay rate Γ of the inflaton varied in space due to a dependence on a light field, and density perturbations would be generated during reheating independently of those generated by the standard inflationary mechanism. In these two scenarios the light scalar fields, not the inflaton, are responsible for the primarily density perturbations. The inflaton just serves to drive and end inflation, and under this assumption the constraints on inflation are considerably lessened. By introducing these light scalar fields one also finds that primordial non-Gaussianity can be very large compared to the single inflaton models. In curvaton models the non-linear parameter $f_{\rm NL} \sim 5/4r$ [1] is a small coefficient (Lyth et al., 2003; Lyth, 2005; Lyth and Rodriguez, 2005); and inhomogeneous/modulated reheating models suggest $f_{\rm NL} \sim \mathcal{O}(1)$ (Dvali et al., 2004b; Zaldarriaga, 2004; Matarrese and Riotto, 2003) or larger given particular decay processes, see articles (Suyama and Yamaguchi, 2008; Battefeld, 2008; Ichikawa et al., 2008; Kohri et al., 2010).

Cosmological modellers have paid attention recently to the DBI field as an alternative to a canonical field. Some earlier works, (Silverstein and Tong, 2004; Alishahiha et al., 2004; Chen et al., 2007; Easson et al., 2008, 2007; Gmeiner and White, 2008; Arroja et al., 2008), have discussed cosmology using a DBI field, and with this interesting source some results are different from those obtained in (Huang et al., 2008; Langlois and Renaux-Petel, 2008; Langlois et al., 2008a,b; Guo and Ohta, 2008). So far only the ordinary light scalar fields were discussed in inhomogeneous reheating, therefore in this note, we focus on the inhomogeneous (modulated) reheating models specifically involving DBI fields. As a toy model to reheat the universe, we assume that the DBI fields can dominate the decay rate. With the variation of the decay rate, the fluctuations can be generated after inflation.

[1] The variable $r = 3\rho_{\sigma\rm dec}/(3\rho_{\sigma\rm dec} + 4\rho_{r\rm dec})$ being $\rho_{r\rm dec}$ the radiation energy density just before the curvaton σ decay with energy $\rho_{\sigma dec}$ at decay point (Lyth and Rodriguez, 2005).

3.2 Basic Mechanism

To reheat the universe, in the scenario of Dvali et al. (2004a) the inflaton couples with ordinary particles. When the inflaton decays, the decay rate has the form $\Gamma \sim \lambda^2 m$, where λ is a stochastic variable and m is the mass of the inflaton. Assuming λ is a function of the scalar fields in the theory, contrary to the standard scenario, the fluctuations in this new scenario are determined by the fluctuations of the decay rate Γ and not the inflaton field ϕ. This means that when two places have a different decay rate, the cosmological evolution in these regions will undergo different processes and eventually result in density perturbations when reheating finishes. Finally, the density perturbations are

$$\frac{\delta\epsilon_{\rm rad}}{\epsilon_{\rm rad}} \propto \frac{\delta\lambda}{\lambda} \propto \frac{\delta\Gamma}{\Gamma} \tag{3.1}$$

where we find the fluctuations in Γ are transferred into density perturbations. More detailed discussions can be found in (Dvali et al., 2004a).

In our model, which is motivated by the papers (Dvali et al., 2004a; Cai et al., 2009), we consider the decay rate to be determined by a DBI field. According to these two papers, we know the light fields are expected to provide a considerable perturbation, and in (Cai et al., 2009) we can see that light DBI-fields lead to a different and larger curvature perturbation. We also get a factor $f_{\rm NL}^{\rm equi}$ which is determined by the sound speed $c_{\rm s}$, which gives a sizable non-Gaussianity.

Expecting to get further understanding of origin of perturbations after inflation, we propose the decay rate to be determined by the DBI field in the scenario of inhomogeneous reheating. To investigate the relationship between the decay rate and the light fields, we generalize Γ to a form $\Gamma_\phi(\sigma) \equiv f(\sigma)$ where the subindex ϕ denotes the inflation era, and σ is the light DBI field. In general Γ varies with the space-time location.

For further discussions, it is necessary to quote some results from (Cai et al., 2009), which described the DBI curvaton scenario and which gives the fluctuations of the light scalar field σ, curvature perturbation ζ and its non-Gaussianity parameter $f_{\rm NL}$.

$$\delta\sigma = \sqrt{c_{\rm s}}\frac{H_*}{2\pi} \tag{3.2}$$

$$\zeta \sim \frac{h_{,\sigma}}{h}\frac{1}{c_{\rm s}^{3/2}}\frac{H_*}{12\pi} \tag{3.3}$$

$$f_{\rm NL} \simeq \frac{5}{2}\left[\frac{3(1-c_{\rm s}^2)^3}{(1-3c_{\rm s}^2)^2} + \frac{4h}{h_{,\sigma}^2}\left(\frac{h_{,\sigma\sigma}}{2} - \frac{h_{,\sigma}^2}{h}\right)\frac{c_{\rm s}^4(1-c_{\rm s}^2)}{1-3c_{\rm s}^2}\right] \tag{3.4}$$

Here the sound speed $c_{\rm s}$ is defined as $c_{\rm s} = \sqrt{1-2h(\sigma)X}$, $X \equiv -\frac{1}{2}g^{\mu\nu}\partial_\mu\sigma\partial_\nu\sigma - \frac{1}{2}g^{\mu\nu}\partial_\mu\phi\partial_\nu\phi$ in which ϕ plays the role of an inflaton field while σ is the DBI field, and $h(\sigma)$ is the warping factor. We stress the amplitude of the curvature perturbation, and more detail can be found in (Cai et al., 2009).

Before discussing the parameters which describe the properties of cosmological evolution, such as curvature perturbations and the non-linear parameter $f_{\rm NL}$, we can expand the decay rate to second order

$$\begin{aligned}\Gamma &= \Gamma_* + \delta^{(1)}\Gamma + \frac{1}{2}\delta^{(2)}\Gamma \\ &= f(\sigma_*) + f'(\sigma_*)\delta\sigma + \frac{1}{2}f''(\sigma_*)(\delta\sigma)^2 \end{aligned} \tag{3.5}$$

Here $'$ denotes the derivative with respective to the DBI-field σ, and H_* and Γ_* represent the Hubble parameter during inflation and the homogeneous value of the decay rate respectively.

Now, let's look at the general representation of the curvature perturbation. Dvali et al. (2004b); Zaldarriaga (2004); Maldacena (2003); Scoccimarro et al. (2004); Bartolo et al. (2004) show that the curvature perturbation ζ can be expressed by the fluctuations of the decay rate, $\delta\Gamma/\Gamma_*$

$$\zeta = -\alpha \log\frac{\Gamma}{\Gamma_*} = -\alpha\frac{\delta\Gamma}{\Gamma_*} \tag{3.6}$$

where the coefficient α can be determined by the quantity Γ_*/H_*. Dvali et al. (2004a) proved that during the inflation era, in the limit $\Gamma_*/H_* \to 0$, $\alpha = 1/6$. Substituting Eq.(3.5) into Eq.(3.6), we can get the curvature perturbation in the linear approximation

$$\zeta = -\sqrt{c_{\rm s}}\frac{f'(\sigma_*)}{f(\sigma_*)}\frac{H_*}{12\pi} \tag{3.7}$$

Note that the final curvature perturbation in this scenario depends not only on the sound speed $c_{\rm s}$ but also on the ratio f'/f which comes from the details of the decay process. They will be discussed in detail in the following sections.

3.3 Non-Gaussianity

Let's now focus on the degree of non-Gaussianity. During inflation, both ϕ and σ are slowly rolling. It is known that the non-Gaussianity of ζ coming from the intrinsic non-Gaussianities of $\delta\phi_*$ and $\delta\sigma_*$ is far below the observational sensitivity. Hence we can treat

$\delta\phi_*$ and $\delta\sigma_*$ as uncorrelated Gaussian random fields with the same amplitude, see (Ichikawa et al., 2008) and references therein.

As we know, the standard inflationary scenario predicts the degree of non-Gaussianity with $f_{\rm NL} \sim 1-n_{\rm s}$ of the perturbation spectrum (Maldacena, 2003; Scoccimarro et al., 2004; Bartolo et al., 2004). By contrast, in the curvaton scenario, significant non-Gaussianities are easily produced because the curvaton density is proportional to the square of the curvaton (Lyth and Rodriguez, 2005), giving $f_{\rm NL} \sim 5/4r$. Some recent works related to DBI fields also give larger positive non-Gaussianities (Huang, 2008b,a; Cai and Xue, 2009; Cai and Xia, 2009; Cai and Wang, 2010) and some related topics have been discussed in the isocurvaton scenario (Li and Wang, 2008; Li and Lin, 2008). Non-Gaussianity in models where density perturbations are produced by spatial fluctuations in the decay rate of the inflaton have been discussed in (Dvali et al., 2004b; Zaldarriaga, 2004). They show that $f_{\rm NL} \sim few$, which is larger than that coming from the inflation model, and possibly accessible to future observations.

The current[2] observational data $-10 < f_{\rm NL}^{\rm local} < 74$ (Komatsu et al., 2011; Larson et al., 2011) permits the primordial non-Gaussianity to be large. In the case of a low energy scale, however, we can safely ignore the contribution of inflaton ϕ_* to the non-Gaussianities, and we just consider the rest of the light scalar fields which are mainly responsible for the generation of non-Gaussianities.

To calculate the local form of non-Gaussianity, for simplicity we assume there is only one DBI field. With the definition of $f_{\rm NL}$ appearing in (Maldacena, 2003; Scoccimarro et al., 2004; Bartolo et al., 2004) (and references therein) it corresponds to

$$\zeta = \zeta_{\rm g} - \frac{3}{5} f_{\rm NL} (\zeta_{\rm g})^2 \tag{3.8}$$

where the coefficient $f_{\rm NL}$ [3] represents the non-Gaussianity parameter of the curvature perturbation. Looking back to Eq.(3.7) up to second order, it gives

$$\zeta = -\frac{1}{6}\left\{ \frac{f'(\sigma_*)}{f(\sigma_*)}\delta\sigma + \frac{1}{2}\left[\frac{f''(\sigma_*)}{f(\sigma_*)} - \left(\frac{f'(\sigma_*)}{f(\sigma_*)} \right)^2 \right] (\delta\sigma)^2 \right\} \tag{3.9}$$

Comparing with Eq.(3.9) and Eq.(3.8), we get the parameter as the function of $f(\sigma)$ and its first and second order derivatives,

$$f_{\rm NL} = 5\frac{\frac{f''(\sigma_*)}{f(\sigma_*)} - \left(\frac{f'(\sigma_*)}{f(\sigma_*)}\right)^2}{\left(\frac{f'(\sigma_*)}{f(\sigma_*)}\right)^2} = 5\left(\frac{f(\sigma_*)f''(\sigma_*)}{f'^2(\sigma_*)} - 1 \right) \tag{3.10}$$

[2] At the time of writing this paper.

[3] Note: In (Wands, 2010) and most other papers, the formula $\zeta = \zeta_{\rm g} + 3/5 f_{\rm NL}(\zeta_{\rm g})^2$ is used, but here we take the opposite sign for $f_{\rm NL}$. The conventions can be linked by taking $f_{\rm NL} \leftrightarrow -f_{\rm NL}$.

Similar results are presented in (Ichikawa et al., 2008). We find that the precise value of $f_{\rm NL}$ depends on specific models, but very large non-Gaussianity $|f_{\rm NL}| \gg 1$ is obtained when $\left|f(\sigma_*)f''(\sigma_*)/f'^2(\sigma_*)\right| \gg 1$ is satisfied. Detailed discussions are given in the following section.

3.4 Discussion

3.4.1 Observable Parameters

According to the calculations in previous sections of this chapter, we have found some results which differ from previous works. For example, from Eq.(3.7), we can see that the curvature perturbation becomes $\mathcal{P}_\zeta^{1/2} \sim \sqrt{c}_{\rm s} H_*/12\pi {\rm M}_*$; here $\rm M_*$ is the mass scale during reheating. In the inflationary background, gravitational waves can be predicted as the tensor fluctuation $\mathcal{P}_{\rm T}^{1/2} \sim H_*/\pi {\rm M_{pl}}$.

(1) At first glance, due to the existence of the sound speed the primordial curvature perturbation, ζ in Eq.(3.7), can be suppressed by the term $\sqrt{c}_{\rm s}$, but we also note that the detailed decay process plays a significant role in determining the final value of the curvature perturbation.

(2) Considering the ratio r of tensor to scalar, here in our model it is given by

$$r = \frac{\mathcal{P}_T}{\mathcal{P}_\zeta} \sim 10^2 \frac{1}{c_{\rm s}} \frac{f^2}{{\rm M_{pl}^2} f'^2} \tag{3.11}$$

Like any linear approximation, in expanding we assume that the decay process has the form of $f(\sigma) \propto (1 + \vartheta\sigma/{\rm M_*} + ...)$ (similarly see (Dvali et al., 2004a; Ichikawa et al., 2008)), where ϑ is small, and $\rm M_*$ is a dimensional parameter representing the mass scale for reheating after inflation ending, and ${\rm m}_\sigma < {\rm M_*} < {\rm M_{pl}}$. If we use $r < 0.36\,(95\%{\rm CL})$ from 7-year WMAP limit in the (Komatsu et al., 2011), then we should impose $f'/f \sim \vartheta/M_*$, so that ${\rm M_*} \sim \vartheta\sqrt{\rm c}_{\rm s}{\rm M_{pl}} \times 10^{-3}$. This means that for very small $c_{\rm s}$, we can get the ${\rm m}_\sigma \ll {\rm M_{pl}}$ which is assumed in the beginning of our consideration.

(3) Contrary to the standard inhomogeneous reheating scenario of (Dvali et al., 2004a), in our model the created fluctuations are of order $\sqrt{c}_{\rm s} H_* f'/f \sim \vartheta\sqrt{c}_{\rm s} H_*/{\rm M_*}$. The relation between the slope of the power spectrum of density perturbations and the inflaton potential

in various scenarios is,

$$\begin{aligned} n-1 &= \frac{d\ln\left((f'/f)^2 c_{\rm s} H_*^2\right)}{d\ln a} && \text{in our model} \\ n-1 &= \frac{d\ln H^2}{d\ln a} && \text{standard inhomogeneous reheating} \\ n-1 &= \frac{d\ln H^2/\epsilon}{d\ln a} && \text{standard inflation scenario} \end{aligned} \tag{3.12}$$

Our result is different from both (Dvali et al., 2004a) and the standard inflationary scenario.

Discussing the spectral index explores to what degree the decay process and the warp space contribute to it. With $c_{\rm s} = \sqrt{1-2Xh(\sigma)}$ and its derivative with respective to DBI field σ, i.e. $c_{\rm s}' = (c_{\rm s}^2-1)/2c_{\rm s} \times h'(\sigma)/h(\sigma)$, then we obtain

$$n-1 = \frac{d\ln H_*^2}{d\ln a} + \left[\frac{c_{\rm s}^2-1}{2c_{\rm s}^2}\frac{h'(\sigma)}{h(\sigma)} + 2\frac{f'(\sigma)}{f(\sigma)}\left(\frac{f(\sigma)f''(\sigma)}{f'^2(\sigma)}-1\right)\right]\frac{d\sigma}{d\ln a} \tag{3.13}$$

where parameter $h(\sigma)$ represents the warped throat and $f(\sigma)$ indicates the decay rate. For simplicity for estimating the contribution to power spectra, we set all $h'(\sigma)/h(\sigma)$ and $f'(\sigma)/f(\sigma)$ as proportional to $1/\sigma$ for easy estimation. By doing this, we can combine the second term as

$$\begin{aligned} n-1 &\sim \frac{d\ln H_*^2}{d\ln a} + \left[\frac{c_{\rm s}^2-1}{2c_{\rm s}^2} + 2\left(\frac{f(\sigma)f''(\sigma)}{f'^2(\sigma)}-1\right)\right]\frac{d\ln\sigma}{d\ln a} \\ &\sim \frac{d\ln H_*^2}{d\ln a} + \left(\frac{c_{\rm s}^2-1}{2c_{\rm s}^2} + \frac{2}{5}f_{\rm NL}\right)\frac{d\ln\sigma}{d\ln a} \end{aligned} \tag{3.14}$$

(A): if $c_{\rm s} \simeq 1$, the decay rate surpasses the contribution from the warped throat. From Eq.(3.13), the effect of the warp throat is reduced. However, in view of the Lagrangian, the system is just reduced to a canonical one, and can be rewritten as a usual dynamic system with $\mathcal{L} = \mathcal{L}(X,\sigma) = -\frac{1}{2}\partial_\mu\sigma\partial^\mu\sigma - V(\sigma)$.

(B): if $c_{\rm s} \ll 1$, it is hard to say which contribution affects the whole term more. Because of the warped factor h, the sound speed $c_{\rm s}$ and the unknown decay process $f(\sigma)$, the model possesses a lot of freedom, but reheating from a warped throat is worthy of investigation in future work.

3.4.2 Some Specific Examples

Interestingly, from Eq.(3.10), the non-Gaussianity is independent of the sound speed in our model even though the curvature perturbation depends on it. This distinguishes from the previous works in DBI field scenario (Huang et al., 2008; Langlois and Renaux-Petel,

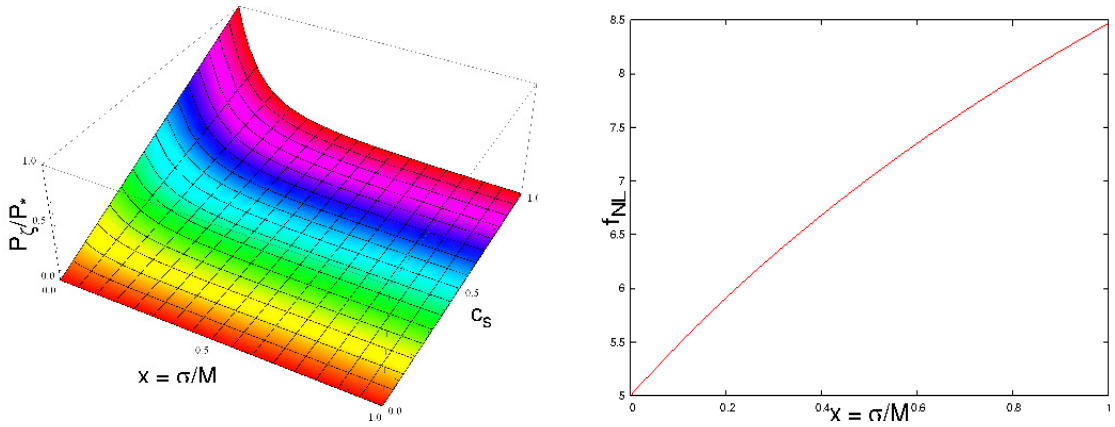

Figure 3.1: (Left) Plot of the ratio $\Re = P_\zeta/P_*$, where P_* indicates the scale-invariant power spectrum $P_* = (H_*/2\pi)^2$. (Right) non-Gaussianity of perturbation. The plots show that the amplitude of $f_{\rm NL}$ is of $\mathcal{O}(1)$, even though $\sigma \ll M$. There, the mass scale for M is lower than inflaton scale H_*.

2008; Langlois et al., 2008b; Cai et al., 2009) where the primordial fluctuations and non-Gaussianities are both enhanced by a low sound speed. Here the non-Gaussianities only depend on the specific decay process.

We wish to know whether a particular decay process exists to generate a large curvature perturbation and also non-Gaussianities. Let's consider some specific toy models able to produce detectable density perturbations and large non-Gaussianity.

(1) We assume that the decay process is described by $f(\sigma) \sim \left(1+6\log\left(1+\sigma/\mathrm{M}\right)\right)^{-1}$. Here M is a mass scale during reheating, which is less than H_*.

In this case with Fig. 3.1, we find $\zeta \sim \sqrt{c_{\rm s}}/\left\{(1+6\log(1+\sigma/\mathrm{M}))(1+\sigma/\mathrm{M})\right\}$ and $f_{\rm NL} = 35/6 + 5\log(1+\sigma/\mathrm{M})$. From the plot on the left hand side, when the speed of DBI field σ reaches its relativistic limit, which means the sound speed $c_{\rm s}$ approaches zero, we get the curvature perturbation converted from the fluctuation of σ to be zero. If the sound speed is approaching 1, meaning corresponding to a canonical system, the curvature perturbation can be of order P_*. However the ratio $\Re$ is less than 1, from the left plot, generally the curvature perturbation of the DBI field through decaying process is suppressed by $c_{\rm s}$, even if the DBI field has a large mass scale.

We can see the non-Gaussianity from the plot on the right hand side. It is independent of the sound speed $c_{\rm s}$. It is possible to obtain a large non-Gaussianity, being of $\mathcal{O}(10)$, if we place suitable coefficients in the decay rate.

(2) If we take for example the form of $(1-\lambda\sigma/M)^{-1/n}$, we could get $f_{\rm NL} \sim \mathcal{O}(1 \sim 10)$ or more. Here λ is just a sign which is used to determine the curvature perturbation

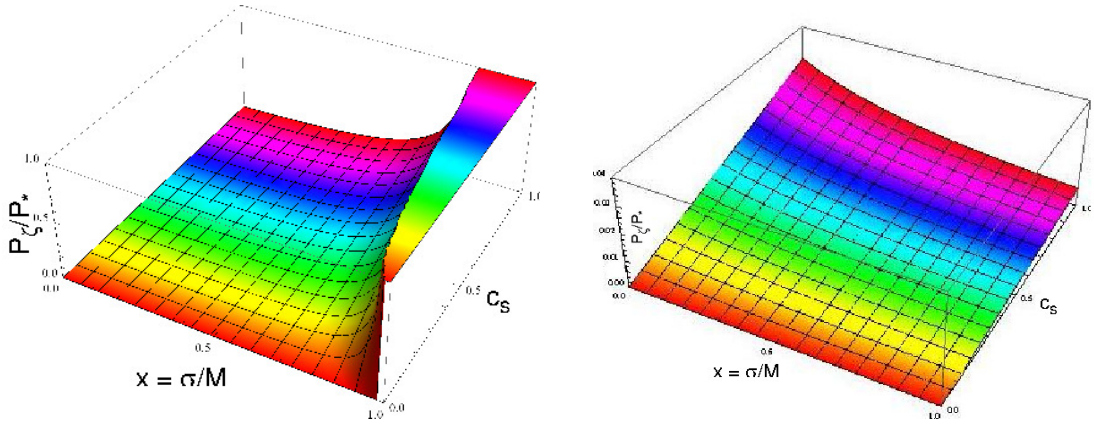

Figure 3.2: Different shapes of the ratio $\Re = P_\zeta/P_*$ with $n > 0$ (Left) and $n < 0$ (Right). Here we place $n = 1$. When $|n|$ is larger than one, the perturbation will be more flat.

together with the power n, while M is a mass scale during reheating.

In Fig. 3.2, we notice the curvature perturbations have different shapes in case with different n and the sound speed c_s overall. The figures show that the perturbations are smoothed in different parametric regions. The non-Gaussianity f_NL of these types of perturbation has the same shape, with $f_\mathrm{NL} \equiv 5n$ regardless of the sign of n, even given the different c_s.

If $c_\mathrm{s} \sim 0$, the curvature perturbation approaches zero too. When c_s gets larger, we can find the possibility of generating a detectable perturbation when $n > 0$ (in the left figure). In contrary, when $n < 0$ (in the right figure), it might not easy to detect the curvature perturbation which is converted from the DBI field during the decay period.

3.5 Summary and Outlook

In this note we proposed a variant on the inhomogeneous reheating model, in which the decay rate of the inflaton is determined by DBI fields. During inflation, the light DBI fields fluctuate and dominate the final density perturbations through the modulated inflaton decay rate. We gave the general expression for the curvature perturbations and non-Gaussianity for this model. The decay rate of the inflaton played an important role in determining their final value. By presenting the generalized expressions for them we showed that the curvature perturbation $\zeta \sim \sqrt{c_\mathrm{s}} f'/f$ depends not only on the particular process of decay but also on the sound speed c_s from the DBI action. Apparently it is

suppressed by sound speed, but due to the uncertain process of decay there will be other possible outcomes. Moreover the non-Gaussianity in our model is independent of $c_{\rm s}$ no matter that ζ depends on it. As discussed in this article, we find the non-linear parameter $f_{\rm NL}$ is independent of the sound speed $c_{\rm s}$ and large non-Gaussianity can be obtained if $\left|f''f/f'^2\right| \gg 1$ is satisfied. As an application we exemplify some kinds of decay process leading to a detectable non-Gaussianity, $f_{\rm NL}$ of $\mathcal{O}(1 \sim 10)$ which is compatible with observational data.

As a byproduct and outlook, comparing Eq.(3.7) with Eq.(3.3), we can rewrite them as $\zeta^{\rm DBI}_{\rm inhomo} \sim -\vartheta_i$ and $\zeta^{\rm DBI}_{\rm curvaton} \sim \vartheta_c/c_{\rm s}^2$ where we define two factors respectively for the above two quantities $\vartheta_i \equiv \sqrt{c}_{\rm s} f'(\sigma_*)/f(\sigma_*)$ and $\vartheta_c \equiv \sqrt{c}_{\rm s} h'(\sigma_*)/h(\sigma_*)$.

If we consider a tachyon condensation, as discussed in (Cai et al., 2009), where the DBI-Curvaton has this kind of exit mechanism rather than oscillation as in usual curvaton model, then the universe can be instantly reheated. However, we presume that in a warped throat, in which a space-time has a strong compactification, that the motion of DBI fields σ or the D-brane itself could be assumed to decay once the inflation ends. Due to the fields having a velocity limit in a D-brane, which could be interpreted by the sound speed $c_{\rm s}$ in DBI action, it is interesting to bridge the decay process and the warp throat with the sound speed, namely $f(\sigma) \simeq h(\sigma)c_{\rm s}^2$. Then we may find that the DBI-Curvaton is a special case in the context of this model if there should exist a decay process in the form of $f(\sigma) \simeq h(\sigma)c_{\rm s}^2$ in a warped throat. To investigate the inhomogeneous reheating mechanism concerning a warped throat is a valuable direction for future work, although many works have been done in the context of a throat (Barnaby et al., 2005; Chen, 2005; Chialva et al., 2006; Kecskemeti et al., 2006; Becker et al., 2007; Alabidi et al., 2010; Kobayashi and Mukohyama, 2009; Zhang et al., 2010).

· Chapter 4 ·

Analytic and Numerical Study on K-inflation

It seems that if one is working from the point of view of getting beauty in one's equations, and if one has really a sound insight, one is on a sure line of progress.

P. A. M. Dirac

We extend the ModeCode software of Mortonson, Peiris and Easther to enable numerical computation of perturbations in K-inflation models, where the scalar field no longer has a canonical kinetic term. Focussing on models where the kinetic and potential terms can be separated into a sum, we compute slow-roll predictions for various models and use these to verify the numerical code. A Markov chain Monte Carlo analysis is then used to impose constraints from WMAP 7-year data ("WMAP7") on the addition of a term quadratic in the kinetic energy to the Lagrangian of simple chaotic inflation models. For a quadratic potential, the data do not discriminate against addition of such a term, while for a quartic ($\lambda\phi^4$) potential inclusion of such a term is actually favoured. Overall, constraints on such a term from present data are found to be extremely weak.

4.1 Introduction

Observations, especially including those from the Wilkinson Microwave Anisotropy Probe (WMAP) (Dunkley et al., 2009; Komatsu et al., 2009, 2011; Larson et al., 2011), are beginning to impose useful constraints on inflationary cosmologies. In particular, a number of papers have made detailed evaluations of constraints on the simplest inflation models, featuring a single canonically-normalized scalar field with unknown potential $V(\phi)$, see for example (Dodelson et al., 1997; Kinney, 2002; Peiris et al., 2003; Leach and Liddle, 2003; Alabidi and Lyth, 2006; Peiris and Easther, 2006a; Kinney et al., 2006; Ringeval, 2008; Kinney et al., 2008; Hamann et al., 2008; Adshead and Easther, 2008; Agarwal and Bean, 2009; Komatsu et al., 2011).

Staying with the single-field paradigm, a more general scenario is available through the K-inflation paradigm. This retains minimal coupling of the scalar field to gravity, but allows the action to have an arbitrary dependence on the field's kinetic energy as well as on its value. This introduces new features, including a sound speed less than the speed of light which may enhance the non-gaussianity in the models. Our aim in this chapter is to impose observational constraints on versions of this more general single-field scenario.

Our strategy is to modify the ModeCode program of Mortonson et al. (2011), which solves the inflationary perturbation mode equations numerically and then interfaces to the CAMB (Lewis et al., 2000) and CosmoMC (Lewis and Bridle, 2002) packages in or-

der to compute the corresponding microwave anisotropies and compare to observational data. This entails a number of modifications to the way that ModeCode handles both the background (homogeneous) evolution equations and the perturbation equations. In this chapter we will focus on the simplest case where the kinetic and potential terms remain sum-separable, and consider only simple forms for each. For the potential we will consider the simplest chaotic inflation models (Linde, 1982, 1983), based on quadratic and quartic potentials. For the kinetic term, we will consider simple monomial and polynomial forms, in particular investigating constraints on addition of a term quadratic in the kinetic energy to the normal canonical form. Future work will explore more complicated forms. Modification of ModeCode to consider specifically the action corresponding to DBI inflation (Sen, 2002b,a) has already been carried out in (Devi et al., 2011). Comparison of K-inflation models to five-year WMAP data using slow-roll methods has been made in (Lorenz et al., 2008a).

4.2 The K-inflation model

The K-inflation model (Armendariz-Picon et al., 1999; Garriga and Mukhanov, 1999) features a single scalar field with the action

$$S = \int \sqrt{-g}\, p(\phi, X) d^4x \,, \tag{4.1}$$

where ϕ is the field value and $X \equiv (1/2)\partial_\mu\phi\partial^\mu\phi$. The function p will play the role of the pressure. A canonical scalar field has $p(\phi, X) = X - V(\phi)$ where $V(\phi)$ is the potential. In this chapter we will focus on models where the kinetic and potential terms can be written as a sum:

$$p(\phi, X) = K(X) - V(\phi) \,, \tag{4.2}$$

where $K(X)$ and $V(\phi)$ are both arbitrary functions to be determined from data.

Given the Lagrangian $p(X, \phi)$ of the considered model, we can obtain observable consequences by the following approach, closely following (Garriga and Mukhanov, 1999).

4.2.1 Background field equations and sound speed

We assume the usual Einstein equations and a spatially-flat Robertson–Walker metric with scale factor a and Hubble parameter $H = \dot{a}/a$. We use the reduced Planck mass, defined

by $M_{\rm Pl}^2 = (8\pi G)^{-1}$, to denote the strength of gravity throughout (with $c = \hbar = 1$ as usual).

First, without needing to consider gravity, we can obtain a relationship between the density ρ of the universe and its pressure p,

$$\dot{\rho} = -3H(\rho + p)\,, \tag{4.3}$$

which is known as the continuity equation, in which the energy–momentum tensor is characterised by the pressure $p(X, \phi)$ and the density

$$\rho(X, \phi) = 2X\frac{dp}{dX} - p \tag{4.4}$$

of this universe.

Second, now invoking a theory of gravity in the form of general relativity, we have the Friedmann equation for flat cosmologies

$$H^2 = \frac{\rho}{3M_{\rm Pl}^2}\,. \tag{4.5}$$

Taking Eq. (4.3) together with Eq. (4.5), we can therefore study the evolution of the scale factor a and the field variable ϕ.

One important quantity, called the 'sound speed', describes the properties of the ϕ field. Regarding the field as a fluid system, we can introduce $c_{\rm s}^2$ as

$$c_{\rm s}^2 = \frac{p_{,X}}{\rho_{,X}} = \frac{p_{,X}}{2Xp_{,XX} + p_{,X}}\,, \tag{4.6}$$

where the comma denotes the partial derivative with respect to X.

4.2.2 Perturbation mode equations

The background state for the field ϕ is given by Eqs. (4.3) and (4.5). However, confrontation of inflationary models with data requires us to evaluate the perturbations they predict. We will just quote the two significant equations, first derived by Garriga and Mukhanov (1999). The scalar and tensor perturbations are described by quantities v and u whose Fourier components in the longitudinal gauge satisfy

$$\frac{d^2v_k}{d\tau^2} + \left(c_{\rm s}^2k^2 - \frac{d^2z/d\tau^2}{z}\right)v_k = 0 \tag{4.7}$$

$$\frac{d^2u_k}{d\tau^2} + \left(k^2 - \frac{d^2a/d\tau^2}{a}\right)u_k = 0 \tag{4.8}$$

respectively. Here, τ is the conformal time, subscript k denotes the momentum space, and the variable k relates to the comoving scale by $\lambda = 2\pi/k$. The curvature perturbation ζ is

related to v by $\zeta = v/z$, while in a flat universe the background variable z can be expressed as

$$z^2 = \frac{a^2(\rho + p)}{c_{\rm s}^2 H^2} \,. \tag{4.9}$$

In momentum space, the canonical quantisation modes v_k and u_k give two different classes of perturbations, the scalar perturbations measured by v_k and the tensor (gravitational wave) perturbations by u_k. From Eq. (4.7), we see that $c_{\rm s}/H$ plays the role of the 'sound horizon', which the k mode leaves by satisfying $c_{\rm s}k = aH$. The power spectrum of the scalar mode can be expressed by

$$\mathcal{P}_\zeta(k) = \frac{k^3}{2\pi^2} \left| \frac{v_k}{z} \right|^2 \,, \tag{4.10}$$

while in Eq. (4.8) the tensor mode leaves the usual horizon by satisfying $k = aH$, with spectrum

$$\mathcal{P}_{\rm t}(k) = \frac{k^3}{2\pi^2} \left| \frac{u_k}{a} \right|^2 \,. \tag{4.11}$$

4.2.3 Power spectra and observables

Solving Eq. (4.7) in the slow-roll approximation gives the expression (Garriga and Mukhanov, 1999):

$$\mathcal{P}_\zeta = \left. \frac{1}{8\pi^2 M_{\rm Pl}^2} \frac{H^2}{\epsilon c_{\rm s}} \right|_{c_{\rm s}k = aH} \,, \tag{4.12}$$

The tensor mode Eq. (4.8) has its usual power spectrum

$$\mathcal{P}_{\rm t} = \left. \frac{2}{\pi^2 M_{\rm Pl}^2} H^2 \right|_{k=aH} \,. \tag{4.13}$$

Having given the mode equations and their spectra, we can study the two most interesting variables, the spectral index $n_{\rm s}$ and the tensor–scalar ratio r. These two quantities can be constrained by observations, such as the existing WMAP data or the forthcoming *Planck* satellite results. Their definitions are

$$n_{\rm s} - 1 \equiv \frac{d\ln \mathcal{P}_\zeta}{d\ln k} \simeq -2\epsilon - \tilde{\eta} - s \tag{4.14}$$

$$n_{\rm t} \equiv \frac{d\ln \mathcal{P}_{\rm t}}{d\ln k} \simeq -2\epsilon \tag{4.15}$$

$$r \equiv \frac{\mathcal{P}_{\rm t}}{\mathcal{P}_\zeta} = 16\epsilon c_{\rm s} \,, \tag{4.16}$$

where the parameters $\epsilon \,, \tilde{\eta} \,, \delta \,, s$ are all small and defined as

$$\epsilon = -\frac{d\ln H}{dN} \quad ; \quad \tilde{\eta} = \frac{d\ln \epsilon}{dN} \quad ; \quad \delta = -\frac{d\ln \dot{\phi}}{dN} \quad ; \quad s = \frac{d\ln c_{\rm s}}{dN} \,, \tag{4.17}$$

through $dN = Hdt$, and we additionally give the tensor spectral index $n_{\rm t}$. Higher-order versions of these expressions, which we do not use here, have been obtained using the uniform approximation (Lorenz et al., 2008b).

All these parameters are calculated at the time when mode k leaves its individual horizon. For the scalar mode k takes the value of $aH/c_{\rm s}$, while for tensor mode k takes aH. As a result, the relation of d/dN to $d/d\ln k$ for the scalars is

$$\frac{d\ln k}{dN} = 1 - \epsilon - s\,. \tag{4.18}$$

Therefore Eq. (4.14) and Eq. (4.15) are then actually divided by Eq. (4.18), whereas s must be taken as zero when adjusting Eq. (4.15) as the sound speed does not enter its horizon-crossing expression.

Note that $\tilde{\eta}$ in Eq. (4.17) is implicitly a function of the usual slow-roll parameters $\epsilon = (M_{\rm Pl}^2/2)(V'/V)^2$ and $\eta = M_{\rm Pl}^2 V''/V$ and other smaller parameters, such as δ.[1] Here and throughout primes are derivatives with respect to ϕ. We will discuss its particular expression in later sections when investigating specific models.

4.3 Slow-roll predictions

In this section, we use the slow-roll approximation to compute the spectral index $n_{\rm s}$ and tensor-to-scalar ratio r for various models. These results are of interest in their own right as they give an indication of the properties of models that will be able to fit the data. Additionally, we will be able to use them to verify that our modifications to ModeCode have been implemented successfully.

4.3.1 General prediction without specifying a potential

We study models where the Lagrangian takes the form

$$p(\phi, X) = K_{n+1}X^n - V(\phi)\,, \tag{4.19}$$

[1] The full expression is

$$\tilde{\eta} = 2\epsilon - 2\left(1 + \frac{Xp_{,XX}}{p_{,X}}\right)\delta + \frac{p_{,X\phi}}{p_{,X}}\phi_{,N}$$

given pressure $p = p(X, \phi)$, where $,N$ indicates the derivative with respect to N. In our current consideration, the pressure has separable X and ϕ, so the last term vanishes. The factor of δ in the second term can be treated as $-(1+\theta)$, where $\theta = 1/c_{\rm s}^2$. Therefore $\tilde{\eta} = 2\epsilon - (1+\theta)\delta$.

where K_{n+1} are constants and n takes integer values.[2] Under this kind of action, we can derive the field equation for the scalar field ϕ from Eq. (4.3) as

$$\dot{X}\rho_{,X} + \dot{\phi}\rho_{,\phi} = -6nK_{n+1}HX^n\,, \tag{4.20}$$

where the subscript $,\phi$ is the derivative with respect to the field.

We now discuss what the models predict under the slow-roll scheme. Therefore by the usual consideration, we assume the density of the universe is dominated by the scalar potential, $H^2 \propto \rho \simeq V$ and replace all appearances of the Hubble parameter H^2 by V. In the field equation Eq. (4.20), we take the first (acceleration) term on the left-hand side to be much less than the second term. Hence it simplifies to

$$V'\dot{\phi} \simeq -6nK_{n+1}HX^n\,. \tag{4.21}$$

Within the slow-roll assumption, we can obtain descriptions of the observable quantities by means of some parameters. From Eq. (4.17) we can identify ϵ as $\epsilon_{_V}$ under the slow-roll assumption, where

$$\epsilon_{_V} = -\frac{1}{2}\frac{V'}{V}\frac{\dot{\phi}}{H}\,. \tag{4.22}$$

With $\ddot{\phi} \ll \dot{\phi}$ under the slow-roll assumption, for later discussion we give the second parameter $\eta_{_V}$ which relates to the first and second-order derivatives of the potential,

$$\eta_{_V} = -\frac{V''}{V'}\frac{\dot{\phi}}{H}\,. \tag{4.23}$$

By the approximation above, we can find a simple relation between these parameters,

$$\frac{\eta_{_V}}{\epsilon_{_V}} = 2\frac{VV''}{V'^2}\,, \tag{4.24}$$

and also we can find the relation

$$\tilde{\eta} = 3\epsilon_{_V} - \delta - \eta_{_V}\,. \tag{4.25}$$

From Eq. (4.21), for later evaluation we can write the ratio $\dot{\phi}/H$ as

$$\frac{\dot{\phi}}{H} = -\alpha(n)\left(\frac{V'}{V^n}\right)^{1/(2n-1)} \tag{4.26}$$

where

$$\alpha(n) = \left(\frac{6^{n-1}}{nK_{n+1}}M_{\rm Pl}^{2n}\right)^{1/(2n-1)}\,. \tag{4.27}$$

[2] With only a single kinetic term, the coefficient K_{n+1} could be removed by rescaling ϕ, adjusting the potential, but for later comparison with cases with more than one term we keep it explicit.

Then

$$\epsilon_{_V} = \frac{1}{2}\alpha(n)\left(\frac{V'^{2n}}{V^{3n-1}}\right)^{1/(2n-1)} \quad ; \quad \eta_{_V} = \alpha(n)\left(\frac{V''^{(2n-1)}}{V^{n}V'^{2n-2}}\right)^{1/(2n-1)} . \tag{4.28}$$

Now we would like to apply the slow-roll approximation to evaluate the most important physical observables. The first is the scalar power spectrum $\mathcal{P}_\zeta$,

$$\mathcal{P}_\zeta \propto \frac{2}{\alpha(n)c_{\rm s}}\left(\frac{V^{5n-2}}{V'^{2n}}\right)^{1/(2n-1)} , \tag{4.29}$$

In this case, we can write the spectral index via Eq. (4.29) as

$$n_{\rm s} - 1 = \frac{1}{2n-1}\left[2n\eta_{_V} - 2(5n-2)\epsilon_{_V}\right] . \tag{4.30}$$

To verify that Eqs. (4.29) and (4.30) are correct for standard inflation, we just need to set $n = 1$, and then we have the power spectrum

$$\mathcal{P}_\zeta = \frac{1}{12\pi^2 M_{\rm Pl}^2}\frac{K_2 V}{2\epsilon_{_V}} , \tag{4.31}$$

and its corresponding spectral index is $n_{\rm s} - 1 = 2\eta_{_V} - 6\epsilon_{_V}$. As a prediction of Eq. (4.30), for the simplest NCI, in which the kinetic term has the form X^2, we can obtain the power spectrum

$$\mathcal{P}_\zeta = \frac{1}{12\pi^2 M_{\rm Pl}^4}\left(\frac{K_3 V^8}{3M_{\rm Pl}^4 V'^4}\right)^{1/3} , \tag{4.32}$$

and its spectral index $n_{\rm s} - 1 = (4\eta_{_V} - 16\epsilon_{_V})/3$.

4.3.2 Predictions for specific models through e-folding N

Thus far we have obtained the formulae for the scalar power spectrum and its spectral index without specifying a particular potential type. In this subsection, we continue the discussion within a class of potential $V(\phi) = A\phi^m$ in the Lagrangian Eq. (4.19), where A denotes the normalisation parameter, and m takes integer values.[3]

The e-folding number N, which measures how much inflation took place, is

$$N = -\int H\, dt\, . \tag{4.33}$$

[3]Following footnote 2, for this form of potential a rescaling of ϕ to eliminate K_{n+1} in the single-term kinetic case would simply renormalize A, which anyway is to be fixed by the density perturbation amplitude. Hence there is a perfect degeneracy between K_{n+1} and A and data can only fix a combination of them.

After observable scales cross the horizon we have $N \sim 50$ until inflation ends. First we evaluate the time variation $H\,dt$ by the time-shift carried by the scalar field ϕ and finally transferred from the gradient change in the potential $V(\phi)$

$$H\,dt = \frac{H}{\dot{\phi}} d\phi = \frac{H}{\dot{\phi}} \frac{1}{V'} dV\,. \tag{4.34}$$

So from the definition of N, and taking the above relation along with Eq. (4.26), we can derive the corresponding relation for N in terms of the scalar potential $V(\phi)$ and its derivatives, rather than with ϕ itself,

$$N = \int_{\rm i}^{\rm e} \frac{H}{\dot{\phi}} \frac{1}{V'} dV\,. \tag{4.35}$$

Under the assumption of slow-roll, by means of the slow-varying parameters, say Eqs. (4.22) and (4.23), we can write Eq. (4.35) as

$$N = -\frac{1}{2} \int_{\rm i}^{\rm e} \frac{1}{\epsilon} \frac{dV}{V}\,. \tag{4.36}$$

Here ϵ (neglecting the subscript) is a function of the potential and its derivatives as well, which have already been denoted by Eqs. (4.22) and (4.23) in the slow-roll approximation. Connecting N with these two slowly-varying parameters leads to the expression for spectral index $n_{\rm s}$.

By taking potential $V(\phi) = A\phi^m$, we obtain

$$N = \frac{m}{\beta(n,m)} \frac{1}{\gamma(n,m)} V^{\beta(n,m)/m} \tag{4.37}$$

where

$$\beta(n,m) = \frac{m(n-1)+2n}{2n-1} \quad ; \quad \gamma(n,m) = \alpha(n) \left(mA^{1/m}\right)^{2n/(2n-1)}\,. \tag{4.38}$$

Then, connecting Eqs. (4.22), (4.23) and Eq. (4.37), we can get the relation between the slow-roll parameters and N

$$\epsilon_{_V} = \frac{m}{2\beta} \frac{1}{N} \quad ; \quad \eta_{_V} = \frac{m-1}{\beta} \frac{1}{N}\,. \tag{4.39}$$

The final formula for the spectral index in Eq. (4.30) is therefore

$$n_{\rm s} - 1 = -\mathcal{I}(n,m) \frac{1}{N}\,, \tag{4.40}$$

where

$$\mathcal{I}(n,m) = \frac{m(3n-2)+2n}{m(n-1)+2n}\,. \tag{4.41}$$

	$n=1$		$n=2$	
	$m=2$	$m=4$	$m=2$	$m=4$
$\alpha(n)$	$M_{\rm Pl}^2/K_2$	$M_{\rm Pl}^2/K_2$	$(3M_{\rm Pl}^4/K_3)^{1/3}$	$(3M_{\rm Pl}^4/K_3)^{1/3}$
$\beta(n,m)$	2	2	2	$8/3$
$\gamma(n,m)$	$4\alpha(1)A$	$16\alpha(1)A^{1/2}$	$2^{4/3}\alpha(2)A^{2/3}$	$2^{8/3}\alpha(2)A^{1/3}$
$\mathcal{I}(n,m)$	2	3	2	$5/2$
$\mathcal{P}_\zeta$	$\gamma_{(1,2)}N^2$	$\gamma_{(1,4)}^2(N/2)^3$	$\sqrt{3}\gamma_{(2,2)}N^2$	$\sqrt{3}\gamma_{(2,4)}^{3/2}(2N/3)^{5/2}$
$n_{\rm s}\big\vert_{N=50}$	0.96	0.94	0.96	0.95
$r\big\vert_{N=50}$	0.16	0.32	0.092	0.14

Table 4.1: Functions and observables for standard inflation and the simplest NCI model $K(X)=K_3X^2$. $\mathcal{P}_\zeta$ is in units of $(12\pi^2M_{\rm Pl}^4)$ and N is taken as 50.

We can separate the two dependencies in Eq. (4.41) so as to examine how the potential and kinetic energy terms contribute:

$$\mathcal{I}=1+\frac{(2n-1)m}{m(n-1)+2n}=1+\frac{m}{\beta}\qquad(n\,,m\geq 1)\,, \tag{4.42}$$

which indicates $\mathcal{I}>1$. We can see, from the above expression, that the spectral index $n_{\rm s}-1$ has a simple relation with the power of the potential in N, Eq. (4.37). In particular, for the quadratic potential $m=2$, $\mathcal{I}$ is independent of n. Therefore, the inflation model driven by this potential will give a spectral index $n_{\rm s}=0.96$ regardless of the power of X in the kinetic term. Further, in terms of $\mathcal{I}(n,m)$ in Eq. (4.42), the scalar power spectrum Eq. (4.12) can be written as

$$\mathcal{P}_\zeta=\frac{1}{12\pi^2M_{\rm Pl}^4}\frac{1}{c_{\rm s}}\gamma^{\mathcal{I}-1}\left(\frac{N}{\mathcal{I}-1}\right)^{\mathcal{I}}\,. \tag{4.43}$$

The class of Lagrangian, Eq. (4.19), has sound speed $c_{\rm s}=1/\sqrt{2n-1}$ which is independent of m. As for Eq. (4.43), given a known e-folding number N after inflation, the scalar power spectrum can be determined directly using the parameter set (n,m), which is the input argument to the two functions $\gamma(n,m)$ and $\mathcal{I}(n,m)$, while for the scalar spectral index we can just use one function $\mathcal{I}(n,m)$. Example values for the functions $\alpha(n)$, $\beta(n,m)$ and $\gamma(n,m)$ with parameter set (n,m) can be seen in Table 4.1.

From Eqs. (4.16), (4.39) and (4.40), we can obtain an expression relating the tensor-to-scalar ratio r and spectral index $n_{\rm s}$

$$r=8\frac{\sqrt{2n-1}\,m}{m(3n-2)+2n}\,(1-n_{\rm s})\,. \tag{4.44}$$

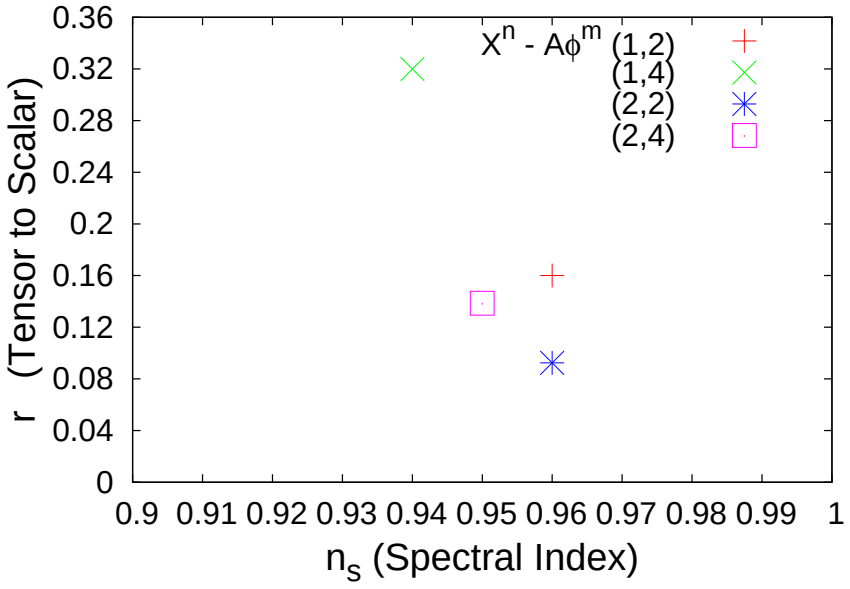

Figure 4.1: Slow-roll predictions for the tensor-to-scalar ratio r and the scalar spectral index $n_{\rm s}$ in standard inflation and the simplest NCI model where $n = 2$ in Eq. (4.19).

We list the observables in Table 4.1, and example values for $n_{\rm s}$ and r can be seen in Figure 4.1.

For canonical inflation, the known relation $n_{\rm s} - 1 = -(m+2)/2N$ is recovered by setting $n = 1$. For $n = 2$, we find

$$n_{\rm s} - 1 = -\frac{4(m+1)}{m+4}\frac{1}{N}\,. \tag{4.45}$$

Figure 4.2 shows the spectral index as a function of m for several n values; when $n > 1$ the spectral index asymptotes to $1 - 4/N$ in the limit of large potential power-law m, unlike the canonical case where $1 - n_{\rm s}$ grows linearly with m and can be large.

4.4 ModeCode for K-inflation

For single-field canonically-normalized inflation models there are many numerical tools which can calculate the primordial power spectra, as well as other characteristics such as the bispectrum and trispectrum of non-gaussianities. Also many of these tools have been interfaced with MCMC codes such as CosmoMC so as to explore the likelihood and carry out parameter estimation. ModeCode (Mortonson et al., 2011) is an example of such

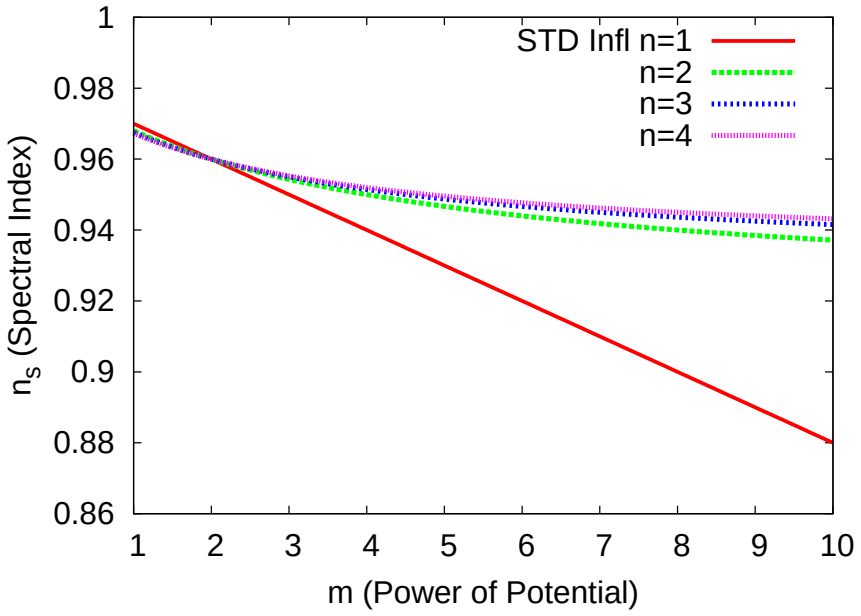

Figure 4.2: Slow-roll predictions for the spectral index with different kinetic power-law n and potential power-law m. This plot assumes the pivot corresponds to $N = 50$.

a programme, which had also recently been interfaced to the MultiNest model selection code (Easther and Peiris, 2012; Norena et al., 2012). Other codes to numerically solve the inflationary mode equations have been described in (Grivell and Liddle, 1996; Martin and Ringeval, 2006; Lesgourgues and Valkenburg, 2007; Lesgourgues et al., 2008; Finelli et al., 2010; Martin et al., 2011).

To study non-canonical models, modifications must of course be made to the code, generalizing both the background and perturbation equations. An example already in the literature is an enhancement to consider the Lagrangian describing DBI inflation, made in (Devi et al., 2011), which is motivated from string scenarios (Sen, 2002b,a) and has been widely studied in the literature. In this chapter we consider a different extension to non-canonical inflation models, at this stage restricted to models where the kinetic energy $K(X)$ and the potential $V(\phi)$ are sum-separable.

4.4.1 Brief description of ModeCode

ModeCode is characterised by free parameters describing the inflationary potential for canonical single-field inflation, and solves the inflationary mode equations numerically, bypassing the slow-roll approximation. It computes the cosmic microwave background

angular power spectra and performs a likelihood analysis and parameter estimation by interfacing with CAMB (Lewis et al., 2000) and CosmoMC (Lewis and Bridle, 2002).

4.4.2 Modifications needed for K-inflation

We implement ModeCode under our umbrella **Kinetic Module Companions (KMC)**. To perform our analysis for NCI models, we build up a full system for initialising the background equations, avoiding slow-roll or any other kind of approximation beyond linear perturbation theory. The parameters which can be explored and the methodology in KMC are as follows.

- Parameters describing the form of the kinetic energy, for example a Taylor expansion of $K(X)$ about $X = 0$ which we have currently implemented up to sixth order (though in the present paper we will only consider up to quadratic order).
- Parameters describing the inflationary potential, for instance the potential can take a polynomial form or be a Taylor series.

We use eigenvalue methods to get the real solutions needed by the background equations, Eqs. (4.4) and (4.21), as well as perturbed equations. Equations to solve simultaneously for $\phi_{,N}$ and H^2 can be explicitly obtained.

4.4.3 Comparison tests

Recovery of ModeCode results for $K(X) = X$

Before running the extended functions, we check we can recover the results of ModeCode with our KMC system. The outputs that ModeCode generates are recovered either by setting our flag use_kinetic=T and setting $K(X) = X$, so that KMC will perform its intrinsic functions for models that can be executed by ModeCode, or just by switching off the KMC functional system by flag use_kinetic=F, leaving KMC to function as the normal ModeCode. We have confirmed that the ModeCode results are then precisely recovered under either method.

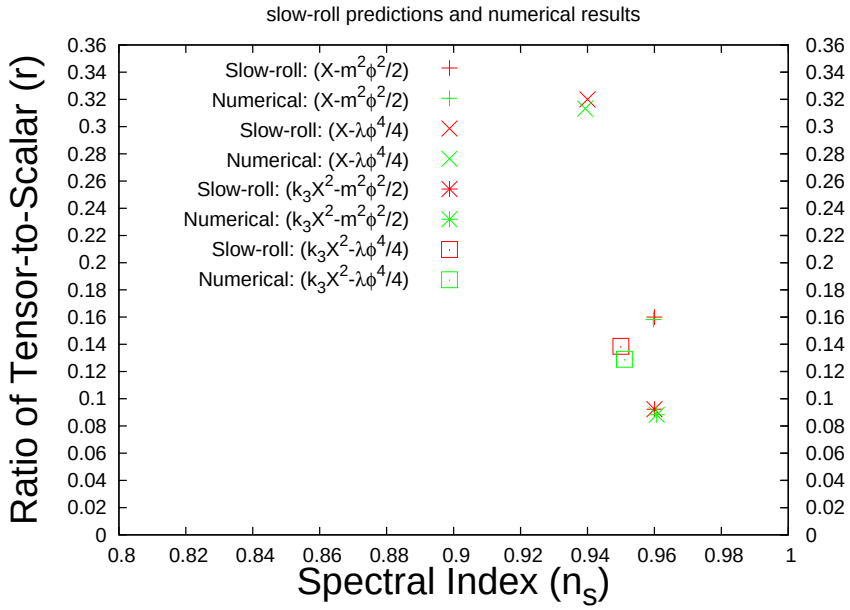

Figure 4.3: Slow-roll predictions and numerical results for standard canonical inflation and the simplest NCI model ($K_3X^2 - A\phi^m$), showing they are consistent. The matter power spectrum amplitude constrains the combination $AK_3^{m/4}$ (from the scaling argument of footnote 3) and the predictions for n_s and r are independent of this. The value of K_3 does determine the e-folding value corresponding to observable scales, but this is not fixed by observations.

Recovery of slow-roll results

Now we compare the slow-roll predictions of the previous section with the numerical results for two types of inflation model. One is the standard inflationary model, with canonical kinetic energy and Lagrangian $p(\phi, X) = X - V(\phi)$. The other is the simplest NCI model, where the kinetic energy takes the form X^2 in the Lagrangian $p(\phi, X) = K_3X^2 - V(\phi)$. Figure 4.3 shows that the recovery of the slow-roll results is very accurate. It is not expected to be absolutely precise because the slow-roll approximation is not perfect, for instance leading to an offset in identification of the $N = 50$ point as well as neglecting higher-order corrections to perturbation observables.

4.5 Parameter explorations with MCMC

4.5.1 Global settings and initial conditions

We now proceed to explore the parameter space of a particular non-canonical type of inflationary model, by means of Markov Chain Monte Carlo (MCMC) methodology. We use the WMAP 7-year data ("WMAP7") version4, and our simulations take 12 chains for each model. We set the pivot scale to $k_{\rm pivot} = 0.05\,{\rm Mpc}^{-1}$. We aim to select an initial field value $\phi_{\rm init}$ which corresponds to 70 e-foldings from the end of inflation, estimated analytically by assuming a single power-law term dominates $K(X)$; if this approximation proves inaccurate it gets adjusted by the numerical code. We then must choose a consistent initial field velocity $\phi_{,{\rm N}{\rm init}}$, as mentioned in Section 4.4.2, a task which has been solved by eigenvalue methods in our KMC numerical modules.

Having developed the KMC code, our aim is to investigate what type of NCI models are supported by observational data. Using the MCMC method, we will perform a likelihood analysis and parameter exploration for some particular NCI models.

4.5.2 Choice of models

In this article, for our numerical work we focus on a particular choice of kinetic term which adds a quadratic term in X to the usual linear one. Investigation of more complex models will be made in future work. Hence our considered NCI model is $p(X,\phi) = K_2X + K_3X^2 - V(\phi)$ with K_3 positive,[4] and we will additionally assume the potential to have a single polynomial term $V(\phi) = A\phi^m$ with $m = 2$ or 4, giving a large-field model. The field ϕ can always be rescaled to set $K_2 = 1$, and the new term with coefficient K_3 can be considered as the first correction term in a Taylor expansion of a general $K(X)$ that reduces to a canonical form in the limit $X \to 0$. While such a model is not particularly realistic, it has the benefit of simplicity and it is interesting to ask whether present data can say anything about the possible values of such a correction. Since in slow-roll inflation

[4] Negative K_3 appears possible in principle, provided X is not too large, but gives models that can have phantom behaviour ($w < -1$) from an overall negative kinetic term, which can be expected to cause instabilities. We note also that the quadratic approximation to the DBI model features a positive coefficient.

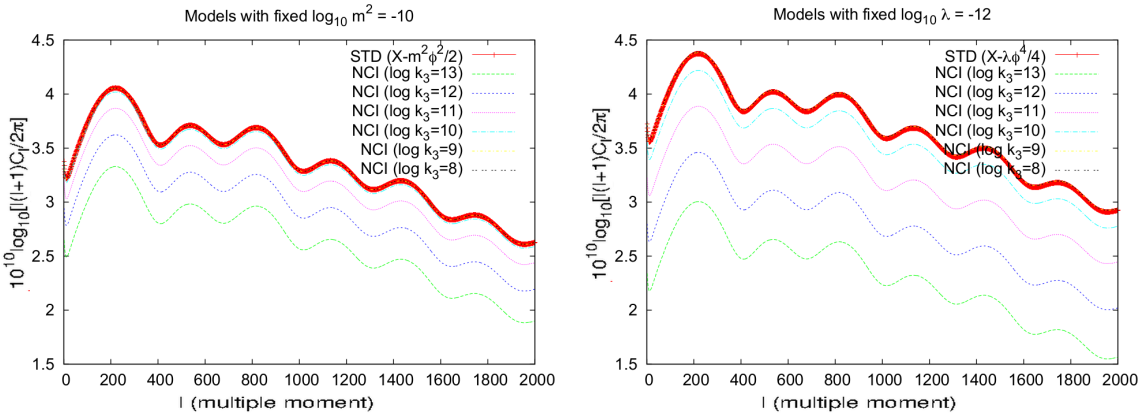

Figure 4.4: The effect of different values of K_3 on the final power spectrum. All numbers in the legend are base-10 logarithms, with the spectrum in units of $\mu\mathrm{K}^2$.

X will be small, we can immediately anticipate that any constraint on K_3 will be very weak, allowing values much greater than one before this correction term could significantly modify the canonical term.

Our free parameters are therefore the power of the potential, which we fix for each investigation, and the values of the amplitude of the potential and the coefficient K_3. Additionally, the value of N_{pivot} corresponding to k_{pivot} can vary as in the original ModeCode. The well-measured amplitude of perturbations will accurately fix a combination of these parameters.

4.5.3 Overview of effects from additional kinetic terms

Before we examine the results from MCMC, we look at the influence of the extra term, K_3X^2 in the kinetic function, on the final power spectrum. The shape of the power spectrum is controlled by a combination of A and K_3 in our considered NCI models. In the left panel of Figure 4.4, we take $\log m^2 = -10$ for potential $m^2\phi^2/2$; introducing K_3 has negligible effect for $K_3 \lesssim 10^{10}$, above which the spectrum starts to decrease as the quadratic kinetic term becomes dominant. In the right panel we see a similar result for $\lambda\phi^4$ with $\lambda = 10^{-12}$. Figure 4.5 shows the spectra for some parameter values chosen so that the spectral amplitude is close to the observed value.

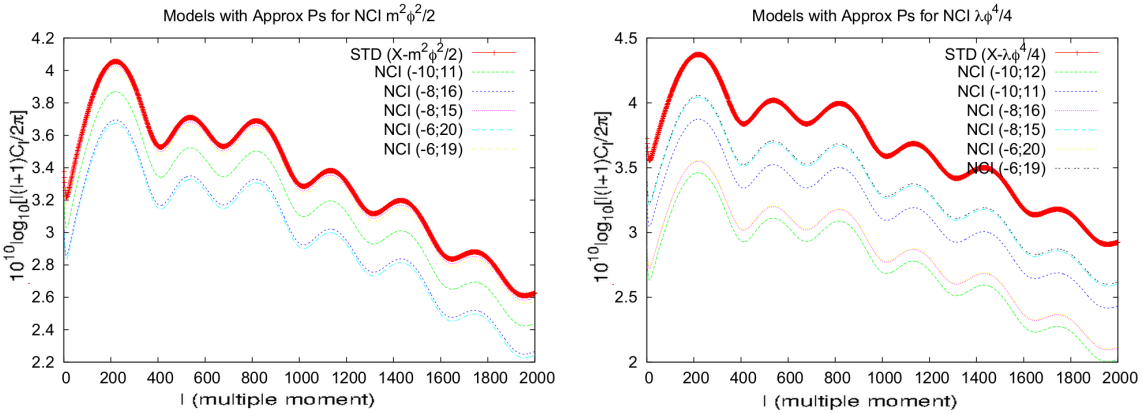

Figure 4.5: The power spectra for various combinations of parameters. For the NCI models, the first number in the key is the exponent of m^2 (left panel) or λ (right panel), while the second number is the exponent of K_3.

Models	Priors		$n_{s,\mathrm{ML}}$	r_{ML}	$-2\ln\mathcal{L}_{\mathrm{ML}}$
(NCI)	$\log A$	$\log K_3$			
$(1,2;2)$	$(-16\,,-4)$	$(0,20)$	0.965	0.080	7469.8
$(1,2;4)$	$(-18\,,-4)$	$(0,20)$	0.957	0.115	7471.8

Table 4.2: Priors for the parameters, $\log A$ and $\log K_3$, and the maximum likelihood (ML) values for n_{s} and r from WMAP7. NCI models with single-term potentials provide a red tilt, $n_{\mathrm{s}} < 1$, and a detectable tensor-to-scalar ratio $r \sim 0.1$.

4.5.4 Interpretation of MCMC explorations

After finishing 12 chains for each model, we have obtained a Gelman–Rubin convergence statistic $R-1 = 0.16$ and 0.012 for the eigenvalues of the covariance matrix in models with quadratic and quartic potentials respectively. The prior ranges and maximum likelihood values are given in Table 4.2, and the posterior distributions in Figures 4.6 and 4.7.

The parameter of principal interest in each case is K_3. In the quadratic potential case, this parameter turns out to be completely unconstrained by the data. This is to be expected, as the quadratic potential gives acceptable observables when the kinetic term is either X or X^2, which are the limits of small and large K_3. The MCMC results show that the fit to data remains acceptable right to the largest values of K_3 that we permit. We clearly see the two limiting behaviours of domination by either the X or X^2 term; for

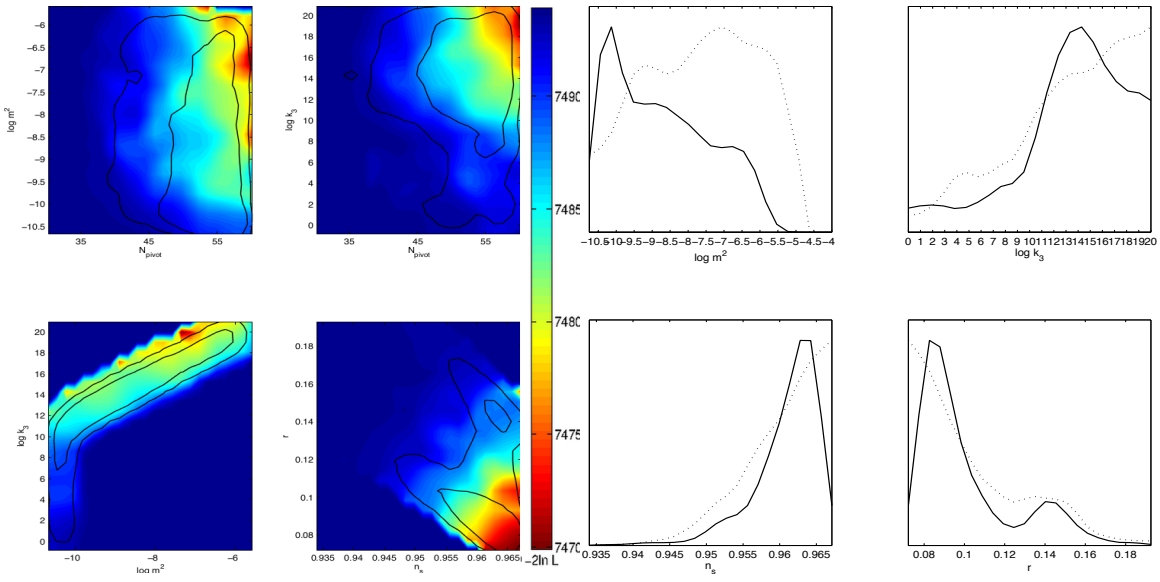

Figure 4.6: Parameter constraints for NCI model with quadratic potential. Left: Constraints on $\log m^2$ and K_3 against $N_{\rm pivot}$ for WMAP7 data. The countours are 68% (inner) and 95% (outer) confidence levels, while the colour scale shows the sample mean likelihood in bins. Right: one-dimensional posterior distributions for the parameters (solid) and the mean likelihoods (dashed). (The colour bar indicates the likelihood of parameter's value, and the red colour within this bar denotes the likelihood for the best-fitted parameters.)

example in the 2D m^2–K_3 constraint plot the former region has constant $\log m^2 \simeq -10$, while the latter has $K_3 \propto m^4$ as implied by taking constant $\mathcal{P}_s$ in the third column of Table 4.1 to obtain the observed amplitude. The bimodal likelihood of r is caused by the different values of this parameter in the two regimes. We also see a very mildly enhanced likelihood in the transition regime $K_3 \simeq 10^{12}$, but all values of K_3 are acceptable Perhaps surprisingly, then, present data can say nothing about the amplitude of a quadratic kinetic term added to the normal canonical one for this potential, and as this is a potential known to fit the data well in the canonical case we can conclude that more generally a quadratic correction term cannot be constrained directly from data.

The quartic potential case shown in Figure 4.7 is more interesting. In the standard cosmology, $K_3 \to 0$, the quartic potential is quite disfavoured by WMAP7. As we would anticipate from the slow-roll results of Section 4.3, the situation for this potential actually improves in the limit of large K_3, as both $n_{\rm s}$ and r move towards the scale-invariant values. Once more the MCMC results show that the fit remains good as the quadratic kinetic term becomes dominant and we find no observational upper limit on K_3 for this potential. This time the distribution for r is unimodal, as only the X^2 domination regime contributes to

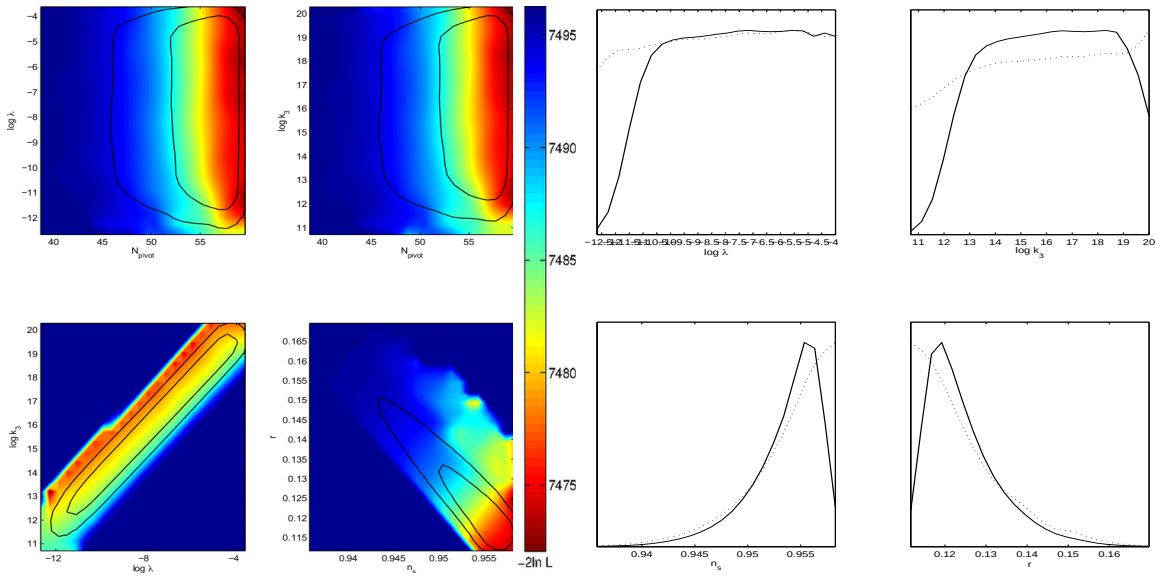

Figure 4.7: Parameter constraints for NCI model with single-term quartic potential. This figure uses the same convention as in figure 4.6. (The colour bar and scale take the same convention in Fig. 4.6.)

the posterior. There is a plausible non-zero lower limit on K_3, though the numerical value of such a limit will be quite prior-dependent. Hence, incorporation of an X^2 term is a method of salvaging the quartic model, though the large value of $K_3 \lesssim 10^{10}$, in Planck units, that is required is unattractive.

4.6 Conclusions

In this chapter we introduced a numerical solver **Kinetic Module Companions (KMC)**, an extension to ModeCode for a class of non-canonical inflation (NCI) models. In this article we have used our code to investigate some simple non-canonical models, which have up to two terms in the kinetic energy and a monomial potential, in order to test the validity of the code and provide some initial scientific results. We found that these models are well able to fit current data, including in the quartic potential case provided the quadratic kinetic term dominates. This is compatible with slow-roll results we obtained in the case of a single kinetic term of power-law form.

As a specific application of the code, we studied the introduction of a quadratic correction K_3X^2 to the normal canonical kinetic term X, with the goal of constraining the

coefficient K_3. In practice, however, K_3 turns out to be unconstrained by data, and indeed the inclusion of a large quadratic term can even improve the fit to WMAP7 data, for instance for a quartic potential which, in the canonical case, is under severe pressure from observations. Accordingly present data allow no leverage whatsoever on radical deviations from the canonical case. In future work we plan a much more comprehensive investigation of possible kinetic and potential forms.

A longer-term objective in this area may be to extend ModeCode to yet more complex forms of single scalar-field action, such as the Galileon (Nicolis et al., 2009) or indeed the Horndeski action (Horndeski, 1974) which is the most general scalar–tensor theory yielding second-order equations of motion. However the many functional degrees of freedom of such actions will no doubt lead to considerable degeneracies given the relatively limited amount of observational information available, which essentially amounts to only a couple of numbers at present. Hence, as we have found here even for the simplest separable K-inflation case, one is likely to need considerable guidance from theory as well as from observations in assessing whether the most general paradigms are useful.

· Chapter 5 ·

Analytic Study on Tachyon and DBI Inflation

Do not be afraid to skip equations.

Roger Penrose

Insanity: doing the same thing over and over again and expecting different results.

Albert Einstein

We present a systematic method for evaluation of perturbation observables in non-canonical single-field inflation models within the slow-roll approximation, which allied with field redefinitions enables predictions to be established for a wide range of models. We use this to investigate various non-canonical inflation (NCI) models, including Tachyon inflation and DBI inflation. The Lambert $\mathcal{W}$ function will be used extensively in our method for the evaluation of observables. In the Tachyon case, in the slow-roll approximation the model can be approximated by a canonical field with a redefined potential, which yields predictions in better agreement with observations than the canonical equivalents. For DBI inflation models we consider contributions from both the scalar potential and the warp geometry. In the case of a quartic potential, we find a formula for the observables under both non-relativistic (sound speed $c_{\rm s}^2 \sim 1$) and relativistic behaviour ($c_{\rm s}^2 \ll 1$) of the scalar DBI inflaton. For a quadratic potential we find two branches in the non-relativistic $c_{\rm s}^2 \sim 1$ case, determined by the competition of model parameters, while for the relativistic case $c_{\rm s}^2 \to 0$, we find consistency with results already in the literature. We present a comparison to the latest *Planck* satellite observations. Most of the non-canonical models we investigate, including the Tachyon, are better fits to data than canonical models with the same potential, but we find that DBI models in the slow-roll regime have difficulty in matching the data.

5.1 Introduction

The slow-roll expansion has proven a powerful tool for calculating perturbation observables in inflationary cosmologies, and its likely applicability is now strongly supported by the observed near scale-invariance of scalar perturbations and the increasingly strong upper limits on the tensor-to-scalar ratio. In the case of canonically-normalized single-field models this formalism, first set down in (Liddle and Lyth, 1992), readily generates results that can be set against observations such as the recent data compilations provided by the *Planck* Collaboration (Ade et al., 2013b). It results from an expansion in the Mukhanov equations (Mukhanov, 1985) that describe scalar and tensor perturbations, which can be solved using Hankel functions. The formalism can be extended to higher order in the small slow-roll parameters (Stewart and Lyth, 1993; Stewart, 2002; Gong and Stewart, 2001, 2002;

Choe et al., 2004), and various non-slow-roll approaches exist such as the δN formalism (Sasaki and Stewart, 1996) and the approaches in (Huston and Malik, 2011; Ribeiro, 2012; Adshead et al., 2013), which are often useful in non-gaussianity investigations (Burrage et al., 2011b). For the power spectra themselves, however, the simple slow-roll approach is typically valid.

There is ongoing interest in the possibility that inflation may be driven by a single field which does not possess a canonical kinetic term, usually referred to as k-inflation (Armendariz-Picon et al., 1999), examples being the Tachyon and the Dirac–Born–Infeld (DBI) field, or the Galileon inflation theories as discussed in (Mizuno and Koyama, 2010; Kobayashi et al., 2010; Burrage et al., 2011a). This motivation is in large part theoretical, but additional observational impetus is being created due to the tightening upper limits on the tensor contribution, as even simple non-canonical models can shift predicted observables closer to scale invariance, e.g in (Li and Liddle, 2012; Unnikrishnan et al., 2012). The slow-roll formalism is readily extended to non-canonical single-field models (Garriga and Mukhanov, 1999; Kinney and Tzirakis, 2008; Ringeval, 2010) (see (Hu, 2011) for recent developments). However, for specific models the calculations necessary to determine the observables may be algebraically challenging.

In this article we propose a new systematic algorithm for carrying out these calculations, through a reframing of the evolution equations in a recursive form and use of field redefinitions to simplify the Lagrangians. We deploy it for a range of non-canonical models to generate theoretical predictions that we set against contemporary observations. The new algorithm will frequently involve the Lambert $\mathcal{W}$ function in order to evaluate desired observables such as the power spectrum and its index. Our approach recovers results in our related papers, which undertake numerical analyses (Li and Liddle, 2012, 2013b). The results from our algorithm give an interpretation of the numerical results, in particular the degeneracy of model parameters (Devi et al., 2011; Li and Liddle, 2012, 2013b). The algorithm also provides another view on reconstructing the inflation model in respect of the observational data, such as those from *Planck* and future data from *Euclid*.

We begin by introducing the framework of the proposed algorithm in Section 5.3, and present the predictions for the power spectrum and its spectral index for various models. We implement the analytic methods in Section 5.4. We will discuss our results for some models in Section 5.5, then model parameter estimations are studied in Section 5.6 as the result of applying those techniques. We summarise in Section 5.7, including a few words on future exploration and possible applications of our algorithm.

5.2 The Models

The general Lagrangian for a single-field model with second-order field equation is an arbitrary function $p(X, \phi)$ of the scalar field ϕ and its kinetic energy $X \equiv \frac{1}{2}\partial_\mu\phi\partial^\mu\phi$. In addition to the general case, in this chapter we will consider four specific Lagrangians within this class:

1. Canonical field with potential $V(\phi)$:

$$p(X, \phi) = BX - V(\phi) \tag{5.1}$$

   where we add the coefficient B denoting the coupling strength of the kinetic energy, though traditionally it is set to 1.

2. Non-Canonical inflation (NCI) model: This features an arbitrary power on the kinetic term and was studied in (Mukhanov and Vikman, 2006; Li and Liddle, 2012; Unnikrishnan et al., 2012), the Lagrangian being

$$p(X, \phi) = BX^n - V(\phi) \tag{5.2}$$

   where n is a positive integer (equal to 1 in the canonical case).

3. Tachyon model: The Tachyon model was introduced by Sen (2002a,b), and later studied by Gibbons (2002); Fairbairn and Tytgat (2002); Kofman and Linde (2002); Piao et al. (2002); Guo et al. (2003). Its Lagrangian is

$$p(X, \phi) = -V(\phi)\sqrt{1 - 2fX} \tag{5.3}$$

   where the warp factor f is a constant.

4. DBI inflation model: Its Lagrangian is given by

$$p(X, \phi) = -\frac{1}{f(\phi)}\sqrt{1 - 2f(\phi)X} - V(\phi) \tag{5.4}$$

   where we follow (Alishahiha et al., 2004) and take the warp factor $f(\phi) \simeq \lambda_s/\phi^4$ with λ_s constant. Some authors, e.g. in article (Silverstein and Tong, 2004), include an additional term $1/f(\phi)$ to cancel the leading-order term from expanding the square root. We have absorbed such a term into $V(\phi)$. The article (Bean et al., 2008) contains a detailed study of one particular regime of this model.

The sound speed is defined as

$$c_{\rm s}^2 = \frac{\delta p}{\delta \rho} = \frac{\partial p/\partial X}{\partial \rho/\partial X}\,, \tag{5.5}$$

and one can show that for both NCI models it is $c_{\rm s} = \sqrt{1-2f(\phi)X}$, where the warp factor takes the unified form as $f = f(\phi)$. This factor is constant in Tachyon models, and a function of the scalar field in the DBI inflation models.

We investigate the observables of interest, being the power spectrum $\mathcal{P}_\zeta$, its spectral index $n_{\rm s}$, and the tensor–scalar ratio r, within the slow-roll approximation. Following the conventions in (Armendariz-Picon et al., 1999; Garriga and Mukhanov, 1999), these are given by

$$\mathcal{P}_\zeta = \frac{1}{8\pi^2}\frac{H^2}{c_{\rm s}\epsilon}\,, \tag{5.6}$$

$$n_{\rm s} - 1 = \frac{d\ln \mathcal{P}_\zeta}{d\ln k} = -(2\epsilon + \eta + s)\,, \tag{5.7}$$

$$r = 16 c_{\rm s}\epsilon\,, \tag{5.8}$$

where the various small parameters are defined by

$$\epsilon = -\frac{d\ln H}{H dt}\,,\ \eta = \frac{d\ln \epsilon}{H dt}\,,\ s = \frac{d\ln c_{\rm s}}{H dt}\,. \tag{5.9}$$

In this chapter, for each case we will focus on power-law potentials, either with general exponent m or the simplest cases $V = \frac{1}{2}m^2\phi^2$ and $V = \frac{1}{4}\lambda\phi^4$. Also we take the reduced Planck mass $M_{\rm Pl}^2 = 1$ for convenience, for instance in the expression for $\mathcal{P}_\zeta$.

5.3 The General Systematic Method

Here we propose a systematic method in the slow-roll regime to obtain and express the final solutions for observables, such as the power spectrum $\mathcal{P}_\zeta$ and spectral index $n_{\rm s}$, as a function of e-folds N.

5.3.1 General formula for the spectral index $n_{\rm s}$

We continue with the general Lagrangian $\mathcal{L} = p(\phi, X)$, noting for later use that any field redefinition to a new field φ, that is a function of ϕ and whose kinetic energy density is $\tilde{X} = \frac{1}{2}\partial_\mu\varphi\partial^\mu\varphi$, still leaves the Lagrangian as a general function $\tilde{p}(\varphi, \tilde{X})$ and hence results in the same field equations in the new variables.

We write down the energy density of the universe, ρ, as usual (Armendariz-Picon et al., 1999; Garriga and Mukhanov, 1999)

$$\rho = 2Xp_{,X} - p\,. \tag{5.10}$$

The Friedmann equations are

$$H^2 = \frac{\rho}{3}\,,\ \dot{H} = -Xp_{,X}\,, \tag{5.11}$$

where we continue to use the convention $M_{\rm Pl}^2 = 1$.

We now define a variable u by

$$u := \frac{1}{\epsilon} = \frac{H^2}{Xp_{,X}}\,. \tag{5.12}$$

We will use Eqs. (5.10), (5.11), (5.12) and their derivatives to obtain the observables for the considered inflationary scenarios in the slow-roll regime.

Eq. (5.11) gives the continuity equation

$$\rho' = 3(\rho + p) = 6Xp_{,X}\,, \tag{5.13}$$

where $'$ indicates derivative w.r.t. the e-folds N. According to Eqs. (5.12) and (5.13) we can write

$$\frac{2}{u} = \frac{\rho'}{\rho}\,. \tag{5.14}$$

This compact form suggests that typically $\epsilon = 1/u \propto 1/2N$, in view of dimensional analysis.

We wish to write the density of the Universe as

$$\rho = \rho(V(\phi), u)\,. \tag{5.15}$$

so that X and $\dot{X}$ will play the role of simplification in recursion relations for u and u', etc. This form is general but useful, since it indicates that the considered quantities, such as the power spectrum, are determined by the potential and a small parameter $1/u$. The final result can be obtained by the perturbation method in terms of the small parameters coming from u and its derivatives (here ϵ, η, $c_{\rm s}$, s). Once we find the solution for the quantity u we can then obtain the potential via Eq. (5.14), where it is a first derivative w.r.t. the scalar field ϕ.

To find an expression for u without assuming a particular form of the Lagrangian, we differentiate Eq. (5.12) w.r.t. N to obtain

$$\frac{u'}{u} \;=\; \frac{2}{u} - \frac{X'}{X}\frac{1+c_{\rm s}^2}{2c_{\rm s}^2} - \frac{p_{,X\phi}}{p_{,X}}\phi'\,, \tag{5.16}$$

In deriving this equation, we have applied the relation $1/c_{\rm s}^2 = 1 + 2Xp_{,XX}/p_{,X}$.

Differentiating Eq. (5.14) w.r.t. N,

$$-\frac{u'}{u} = \frac{\rho''}{\rho'} - \frac{\rho'}{\rho} = \frac{2}{u}\left(\frac{\rho''\rho}{\rho'^2} - 1\right), \tag{5.17}$$

and the relation $X = \frac{1}{2}H^2\phi'^2$ gives

$$\frac{X'}{X} = 2\left(\frac{\phi''}{\phi'} + \frac{1}{u}\right). \tag{5.18}$$

Eq. (5.18) can be used to eliminate the field-dependent terms, such as X'/X and ϕ'/ϕ, which are present in Eqs. (5.16) and (5.17).

The quantity u' has a clear meaning, namely

$$u' = \frac{\eta}{\epsilon}. \tag{5.19}$$

Once u is obtained, we will have an explicit relation between η and ϵ.

Exact formula for $u(c_{\rm s})$

We now use Eq. (5.13) to reformulate Eq. (5.16) as,

$$u' = 2\left(1 - \frac{u}{2}\frac{p_{,X\phi}\phi'}{p_{,X}}\right) - 3(1 + c_{\rm s}^2)\left(1 - \frac{u}{2}\frac{\rho_\phi\phi'}{\rho}\right)u\,. \tag{5.20}$$

Equation (5.20) is derived from the field equation without any assumptions or model specification. It is general and has a quite symmetric form, from which we can get some descriptive results by inserting or approximating Eq. (5.14). For example, qualitatively, if one approximates $\rho \sim V$, then for the following two models we will have

- Canonical inflation

  This type of inflation model has Lagrangian $\mathcal{L} = X - V(\phi)$. Then according to the equation above, we will have $\epsilon = 1/2N$, and $\eta = 2\epsilon = 1/N$, due to

  $$p_{,X\phi} \equiv 0\,,\ \frac{2}{u} \simeq \frac{\rho_\phi\phi'}{\rho} = \frac{V_{,\phi}\phi'}{V}\,. \tag{5.21}$$

- Tachyon models

  The Lagrangian for this model is $\mathcal{L} = -V(\phi)\sqrt{1 - 2fX}$, where f is a constant. As in the analysis above, we find $\epsilon =$ const. due to,

  $$\frac{p_{,X\phi}\phi'}{p_{,X}} \equiv \frac{V_{,\phi}\phi'}{V} \equiv \frac{\rho_\phi\phi'}{\rho} \simeq \frac{2}{u}\,. \tag{5.22}$$

The outcomes are concise, but the approximate results of Eqs. (5.21) and (5.22) are only for qualitative understanding. We cannot make this approximation to eliminate any term in Eq. (5.20). The evolution equation for u is derived from the exact equation of motion, and if one wants to make an assumption on any term in Eq. (5.20), one must also rederive the evolution equation for u. In the next subsection we address this issue. Therefore, although we have obtained this equation, it does not yet lead to a clear understanding for the observables for given model.

Predictions within the slow-roll approximation

We need to derive a suitable equation for u. In the following, we will apply a well-defined approximation scheme to derive results based on Eqs. (5.12), (5.13), (5.16), and (5.17). In obtaining the observables, we use the variable u and its derivatives.

In the slow-roll regime, the following equation is obtained after expanding Eq. (5.13)

$$\rho_{,\phi}\phi' \simeq 6Xp_{,X} \tag{5.23}$$

Then Eq. (5.14) can be written as

$$\frac{2}{u} = \frac{\rho_{,\phi}\phi'}{\rho}\,, \tag{5.24}$$

Then the full Eq. (5.20) will not applicable because it is derived from the full equation of motion for scalar field. We need to find the derivative of X' from Eq. (5.23) in order to get a similar equation for ϵ and $c_{\rm s}$, by eliminating X'/X in Eq. (5.16). In view of this, we obtain the following equation,

$$\frac{2}{u}\frac{\rho_{,\phi\phi}\rho}{\rho_{,\phi}^2} + \frac{\phi''}{\phi'} = \frac{X'}{X}\frac{1+c_{\rm s}^2}{2c_{\rm s}^2} + \frac{p_{,X\phi}\phi'}{p_{,X}} \tag{5.25}$$

We also define a variable δ,

$$\delta \equiv \left(\frac{\rho_{,\phi\phi}\rho}{\rho_{,\phi}^2} - \frac{1}{2}\right) \tag{5.26}$$

for later convenience. Assembling Eqs. (5.16), (5.18), (5.23), (5.25), and (5.26) we eliminate $Xp_{,X}$, ϕ''/ϕ' and X'/X, but we keep the sound speed $c_{\rm s}$ as it can be related to the variable u. After some effort, we can obtain the final result for Eq. (5.16),

$$u' = 2\left[1 - \delta(1+c_{\rm s}^2)\right] + \frac{p_{,X\phi}\phi'}{p_{,X}}uc_{\rm s}^2\,. \tag{5.27}$$

As we have noted in Eqs. (5.21) and (5.22), the last term in the above equation can now be approximated and then the whole equation can be simplified and solved.

5.3.2 Predictions for two classes of models

Using Eq. (5.27) we consider some classes of inflation models. Unless explicitly stated, the following discussion will consider a monomial potential of the form $V \propto \phi^m$. This will provide a constant $\delta = 1/2 - 1/m$, independent of the field value itself.

Variable separable class This class of inflation models includes two subclasses: Sum-Separable Models (**SSMs**) and Product-Separable Models (**PSMs**).

- ⋆ **SSMs:** Here we have separate terms for ϕ and X which are added together, for example $\mathcal{L} = BX^n - A\phi^m$.[1] In this class, similarly to Eq. (5.21), we have the following useful relations

$$\rho(V(\phi), u) = \frac{V(\varphi)}{1 - 1/3u}\,,\; p_{,X\phi} \equiv 0\,,\; c_{\rm s}^2 \equiv \frac{1}{2n-1}\,, \tag{5.28}$$

which can be substituted into Eq. (5.27). Then we can obtain a compact form, recovering the results we found for this model in (Li and Liddle, 2012):

$$u' = 2\frac{\beta}{m}\,,\; \beta = \frac{(n-1)m + 2n}{2n-1}\,. \tag{5.29}$$

Solution for u: According to the equation above, the solution is explicitly obtained as

$$\epsilon = \frac{m}{\beta}\frac{1}{2N}\,. \tag{5.30}$$

We have a model independent η according to Eqs. (5.19), (5.29) and (5.30),

$$\eta = 2\frac{\beta}{m}\epsilon \equiv \frac{1}{N}\,. \tag{5.31}$$

under the linear assumption by considering only the leading-order small parameter, such as ϵ. We see that the parameter ϵ depends on the exponents m and n of the given model, while the parameter η does not.

Power spectrum $\mathcal{P}_\zeta$, spectral index $n_{\rm s}$, and tensor-to-scalar ratio r: Now that we have obtained the solution for u expressed by Eq. (5.30), we can use Eqs. (5.23), (5.24), and (5.29) to find the scalar potential $V = A\phi^m$ in terms of e-folds N. We recall that Eq. (5.23) gives the slow-roll prediction

$$V' = 6^{1-n} nB \frac{V^{n-1}}{(\beta N)^{2n}} \left(\frac{V}{A}\right)^{2n/m}\,, \tag{5.32}$$

[1] Actually when the kinetic term consists of a single monomial term, any constant prefactor can readily be set to unity without loss of generality by a field rescaling.

and Eq. (5.24) gives

$$\frac{\rho'}{\rho} \simeq \frac{V'}{V} = \frac{2}{u}\,. \tag{5.33}$$

Finally we obtain the potential V as

$$V = \left(\frac{m6^{n-1}}{n}\,\frac{A^{\frac{2n}{m}}}{B}\right)^{\frac{m}{\beta}\frac{1}{2n-1}} (\beta N)^{m/\beta}\,. \tag{5.34}$$

Therefore we can now write down the power spectrum from Eq. (5.6) and its spectral index from the Eq. (5.7),

$$\mathcal{P}_\zeta = \frac{\sqrt{2n-1}}{12\pi^2}\frac{\beta}{m} \times \left(\frac{m\beta^{2n-1}6^{n-1}}{n}\,\frac{A^{\frac{2n}{m}}}{B}\right)^{\frac{m}{\beta}\frac{1}{2n-1}} \times N^{\frac{m}{\beta}+1}\,, \tag{5.35}$$

$$n_\mathrm{s} - 1 = -2\left(1+\frac{m}{\beta}\right) \times \frac{1}{2N}\,, \tag{5.36}$$

$$r = 16\frac{m}{\beta}\frac{1}{2N}\,. \tag{5.37}$$

⋆ **PSMs**: These take the form $\mathcal{L} = -K(X)V(\phi)$ where both $K(X), V(\phi) > 0$, the Tachyon being an example. We will still have the following relations, analogous to the case in Eq. (5.22),

$$\rho_{,\phi} \propto V_{,\phi}\,,\ \frac{p_{,X\phi}\phi'}{p_{,X}} \equiv \frac{V_{,\phi}\phi'}{V} = \frac{2}{u}\,, \tag{5.38}$$

which leads Eq. (5.27) to be,

$$u' = 2(1-\delta)(1+c_\mathrm{s}^2)\,. \tag{5.39}$$

Here we have an implicit function, the sound speed $c_\mathrm{s}^2 = c_\mathrm{s}^2(u)$. To get an explicit result for model observables, such as $\mathcal{P}_\zeta$ and $n_\mathrm{s} - 1$ via this differential equation (5.39), we first need to specify the particular form of c_s^2 in terms of u. In general it is not straightforward to solve this equation due to the undetermined sound speed, but this is possible for the Tachyon Models as presented in Section 5.4.1.

A more general ansatz Not all Lagrangians are sum or product separable, of course; the Tachyon is product-separable but the DBI case is neither. To set up formalism to deal with the latter, we consider the more general Lagrangian

$$\mathcal{L} = -\left(W(\phi)K(X) + U(\phi)\right)\,. \tag{5.40}$$

This contains the SSM and PSM as special cases, respectively W constant and $U \propto W$. In its conventional form, Eq. (5.4), the DBI model does not take this form, but we will

show below that it can be written in this form via a field redefinition. Although we will not undertake a general study for the above ansatz, due to the complexity of the analysis, we will use the DBI case to illustrate our procedure on Lagrangians of this class.

5.4 Application of the Systematic Method to Two Models

5.4.1 Tachyon models

We now consider the Tachyon model given by Eq. (5.3) and apply Eq. (5.39). At this point we don't have to impose any simplification since the Lagrangian already takes the product-separable form. However, we will implement a field-redefinition approach to rederive these results in a different way in Section 5.5.1.

For this type of model, the relation between u and the sound speed $c_{\rm s}$ is

$$\epsilon = \frac{1}{u} = \frac{3}{2}(1 - c_{\rm s}^2)\,, \tag{5.41}$$

while the energy density ρ is

$$\rho(V(\phi), u) = \frac{V(\phi)}{\sqrt{1 - 2/3u}} \simeq V(\phi)\,. \tag{5.42}$$

Then we can solve for u according to Eq. (5.39), which can be written as

$$u' = 4\mu\left(1 - \frac{1}{3u}\right)\,,\ \mu = 1 - \delta = \frac{1}{2} + \frac{1}{m}\,. \tag{5.43}$$

The solution for $\epsilon = 1/u$ is therefore

$$N = \frac{1}{4\mu}\left[\frac{1}{\epsilon} + \frac{1}{3}\ln\left(\frac{3}{\epsilon} - 1\right)\right]. \tag{5.44}$$

The solution can be inverted using the Lambert $\mathcal{W}$ function[2] so we will have,

$$u = \frac{1}{\epsilon} = 1 + \mathcal{W}(e^{x-1})\,,\ x = 12\mu N\,. \tag{5.45}$$

[2]Two useful properties of the Lambert $\mathcal{W}$ function (Wikipedia, 2013) are $\mathcal{W}(e) = 1$ and its asymptotic behaviour for any real $x \geq e$ (Hoorfar and Hassanij, 2008),

$$L_1 - L_2 + \frac{1}{2}L_3 \leq \mathcal{W}(x) \leq L_1 - L_2 + \frac{e}{e-1}L_3$$

where $L_1 = \ln x,\ L_2 = \ln\ln x,\ L_3 = L_2/L_1$.

As μ is of order one, $x \gg 1$ for any N of interest, which means that $\epsilon \ll 1$ will always hold. Then we can obtain the following relations

$$\epsilon = \frac{1}{2\mu}\frac{1}{2N} \tag{5.46}$$

$$\eta = 4\mu\epsilon\left(1-\frac{\epsilon}{3}\right) = \frac{1}{N}\left(1-\frac{1}{6\mu}\frac{1}{2N}\right) \simeq \frac{1}{N}\,. \tag{5.47}$$

To find the power spectrum, we need to find the relation of ϕ to N. To achieve this, we combine Eq. (5.23) with Eqs. (5.38), (5.41), and (5.46) and find the potential V in terms of N and the model parameters A, λ_s,

$$V = \kappa N^{1/2\mu}\,,\ \kappa = \left(2m^2\mu\frac{c_{\rm s}A^{2\mu-1}}{\lambda_s}\right)^{1/2\mu}\,. \tag{5.48}$$

According to Eq. (5.6) the scalar power spectrum is

$$\mathcal{P}_\zeta = \frac{1}{12\pi^2}c_{\rm s}^{1/2\mu-1}\times\left(m^2(2\mu)^{1+2\mu}\frac{A^{2/m}}{\lambda_s}\right)^{1/2\mu}\times N^{1+1/2\mu}\,. \tag{5.49}$$

The spectral index receives contributions from the last term and also from the time variation of the sound speed $c_{\rm s}$, but we will now see that the latter term does not contribute at lowest order in slow-roll. To check this, we need s which is

$$s = -\frac{c_{\rm s}'}{c_{\rm s}} = \frac{1-c_{\rm s}^2}{2c_{\rm s}^2}\frac{X'}{X}\,. \tag{5.50}$$

Combining with u' from Eq. (5.27), we have

$$u' = -\frac{1+c_{\rm s}^2}{2c_{\rm s}^2}\frac{X'}{X}u\,, \tag{5.51}$$

and therefore

$$s = \eta\frac{-\epsilon/3}{1-\epsilon/3} = -\frac{4}{3}\mu\epsilon^2\,,\ \frac{X'}{X} = 4(\delta-1)\epsilon c_{\rm s}^2\,. \tag{5.52}$$

The spectral index is then

$$n_{\rm s}-1 = -(2\epsilon+\eta+s) = -(2+4\mu)\epsilon+\frac{8}{3}\mu\epsilon^2\,. \tag{5.53}$$

Retaining only the lowest-order terms in slow-roll, as required for consistency as only those have been included throughout, we have the spectral index $n_{\rm s}$ and r as

$$n_{\rm s}-1 = -\frac{2m+2}{m+2}\frac{1}{N}\,, \tag{5.54}$$

$$r = \frac{8c_{\rm s}}{\mu}\frac{1}{2N} \simeq \frac{8m}{m+2}\frac{1}{N}\,. \tag{5.55}$$

This indicates that the spectral index is always red tilted, $n_{\rm s} < 1$, in Tachyon models. The number of e-folds between observable perturbation generation and the end of inflation, usually taken to be $N \simeq 50$ (Liddle and Leach, 2003). So take an example for quadratic potential where $m = 2$, we will have $n_{\rm s} = 0.97$ and $r = 0.08$ at pivot $N_* = 50$.

5.4.2 DBI inflation models

The DBI action, as already given in Eq. (5.4), is

$$p(\phi, X) = -\frac{1}{f(\phi)}\sqrt{1 - 2f(\phi)X} - V(\phi) \tag{5.56}$$

where the sound speed $c_{\rm s} = \sqrt{1-2f(\phi)X}$ and the warp factor is $f(\phi) = \lambda_s/\phi^4$. If the last term V is zero the model reduces to the Tachyon model with a constant potential, but we are not interested in this case here; instead we are going to discuss a more general case in the following subsections.

Field redefinition To proceed with our investigation using the method of the previous sections, and in view of simplifying the later calculations, we apply a field redefinition $\varphi = 1/\phi$ to the DBI action (5.4). A variant of this technique will also be used in studying the Tachyon model in Section 5.5. However, we will now focus on the current case, where the Lagrangian for DBI inflation with a potential $V = A\phi^m$ becomes

$$\varphi = \frac{1}{\phi},\ W(\varphi) = \frac{1}{\varphi^4},\ \tilde{V}(\varphi) = A\varphi^{4-m} \tag{5.57}$$

$$\mathcal{L} = -W(\varphi)\left(\frac{1}{\lambda_s}\tilde{c}_{\rm s} + \tilde{V}(\varphi)\right),\ \tilde{c}_{\rm s} = \sqrt{1 - 2\lambda_s\tilde{X}}\,, \tag{5.58}$$

The notation $\tilde{X}$ stands for the kinetic term after applying the field redefinition. With this new field definition, the DBI action falls in the class defined by Eq. (5.40).

The energy density ρ is

$$\rho = W(\varphi)\left(\frac{1}{\lambda_s c_{\rm s}} + \tilde{V}(\varphi)\right) = \frac{3}{2}\frac{W}{\lambda_s}\frac{1-c_{\rm s}^2}{c_{\rm s}}u\,. \tag{5.59}$$

We have a sound speed (for later convenience, we use the same notation $c_{\rm s}$ for sound speed instead of $\tilde{c}_{\rm s}$) which is of the same form as for the Tachyon. The above action in Eq. (5.58) will induce an equation of motion,

$$\frac{\ddot{\varphi}}{c_{\rm s}^2} + 3H\dot{\varphi} + \left[\frac{W'}{W}\frac{1}{\lambda_s} + c_{\rm s}\tilde{V}\left(\frac{W'}{W} + \frac{\tilde{V}'}{\tilde{V}}\right)\right] = 0\,, \tag{5.60}$$

Rearranging Eq. (5.60) it can be reformulated as

$$\frac{\ddot{\varphi}}{c_{\rm s}^2} + 3H\dot{\varphi} + \frac{W'}{\lambda_s W}\left[1 + \lambda_s c_{\rm s}\tilde{V}\left(1 + \frac{\tilde{V}'}{\tilde{V}}\frac{W}{W'}\right)\right] = 0\,. \tag{5.61}$$

where the Hubble rate is

$$H^2 = \frac{u}{2}\frac{W}{\lambda_s}\frac{1-c_{\rm s}^2}{c_{\rm s}}\,. \tag{5.62}$$

Also Eq. (5.61) suggests the same form as the Tachyon, if the potential V is constant.

Predictions for the quartic potential

In this section we will consider the quartic potential $V = \lambda\phi^4/4$, which will provide a simple form of differential relation in Eq. (5.39) for $u = 1/\epsilon$ and its first derivative. We can write

$$\rho = \frac{W(\varphi)}{\lambda_s c_{\rm s}}(1+\alpha c_{\rm s}) \quad , \quad \alpha = A\lambda_s = \frac{\lambda_s \lambda}{4} = {\rm const}\,, \tag{5.63}$$

$$\delta = \frac{W_{,\varphi\varphi}W}{W_{,\varphi}^2} - \frac{1}{2} \equiv \frac{3}{4} \quad , \quad \epsilon = \frac{3}{2}\frac{1-c_{\rm s}^2}{1+\alpha c_{\rm s}}\,. \tag{5.64}$$

Unlike the case of Tachyon models, for the quartic potential model in DBI inflation we have a constant δ. We now have the approximate equation for relation (5.23),

$$\frac{2}{u} = \frac{\rho_{,\varphi}\varphi'}{\rho} \equiv \frac{W_{,\varphi}\varphi'}{W} = \frac{p_{,\tilde{X}\varphi}\varphi'}{p_{,\tilde{X}}}\,. \tag{5.65}$$

Also, we can readily solve Eq. (5.65) so that we can write down the power spectrum $\mathcal{P}_\zeta$ and its spectral index $n_{\rm s}$. This is simplified because of the field redefinition, in contrast to the conventional treatment where one could not get a slow-roll solution for $\mathcal{P}_\zeta$ etc. According to Eq. (5.23) and Eqs. (5.61) and (5.65) we have[3]

$$3X = \epsilon\frac{1+\alpha c_{\rm s}}{\lambda_s}\,, \tag{5.66}$$

which then solves φ and the redefined warp factor $W(\varphi)$,

$$W = 64 c_{\rm s}^2 \frac{1}{\epsilon^2}\,. \tag{5.67}$$

Then we have $\mathcal{P}_\zeta$ to be

$$\mathcal{P}_\zeta = \frac{8}{3\pi^2}\frac{1+\alpha c_{\rm s}}{\lambda_s}\frac{1}{\epsilon^3}\,, \tag{5.68}$$

Now we notice that there is another relation for ϵ in Eq. (5.64), so the above expression can be written in another equivalent form,

$$\mathcal{P}_\zeta = \frac{4}{\pi^2}\frac{1-c_{\rm s}^2}{\lambda_s}\frac{1}{\epsilon^4}\,. \tag{5.69}$$

These formulae may be used interchangeably. Considering the two asymptotic limits for the sound speed $c_{\rm s} = 0$ or 1, either of the above leads to the prediction for the power spectrum. In the limit $c_{\rm s} \to 1$, Eq. (5.68) straightforwardly indicates the leading dependence for $\mathcal{P}_\zeta$

[3] One can just expand Eq. (5.64) to obtain this relation, but for consistency of our treatment we present the same procedure as followed in the previous sections.

of order $1/\lambda_s\epsilon^3$; While in the case $c_{\rm s} \to 0$ we may use the second expression for the power spectrum $\mathcal{P}_\zeta$ by Eq. (5.69), also we will find that in this limit it also recovers the usual prediction for the power spectrum $\mathcal{P}_\zeta = 4/\pi^2\lambda_s\epsilon^4$ when the inflaton field moves relativistically in DBI inflation.

We would however like to go further in obtaining the expression for $\mathcal{P}_\zeta$ for the reason that in either of the expressions above, which have two or three small parameters, it remains unclear where the model degeneracies lie. Therefore, as in previous sections, we are going to find an expression for u in terms of e-folds N. To do this, following Eq. (5.39), we obtain a similar equation for u

$$u' = \frac{1}{2}(1+c_{\rm s}^2)\,. \tag{5.70}$$

However, as u is a rational function of $c_{\rm s}$ (see Eq. (5.64)), we will use another approach to obtain the solution for u.

Assembling all of Eqs. (5.16), (5.58), and (5.65), we will have the ODEs below

$$\frac{u'}{u} = -\frac{\tilde{X}'}{2\tilde{X}}\frac{1+c_{\rm s}^2}{c_{\rm s}^2} - \left(\frac{2}{u} - \frac{p_{,\tilde{X}\varphi}\varphi'}{p_{,\tilde{X}}}\right) \tag{5.71}$$

$$\frac{c_{\rm s}'}{c_{\rm s}} = -\frac{1-c_{\rm s}^2}{c_{\rm s}^2}\frac{\tilde{X}'}{2\tilde{X}} = -s\,. \tag{5.72}$$

We turn to investigate the evolution equation (5.72) for the sound speed, whose evolution is very simple due to the field redefinition to φ-field space.

We can solve the relation for $\tilde{X}'/\tilde{X}$ by using Eqs. (5.65), (5.70), and (5.71)

$$\frac{\tilde{X}'}{\tilde{X}} = -\frac{c_{\rm s}^2}{u}\,, \tag{5.73}$$

then we get the evolution equation for sound speed $c_{\rm s}$,

$$c_{\rm s}' = \frac{3}{4}\frac{(1-c_{\rm s}^2)^2}{1+\alpha c_{\rm s}}c_{\rm s}\,. \tag{5.74}$$

The solution is obtained as follows

$$N = \frac{1}{\epsilon} + \frac{2}{3}\left(\ln\frac{c_{\rm s}^2}{1-c_{\rm s}^2} + \frac{\alpha}{2}\ln\frac{1+c_{\rm s}}{1-c_{\rm s}}\right). \tag{5.75}$$

We are interested in the predictions in the different limits of the sound speed $c_{\rm s}^2$, although we cannot explicitly invert the general results.

⋆ *Non-relativistic case*

It is not generally possible to invert the relation for ϵ and the e-folds N since α is an important parameter. Then we will not have the full expression for the scalar power

spectrum. However, in the non-relativistic case the condition $c_{\rm s}^2 \sim 1$ can be applied such that the latter terms are negligible. So we will have the approximate solution for $\epsilon \simeq 1/N$. Then by this relation, we obtain the redefined scalar field φ,

$$W(\varphi) = \tau N^2 \,,\; \tau = 64 c_{\rm s}^2 \,. \tag{5.76}$$

Finally we have the scalar power spectrum by Eq. (5.6) as[4]

$$\mathcal{P}_\zeta \simeq \frac{8}{3\pi^2}\frac{1+\alpha}{\lambda_s} N^3 \propto \left(A + \frac{1}{\lambda_s}\right) N^3 \,. \tag{5.77}$$

Therefore we can obtain the spectral index according to Eq. (5.7)

$$n_{\rm s} - 1 \simeq -\frac{3}{N} \,. \tag{5.78}$$

This relation can also be derived from the differential system. We can evaluate the two small parameters according to Eqs. (5.19), (5.70), and (5.72),

$$\eta = \frac{1+c_{\rm s}^2}{2}\epsilon \,,\; s = -\frac{1-c_{\rm s}^2}{2}\epsilon \,, \tag{5.79}$$

to obtain the spectral index which is then presented as,

$$n_{\rm s} - 1 = -(2\epsilon + \eta + s) = -(2 + c_{\rm s}^2)\epsilon \,, \tag{5.80}$$

in terms of ϵ and $c_{\rm s}$. From Eq. (5.80) we find that for a quartic potential the spectrum is always red tilted, since $2 + c_{\rm s}^2 > 0$ is always satisfied regardless of the warp strength or the mass of the scalar field. Also if the DBI scalar field rolls asymptotically in the manner of a canonical field in which $c_{\rm s}^2 \to 1$, then we have $n_s \to 1 - 3/N_* = 0.94$ at $N_* = 50$. This result is obviously recovered due to the canonical-like inflation with a quartic potential.

One should note that the relation in Eq. (5.80) does *not* require any limit for $c_{\rm s}$. It can also be applied when $c_{\rm s}^2 \ll 1$, but if that is the case we should modify the value for $\epsilon \simeq 2/N$. We will see this below.

⋆ *Relativistic case*

The behaviour of DBI inflaton can be relativistic, which corresponds to the limit

[4] To determine τ, we applied Eq. (5.24). It is a bit tricky to determine the constant τ in this case. This relation is for $c_{\rm s}^2 \to 1$; one should replace $1 - c_{\rm s}^2$ with $(1 + \alpha c_{\rm s})$ via the definition of ϵ. Then one finds this proportionality coefficient is exactly $64 c_{\rm s}^2$.

$c_s^2 \ll 1$. In this case, we can also use the method from this section. Unlike the case of $c_s^2 \to 1$ we only need to approximate $\epsilon \sim 2/N$.[5]

Therefore, according to Eq. (5.7) and Eq. (5.7), we can respectively write down the relation for the redefined scalar field φ, the scalar power spectrum and its spectral index as follows

$$W = \xi N^4 \quad , \quad \xi \simeq \left(\frac{3}{\alpha}\right)^2 , \tag{5.81}$$

$$\mathcal{P}_\zeta = \frac{1}{4\pi^2}\frac{1}{\lambda_s}N^4 , \tag{5.82}$$

$$n_s - 1 = -\frac{4}{N} . \tag{5.83}$$

To derive the proportionality constant in Eq. (5.81), we have used the speed limit relation $\lambda_s\dot{\varphi}^2 \sim 1$. While deriving Eqs. (5.81) and (5.82), we have also applied the relation $\alpha c_s \epsilon \simeq 3/2$ for this relativistic case. These relations can be obtained by inserting $c_s^2 \ll 1$ into Eq. (5.64).

Since we can have slow-roll solutions for ϵ in each case, we can just substitute either solution to the power spectrum into Eq. (5.68) or Eq (5.69). Eventually we will have the predictions as above. We can see both predictions for the power spectrum for DBI inflation with quartic potential are valid. However, the first one (5.68) will reduce to the conventional canonical inflation with quartic potential in the non-relativistic limit, while Eq. (5.69) will give the prediction for it in the relativistic limit.

5.4.3 Comparison to *Planck* constraints

We have studied several models and derived their predictions within the slow-roll approximation. Now we present these predictions by visualising them against the latest constraints on inflation models compiled by the *Planck* collaboration (Ade et al., 2013b). The *Planck*+WP observational data favours a concave potential for viable canonical inflation models and limits the tensor-to-scalar ratio below $r = 0.11$ at 95% confidence. In Figure 5.1 we can see that for canonical inflation models with the polynomial potential $V \propto \phi^m$, the $m = 3, 4$ cases are ruled out by the observational requirements, while potentials with

[5] This relation can be obtained either from Eq. (5.74) by inserting $c_s^2 \to 0$, or using limiting properties for the third term in Eq. (5.75) which is $\log \frac{1+c_s}{1-c_s} \to 2c_s$. In this limit, we will infer another relation for $\alpha c_s \epsilon \simeq 3/2$.

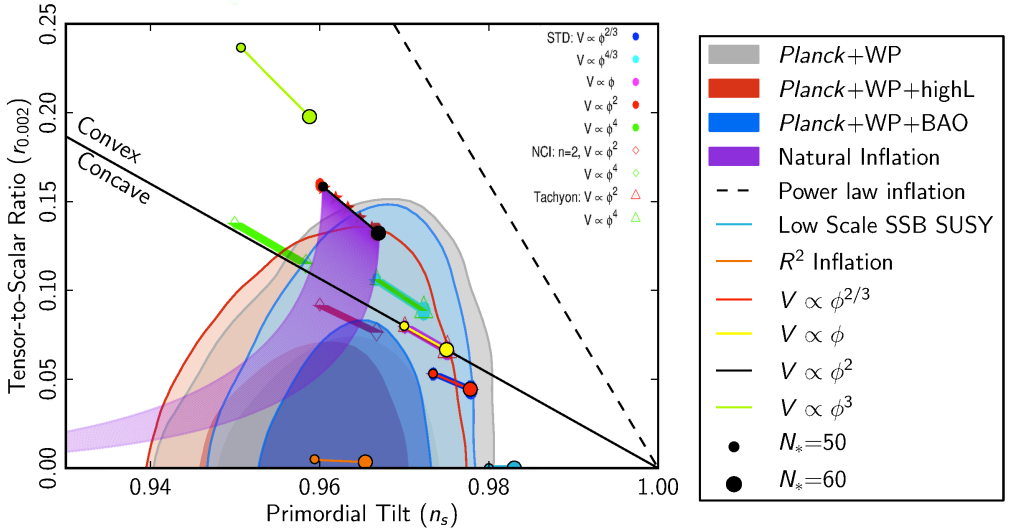

Figure 5.1: Slow-roll predictions for several inflation models alongside constraints from *Planck* and other probes. For $(r\,, n_{\rm s})$ data, we have used Eqs. (5.36, 5.37) for both canonical inflation models ("STD" as labeled in this figure) and $BX^2 - V(\phi)$ models ("NCI: n=2," as labeled in this figure), while Eqs. (5.54, 5.55) for Tachyon models. [Based on an image from Ade et al. (2013b), original image credit ESA/*Planck* Collaboration.]

$m = 2/3,\ 1,\ 4/3$ and 2 are within 95% confidence, though at $N_* = 50$ the quadratic potential ($m = 2$) lies outside the 95% confidence region (Ade et al., 2013b).

This plot shows two of our models. The first is the NCI model where the Lagrangian has the form $\mathcal{L} = BX^2 - V(\phi)$, where both quadratic potential (red diamond) and quartic potential (green diamond) are located within the observationally-permitted region. The second is Tachyon inflation; the figure shows that the quadratic potential (red triangle) is well within the permitted region, while the quartic potential is marginal with only the large e-foldings case $N_* = 60$ lying within the 95% confidence region.

The polynomial potential in NCI-X^2 models and tachyon inflation model can be considered as reshaped by the non-canonical term, and these reshaped potentials can correspond to standard inflation models. In X^2 models the quadratic potential is reshaped to $m \in (2/3, 1)$ and the quartic potential to $m \in (1, 4/3)$. In Tachyon models, the quadratic potential is reshaped to $m = 1$ and the quartic potential to $m = 4/3$. This reshaping in Tachyon models can be found in the following section.

One may infer from the figure that if the inflaton rolls in a polynomial potential $V \propto \phi^m/m$ with higher m, the higher-order kinetic term X^n in NCI models may be supported by current observational datasets such as *Planck* and BAO. These models can potentially

give significant non-gaussianity while satisfying power spectrum constraints, since large non-gaussianity occurs via a small sound speed c_s, which the NCI-X^n models can provide with $c_s^2 = 1/(2n-1)$.

5.5 Implementation Methods for Particular Cases

For some particular models, there may be more direct treatments. For example for Tachyon models, we can take advantage of a field redefinition, along with the assumption $\epsilon \ll 1$ which in turn implies that $c_s \to 1$. This method leads the same prediction as those obtained in Section 5.4, as we show next. For DBI inflation with a quadratic potential, the methods in Section 5.4 require a lot of effort in order to obtain the observables, but initially applying a slow-roll assumption gives results for the model predictions. The following methods can be considered as an implementation of the systematic approach in Section 5.3.

5.5.1 Field redefinition in Tachyon models

A more direct approach to the observables is possible for Tachyon models, as a combination of the slow-roll approximation and a field redefinition allows the theory to be approximated by a canonical Lagrangian. Starting from

$$P(X,\phi) = -V\sqrt{1-2fX}, \tag{5.84}$$

and making the slow-roll assumption $fX \ll 1$, we can approximate it by a different non-canonical model with Lagrangian

$$P(X,\phi) \simeq VfX - V. \tag{5.85}$$

This can be transformed to a canonical action if we can find a new field φ, with corresponding kinetic energy $\tilde{X} = \frac{1}{2}\partial_\mu\varphi\partial^\mu\varphi$, such that $\tilde{X} = VfX$. This can be done in principle for any well-defined potential, though not always analytically. Again focussing on the monomial potential $V(\phi) = A\phi^m$, the required transformation is

$$\varphi = \frac{2\sqrt{Af}}{m+2}\,\phi^{1+m/2}\,, \tag{5.86}$$

so that we have $V(\varphi)$ as,

$$V(\varphi) = \varphi^{\frac{2m}{m+2}}\left(\frac{m+2}{2}A^{\frac{1}{m}}f^{-\frac{1}{2}}\right)^{\frac{2m}{m+2}} \tag{5.87}$$

By completing the above transformation, then the original Lagrangian (5.84) can be re-written within this approximation as

$$P(X,\phi) \to \tilde{P}(\tilde{X},\varphi) = \tilde{X} - \tilde{A}\varphi^{\frac{2m}{m+2}}\,, \tag{5.88}$$

where the normalisation coefficient became

$$\tilde{A} = \left(\frac{m+2}{2}\right)^{\frac{2m}{m+2}} \left(A^{1/m} f^{-1/2}\right)^{\frac{2m}{m+2}}\,, \tag{5.89}$$

The usual results for canonical inflation with $V(\varphi) \propto \varphi^{\alpha}$ then apply, giving a spectral index and tensor–scalar ratio as follows (Liddle and Lyth, 1992)

$$n_{\rm s} - 1 = -\frac{2+\alpha}{2N} = -\frac{2m+2}{m+2}\frac{1}{N} \tag{5.90}$$

$$r = \frac{4\alpha}{N} = \frac{8m}{m+2}\frac{1}{N} \tag{5.91}$$

These match the results we found in Section 5.4.1.

We therefore conclude that, provided our slow-roll assumption holds, a power-law potential in a Tachyon model behaves as if it were a canonical model but with a different power which is smaller (and indeed never bigger than 2). For example, the quadratic potential $m = 2$ rescales to a linear potential $V(\varphi) = 2\sqrt{A/f}\,\varphi$, while the quartic potential $m = 4$ rescales to

$$V(\varphi) = \left(\frac{3A^{1/4}}{\sqrt{f}}\right)^{4/3} \varphi^{4/3}\,, \tag{5.92}$$

The upper limit for the rescaled potential is the quadratic type $V(\varphi) = \hat{A}\varphi^2$, which in canonical inflation is well explored and permitted by present data including that from the *Planck* satellite (Ade et al., 2013b). Consequently, as long as the slow-roll assumption made at the start is valid, we expect this potential to match the observational data for any value of the power-law, unlike in the canonical case.

These results explain the degeneracy between the potential normalization and f found numerically in (Devi et al., 2011) and also confirmed in recent work (Li and Liddle, 2013b). As the spectral index and tensor–scalar ratio match observations, the only parameter tightly constrained by observations is the potential normalization in the φ representation. Hence we predict a perfect degeneracy $A \propto f$ in the quadratic case and $A \propto f^2$ in the quartic case.

We can also now check the validity of the slow-roll assumption made to obtain these solutions. Within the canonical frame, it is well known that the slow-roll approximation $\tilde{X} \ll V(\varphi)$ is valid. Hence $VfX \ll V$, and hence $fX \ll 1$ as required for our original approximation in the Lagrangian. This shows the self-consistency of the slow-roll

approximation we have deployed. Nevertheless, it remains possible that there are other observationally-valid solutions that do not obey the slow-roll condition. In order to investigate this possibility, a numerical analysis is required — see the recent work in (Li and Liddle, 2013b).

5.5.2 DBI inflation with a quadratic potential

We now carry out a similar procedure for DBI inflation with a quadratic potential. According to Eq. (5.60), in which the first term is negligible compared to the second term (see Appendix A), we can obtain an approximate slow-roll equation,

$$3H\dot{\varphi} \simeq -\frac{W'}{W}\frac{1}{\lambda_s}\left(1+\frac{m}{4}\alpha c_s\varphi^{4-m}\right)\,,\ \alpha = A\lambda_s\,. \tag{5.93}$$

With the quadratic potential $\tilde{V} = A\varphi^2$ and the warp factor in form of $W(\varphi)$, the Hubble rate in Eq. (5.62) and the slow-roll equation in Eq. (5.93) for scalar field φ simplifies to

$$3H^2 = \frac{1}{\lambda_s c_{\rm s}\varphi^4}y\,,\ , \tag{5.94}$$

$$3H\dot{\varphi} \simeq \frac{2}{\lambda_s\varphi}(1+y)\,, \tag{5.95}$$

$$y = 1+\alpha c_{\rm s}\varphi^2\,. \tag{5.96}$$

We note that $y > 1$ since $\alpha > 0$ always holds, so we can immediately obtain the parameters δ and ϵ as

$$\delta = \frac{\dot{\varphi}}{H\varphi} = \frac{2}{\alpha}\left(\frac{y+1}{y}\right)(y-1)\,, \tag{5.97}$$

$$\epsilon = \frac{\dot{\varphi}^2}{2}\frac{1}{H^2}\frac{1}{c_{\rm s}\varphi^4} = \frac{2}{\alpha}\left(\frac{y+1}{y}\right)^2(y-1)\,. \tag{5.98}$$

We wish to find the relation between the field φ and the e-folds N via the relation

$$N = -\int H dt = -\int \frac{d\varphi}{\varphi}\frac{1}{\frac{\dot{\varphi}}{H\varphi}} = -\int \frac{d\varphi}{\varphi}\frac{1}{\delta}\,. \tag{5.99}$$

According to Eq. (5.96) we can derive the relation for dy and $d\varphi$ as,

$$\frac{dy}{y-1} = 2\frac{d\varphi}{\varphi}\left(1+\frac{1}{2}\frac{s}{\delta}\right) \sim 2\frac{d\varphi}{\varphi}\,. \tag{5.100}$$

where s is the small parameter defined in Eq. (5.9). To approximate the last term in Eq. (5.100), we have used the relation[6]

$$\frac{s}{2\delta} = \frac{s}{\epsilon}\frac{y+1}{2y} < \frac{s}{\epsilon} \ll 1\,. \tag{5.101}$$

[6]The approximation $s \ll \epsilon$ cannot tell us $c_{\rm s}^2 \sim 1$ even though $s \sim 0$. However, in Appendix B we show that we indeed have $c_{\rm s}^2 \sim \mathcal{O}(1)$ if using the relation (5.100) for approximation.

Now we can obtain N under this approximation. Substituting Eq. (5.97) into Eq. (5.99) and applying Eq. (5.100), we have

$$N = -\frac{\alpha}{4}\int \frac{ydy}{(y-1)^2(y+1)}\,, \tag{5.102}$$

and its solution is,

$$\frac{8N}{\alpha} = \frac{1}{y-1} + \frac{1}{2}\ln\frac{y+1}{y-1}\,, \quad (y>1, c_{\rm s}\simeq 1)\,. \tag{5.103}$$

For the quadratic potential $V\propto\phi^2$ we will recover a relation for $\varphi^{-2}=\phi^2=4N=2mN$ when $y\gg 1$ according to the above equation. This is the slow-roll prediction for the quadratic potential in canonical inflation, where the sound speed is exactly $c_{\rm s}^2=1$, and hence applies if DBI inflation with a quadratic potential is approximated by canonical inflation.

Equation (5.103) is the general relation between the scalar field φ (or ϕ) and N. Note that y can be either of order 1 or much greater, according to the calculation in Appendix B, even when we impose the constraint $c_{\rm s}^2\sim\mathcal{O}(1)$.

We can write the Eq. (5.103) in terms of the Lambert $\mathcal{W}$ function as follows:

$$y = 1+\frac{2}{\theta(x)} = 1+\frac{2}{\mathcal{W}(e^{x+1})-1}, \qquad (\text{at } c_{\rm s}\simeq 1)\,, \tag{5.104}$$

where $x=16N/\alpha$. Therefore we can write the δ and ϵ according to Eqs. (5.97) and (5.98)

$$\delta = \frac{8}{\alpha}\frac{\mathcal{W}}{\mathcal{W}^2-1}\,, \tag{5.105}$$

$$\epsilon = \frac{16}{\alpha}\frac{\mathcal{W}}{\mathcal{W}^2-1}\frac{\mathcal{W}}{\mathcal{W}+1}\,, \tag{5.106}$$

$$N = \frac{\alpha}{16}(1+\mathcal{W}+\ln\mathcal{W})\,. \tag{5.107}$$

They imply $\epsilon\sim 1/N$. We now can treat Eqs. (5.106) and (5.107) as parametric equations for δ, ϵ and $1/N$, respectively, with parameter θ.

By denoting $\beta=(1+1/\mathcal{W})^2$ we can also write

$$\beta = \begin{cases} 1\,, & \mathcal{W}\gg 1 \Longleftrightarrow \alpha\ll 16N \qquad (5.108)\\ 4\,, & \mathcal{W}\to 1 \Longleftrightarrow \alpha\gg 16N \qquad (5.109)\end{cases}$$

Since this quantity (ratio) is monotonically increasing to 4 with α, it will never contribute a term like $1/N$, so we can regard this ratio β as a 'pseudo-constant'. Therefore according to Eqs. (5.106) and (5.107) we represent the parameter θ as

$$\theta = \beta\frac{16}{\alpha\epsilon} \qquad , \qquad \theta\alpha\sim 16\beta N\,. \tag{5.110}$$

where the second relation is approximated by setting $\epsilon \sim 1/N$ for later convenience in discussion. The parameters θ and α, due to the relation in Eq. (5.110), will be treated interchangeably when we discuss the parameter constraints in a later section.

We will use these relations to generalise our conclusions below. So far we have completed the slow-roll calculation for DBI inflation with a quadratic potential. Now we need to evaluate the power spectrum $\mathcal{P}_\zeta$ and its spectral index. According to Eq. (5.6) and the variables which have been derived in Eqs. (5.94), (5.96), (5.105), (5.106) and (5.110), the power spectrum $\mathcal{P}_\zeta$ is written as,

$$\mathcal{P}_\zeta = \frac{1}{48\pi^2}\frac{1}{\epsilon}\frac{\alpha^2}{\lambda_s}\theta\left(1+\frac{\theta}{2}\right) = \frac{1}{96\pi^2}\frac{\alpha^3}{\lambda_s}\frac{(\mathcal{W}^2-1)^2(\mathcal{W}+1)}{W^2}\,, \tag{5.111}$$

where N_* is the e-folds number at the end of the DBI inflation. According to Eq. (5.110), the power spectrum $\mathcal{P}_\zeta$ in Eq. (5.111) provided from the quadratic potential in DBI inflation can also be rewritten in terms of ϵ together with model parameters,

$$\mathcal{P}_\zeta = \frac{1}{3\pi^2}\left(\beta\frac{A}{\epsilon^2} + 8\beta^2\frac{1}{\lambda_s\epsilon^3}\right). \tag{5.112}$$

We can see that the slow-roll prediction for the power spectrum has terms due to the scalar potential denoted by its scale A, and the warp geometry denoted by the strength λ_s. This is a new output from our slow-roll calculation, in comparison to the conventional approach where the first term appears only. Since in that case the model has been always studied at $c_{\rm s} \sim 1$ initially, the DBI action is reduced to the canonical type, which no doubt will only present a limited prediction that is the first term in our generalised equation in Eq. (5.112).

According to Eqs. (5.7) and (5.111), we obtain the spectral index as

$$n_{\rm s} - 1 = -(2\epsilon + \eta)\,. \tag{5.113}$$

The spectral index here is exactly derived from Eq. (5.111). There is no significant contribution from the derivatives of the sound speed, since $c_{\rm s} \sim 1$ or from Eq. (5.101) which tells us that the third parameter s is much less than ϵ. We only need to work out the second parameter η via the result for ϵ, so that,

$$\eta = \frac{\mathcal{W}^2 - \mathcal{W} + 2}{\mathcal{W}^2}\epsilon\,. \tag{5.114}$$

Then by means of Eq. (5.7), we have the result for the spectral index,

$$n_{\rm s} - 1 = -3\epsilon\frac{\mathcal{W}^2 - \mathcal{W}/3 + 2/3}{\mathcal{W}^2}, \quad (\mathcal{W} > 1)\,. \tag{5.115}$$

However, this formula does not give a clear understanding of the spectral index, unlike the one in Eq. (5.113). However, we can check that the relations for the spectral index will

have the same asymptotic behaviour (at $c_{\rm s}\sim 1$)

$$n_{\rm s}-1=\begin{cases}-\dfrac{2}{N_*} & \mathcal{W}\to 1\Longleftrightarrow \alpha\gg 16N\ , \qquad (5.116)\\ -\dfrac{3}{N_*} & \mathcal{W}\gg 1\Longleftrightarrow \alpha\ll 16N\ . \qquad (5.117)\end{cases}$$

where one can derive the ϵ as

$$\epsilon=\begin{cases}\dfrac{1}{2N_*} & \mathcal{W}\to 1\Longleftrightarrow \alpha\gg 16N\ , \qquad (5.118)\\ \dfrac{1}{N_*} & \mathcal{W}\gg 1\Longleftrightarrow \alpha\ll 16N\ . \qquad (5.119)\end{cases}$$

Finally, in terms of $(N,x;\mathcal{W}(e^{1+x}))$, we present both the spectral index $n_{\rm s}$ and the tensor-to-scalar ratio r as,

$$n_{\rm s} = 1-\frac{1}{N}\frac{x}{\mathcal{W}-1}\frac{3\mathcal{W}^2-\mathcal{W}+2}{(\mathcal{W}+1)^2},\quad (\mathcal{W}>1)\,, \qquad (5.120)$$

$$r = \frac{16c_{\rm s}}{N}\frac{x}{\mathcal{W}-1}\frac{\mathcal{W}^2}{(\mathcal{W}+1)^2},\quad (\mathcal{W}>1, c_{\rm s}\sim 1)\,. \qquad (5.121)$$

where $x=16N/\alpha$, and the sound speed can be obtained from $c_{\rm s}^2=1-2\epsilon/[3(\mathcal{W}-1)]$. Since $x>0$ and $\mathcal{W}>1$, the spectral index is always red tilted. We can see that the prediction for both n_s and r are model parameter dependent, in view of $\alpha=M^2\lambda_s/2$. DBI inflation, however, does not provide a simple form for the spectral index n_s and the tensor-to-scalar ratio r as in previous models, where these quantities can be expressed as a function of the variable set (n,m,N). This model has another variable α which can play an important role in determining the value of $n_{\rm s}$ and r.

These results, for the power spectrum in Eq. (5.112) and spectral index in Eq. (5.121), are derived in the non-relativistic limit $c_{\rm s}\sim 1$. Meanwhile, we can evaluate the following relation

$$\frac{23}{24}<\frac{\mathcal{W}^2-\mathcal{W}/3+2/3}{\mathcal{W}^2}<\frac{4}{3}\qquad (\mathcal{W}>1)\,, \qquad (5.122)$$

which appeared in Eq. (5.115). Therefore we will have a leading contribution for the spectral index $n_{\rm s}-1=\mathcal{O}(\epsilon)$ when the DBI inflaton field moves with $c_{\rm s}\sim 1$.

Figure 5.2 shows the predictions against data. We see that for any available model parameter α DBI inflation has difficulties in providing the required observables, as the results lie above the $m=2$ canonical model which is coming under observational pressure, particularly with $N_*=50$. But for larger pivot e-folds, for example $N_*=60$, the DBI model with this quadratic potential has the possibility to match observations. Note incidentally that our predictions meet those of natural inflation (the purple shaded region), which approach the canonical quadratic case from below.

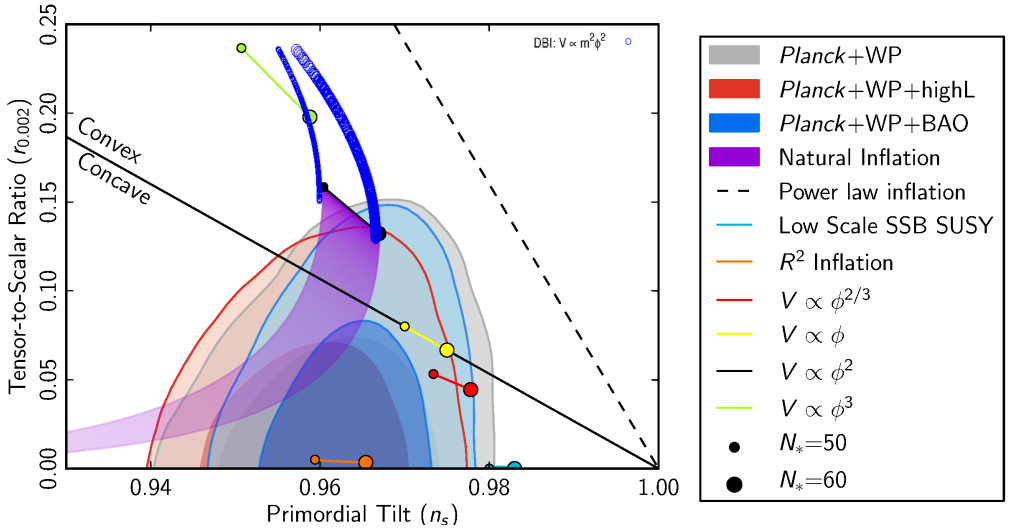

Figure 5.2: Slow-roll predictions for the DBI inflation with quadratic potential and the *Planck* constraints on inflation models. For $(r\,, n_{\rm s})$ data, we have used Eqs. (5.120, 5.121) for this plot. [Based on an image from Ade et al. (2013b), original image credit ESA/*Planck* Collaboration.]

Our result is different from the result that $n_{\rm s}-1=\mathcal{O}(\epsilon^2)$ in work by Alishahiha et al. (2004). The difference between these results is that ours is in the $c_{\rm s}\to 1$ limit, while theirs applies in the warp-factor dominated regime of $c_{\rm s}\to 0$, a limit in which we are able to reproduce their result. To show this we start with the the Hubble parameter H^2 and the sound speed $c_{\rm s}^2$ given by

$$3H^2=\frac{1}{\varphi^4}\frac{y}{\lambda_s c_{\rm s}}\quad,\quad \epsilon=\frac{3}{2}\frac{1-c_{\rm s}^2}{y}\,. \tag{5.123}$$

So at $c_{\rm s}\to 0$, which also means $y\gg 1$ if we focus on $\epsilon\ll 1$, according to Eq. (5.98) we have the following approximate relations

$$3H^2\simeq\frac{3}{2\lambda_s\epsilon}\frac{1}{c_{\rm s}\varphi^4}\quad,\quad \epsilon\simeq\frac{3}{2}\frac{1}{y}\quad,\quad \alpha=\frac{3}{\epsilon^2}\,. \tag{5.124}$$

Therefore, according to Eqs. (5.6) and (5.7) we have

$$\mathcal{P}_\zeta = \frac{1}{16\pi^2}\frac{1}{\lambda_s\epsilon^2}\frac{1}{c_{\rm s}^2\varphi^4}=\frac{1}{16\pi^2}\frac{1}{\lambda_s\epsilon^2}\frac{\alpha^2}{(y-1)^2}\,, \tag{5.125}$$

$$n_{\rm s}-1 = -\left(-2\frac{\epsilon'}{\epsilon}-2\frac{y'}{y-1}\right)=2\frac{y'}{y}\frac{1}{y-1}\,. \tag{5.126}$$

Using the relation in Eq. (5.124), we can simplify them to be

$$\mathcal{P}_\zeta = \frac{1}{4\pi^2}\frac{1}{\lambda_s\epsilon^4}\,, \tag{5.127}$$

$$n_{\rm s}-1 = \frac{4}{3}\epsilon\eta\propto\mathcal{O}(\epsilon^2)\,. \tag{5.128}$$

θ or α	$\frac{1}{N_*}$	$\epsilon(\theta)$	$\epsilon(N_*)$	$\mathcal{P}_\zeta(\epsilon)$	$\mathcal{P}_\zeta(N_*)$	$n_\mathrm{s}-1$	**Domination**
$\theta \to 0$ or $\alpha \gg 16N_*$	$\frac{8}{\alpha\theta}$	$\frac{4}{\alpha\theta}$	$\frac{1}{2N_*}$	$\frac{A}{\epsilon^2}$	$\propto AN_*^2$	$-\frac{4}{2N_*}$	**Scalar Potential**
$\theta \gg 1$ or $\alpha \ll 16N_*$	$\frac{16}{\alpha\theta}$	$\frac{16}{\alpha\theta}$	$\frac{1}{N_*}$	$\frac{1}{\lambda_s\epsilon^3}$	$\propto \frac{N_*^3}{\lambda_s}$	$-\frac{6}{2N_*}$	**Warp Geometry**

Table 5.1: Predictions for the observables in DBI inflation with a quadratic potential, in each limit for θ. At other values of θ, the outcome is determined by both the scalar potential and the warp geometry (see Eq. (5.111) or Eq. (5.112)). These results are obtained under the assumption in Eq. (5.100), which requires the sound speed $c_\mathrm{s}^2 \sim \mathcal{O}(1)$. Also note that $\theta = \mathcal{W} - 1$.

since ϵ, $\eta = -\epsilon'/\epsilon = y'/y$ are of the same order. As this regime predicts that $n_\mathrm{s} - 1$ is very close to one, it is under strong pressure from observations.

To summarise our results in the slow-roll approximation, we obtained formulae for the power spectrum $\mathcal{P}_\zeta$ in Eq. (5.111) or (5.112) and its spectral index n_s in Eq. (5.113). We present all the relations in each limit in Table 5.1.

Finally, it is worth mentioning that we can also make predictions for the case where the sound speed $c_\mathrm{s}^2 \ll 1$ in the same manner that we have just applied. We can obtain the solution in this relativistic case, but the relation $\epsilon = \epsilon(N)$ is not obviously applicable from the e-folds $2/(y^2-1) \propto \mathcal{W}(N)$ which, according to Eq. (B.20), can be obtained from Eq. (5.99).

5.6 Model Parameter Estimation

We now discuss parameter estimation for the models investigated in the previous sections. Throughout this paper, the potential considered possesses only one free parameter. Since the amplitude of the scalar power spectrum is accurately determined to be about 2.5×10^{-9} from observational data, we can now estimate the model parameters for each case, for example taking the pivot e-folds to be $N_* = 50$.

5.6.1 Sum-separable models

We take the expression of the scalar power spectrum from Eq. (5.35) and apply a (base 10) logarithm, giving

$$\log A = \frac{m}{2n}\left[\log B - \frac{6.53 + (1+\frac{m}{\beta})\log N + \log(\frac{\beta}{m}\sqrt{2n-1})}{\frac{m}{\beta}\frac{1}{2n-1}} - \log\left(\frac{m6^{n-1}}{n}\beta^{2n-1}\right)\right] \tag{5.129}$$

where the value -6.53 is derived from $\log_{10}(12\pi^2 \times 2.5 \times 10^{-9})$. Note that the model parameter A denotes the amplitude appearing in the potential $V(\phi) = A\phi^m = \lambda_p\phi^m/m$ after the coefficient of the kinetic term has been rescaled to unity. For example, for the quadratic potential $A = M^2/2$ where M^2 is the mass of field, while for the quartic potential $A = \lambda/4$.

As an application of this formula, we consider the canonical inflation cases where $n = 1$ and $m = 2, 4$. Then we will obtain an estimate for the mass scale for the quadratic and quartic potential respectively. Then

$$\log M^2 \simeq -10.2\,, \tag{5.130}$$

$$\log\lambda \simeq -12.5\,. \tag{5.131}$$

For NCI models, a similar analysis can be performed.

5.6.2 Tachyon models

For the Tachyon model, we consider the results in Section 5.4.1. From Eq. (5.49) we find the relation between A and λ_s to be

$$\log\lambda_s = \frac{2}{m}\log A + 2(\mathbf{A}+\mathbf{B}+\mathbf{C}) + (1+2\mu)\log(2N) \tag{5.132}$$

$$\mathbf{A} = -\mu\log(12\pi^2 \times 2.5 \times 10^{-9}) = 6.53\mu,\ \mathbf{B} = \log m + \left(\frac{1}{2}+\mu\right)\log\mu,\ \mathbf{C} = -\frac{1}{m}\log c_{\rm s}\,.$$

The equation for $\mathbf{C} \sim 0$ above is approximate due to the condition $1/3 < c_{\rm s} < 1$, and particularly $c_{\rm s} \sim 1$ if $\epsilon \ll 1$. Therefore, for the quadratic potential $A = M^2/2\,, m = 2\,, \mu = 1$, we can evaluate the parameters as,

$$\log\lambda_s = \log\frac{M^2}{2} + 19 + 2\log 2 \simeq \log M^2 + 19.3\,, \tag{5.133}$$

For the quartic potential, $A = \lambda/4\,, m = 4\,, \mu = 3/4$, the parameters are

$$\log\lambda_s = \frac{1}{2}\log\frac{\lambda}{4} + 18.2 \simeq \frac{1}{2}\log\lambda + 17.9\,. \tag{5.134}$$

These results are supported by our numerical analysis in (Li and Liddle, 2013b).

5.6.3 DBI models

Quadratic potential We only study the parameter estimation for the case of $c_{\rm s}^2 \sim 1$, as in Section 5.5.2, as otherwise that it is hard to find the required function $\epsilon = \epsilon(N)$. For this reason, for the quadratic potential we present the results in the *non-relativistic case* only.

According to the results in Section 5.5.2, though the formulae for the power spectrum are complicated, we can still approximate the value for α which encodes the scale of the potential (A) and the strength of the warped geometry (λ_s). According to Eq. (5.111), the combined contribution from these indicates that

$$\theta \sim 2 \quad \text{or} \quad \alpha \gtrsim 8N\,. \tag{5.135}$$

Taking the logarithm of this relation (5.135) at the pivot scale $N_* = 50$ we have the linear equation

$$l \equiv \log M^2 + \log \lambda_s \simeq 2.9\,. \tag{5.136}$$

The relation in Eq. (5.135) gives us two possibilities for the locations or choices for the model parameters $A\,, \lambda_s$ at some critical value such as $\alpha \sim 8N_*$. We will see according to Eq. (5.136) and Eq. (5.62) that larger α implies a strong contribution from the scalar field potential. In the other case, α smaller than the critical $8N_*$, inflation will be dominated by the warped geometry.

Recalling Table 5.1, we already have the relation between θ and e-folds N. Therefore we can approximate the model parameter range, as presented in Table 5.2. This table also indicates the value $\log m^2 + \log \lambda_s \sim 3$ (or similar) should be found in parameter space; a similar result is found numerically in (Li and Liddle, 2013b). Above this critical value DBI inflation will be dominated by the scalar field potential, while on the other side the warp geometry will dominate.

Quartic potential The power spectrum was obtained in Section 5.4.2. Following the discussion there, we can approximate the prediction for model parameters at the $N_* = 50$. We note that in this case, although we can still constrain model parameters by requiring the correct amplitude of density perturbations at the pivot scale, the models typically do not lie in the within the 95% confidence region of the $n_{\rm s}$–r plane.

α	$\log M^2 + \log \lambda_s$	**Domination**
$\alpha \gg 8N_*$	> 2.9	**Scalar Potential**
$\alpha \ll 8N_*$	< 2.9	**Warp Geometry**

Table 5.2: Constraints on the model parameters in DBI inflation with quadratic potential. The model parameters, A and λ_s, are correlated along the line $l := \log M^2 + \log \lambda_s$. The parameter $\alpha = A\lambda_s = M^2\lambda_s/2$, where M^2 is the mass scale of the scalar potential and λ_s the strength of the warp factor.

⋆ *Non-relativistic case*

According to Eq. (5.77) in the non-relativistic limit where $c_{\rm s} \sim 1$

$$\log \lambda_s - \log(1+\alpha) \simeq 13.1\,, \tag{5.137}$$

for the parameter correlation. We can estimate the bound for each parameter with different α. If $\alpha \ll 1$ then we can expect the low bound value for the strength λ_s for warp factor,

$$\log \lambda_s \gtrsim 13.2\,, \tag{5.138}$$

while in the limit $\alpha \gg 1$, we will have the upper bound for strength λ of the scalar potential,

$$\log \lambda < -13.1 + \log 4 \simeq -12.5\,. \tag{5.139}$$

This is the observational value for canonical inflation with a quartic potential.

⋆ *Relativistic case*

Similarly we consider the case $c_{\rm s} \ll 1$ from Eq. (5.82), obtaining

$$\log \lambda_s \simeq 13.8\,. \tag{5.140}$$

Hence to have relativistic motion during inflation, the strength of the warp geometry must take this value. We cannot see a relation for the parameter A for the potential if we just consider the power spectrum in Eq. (5.82), but if we recall the footnote in Section 5.4.2 when deriving Eq. (5.82), we have an asymptotic condition relevant to both parameters A and λ_s:

$$\alpha\epsilon c_{\rm s} \sim 1.5\,, \tag{5.141}$$

where $\epsilon = 2/N$ in the relativistic case. So the asymptotic relation between λ and λ_s is

$$\log \lambda_s + \log \lambda \sim \log \frac{3N_*}{c_{\rm s}} \simeq 2.2 - \log c_{\rm s}\,. \tag{5.142}$$

We can evaluate this equation at some values of c_s. For example, for $c_s \sim 0.01$, which is of the same order as ϵ, we will have $\log \lambda_s + \log \lambda \sim 4.2$.

All these parameter estimation cases have also been examined using MCMC methods, and the results from our CosmoMC (Lewis and Bridle, 2002) exploration are presented in our companion paper II.

5.7 Conclusions

In this chapter we have developed and applied a systematic method for deriving observational predictions in non-canonical single-field inflation models, using the slow-roll approximation encoded as a differential equation for $u = 1/\epsilon$ rather than as a set of slow-roll parameters. We have given explicit calculations for several such models, including the tachyon and DBI cases, deriving observables such as the power spectrum $\mathcal{P}_\zeta$ and its spectral index n_s in terms of e-folds N. For some models we also present the results in terms of slow-varying parameters rather than N, when we are unable to explicitly solve the transcendental equation for ϵ and c_s, for example in DBI inflation with quartic potential.

The use of field redefinition is another key methodology in this chapter. It can simplify the process of finding the solution for u, and in terms of the redefined scalar field the reshaped potential can reveal the degeneracy of model parameters which includes both the strength of the kinetic energy and the strength of the potential energy. By this method, in Tachyon models we have obtained an explicit correlation of f and λ which has previously been found only via numerical calculation. For the DBI inflation models, we have also obtained for the first time a similar formula describing the correlations between its two model parameters, though they are not as explicit as the relation in the Tachyon model.

While this method cannot give a full exact solution, as obtained either via non-slow-roll approaches or by numerical exploration, it can nevertheless offer some advantages for modelling inflationary cosmology. For one thing it may suggest to reconstruct the Lagrangian which will potentially give an explicitly solvable relation for $c_s^2 = c_s^2(u)$. For another, it can provide a quick parameter estimation since the power spectrum, which is accurately determined from the observational data, is also formulated via slow-varying parameters. In other words, given the Lagrangian or potential, by finding the $p_{,X\varphi}$ and then the variable u, we can solve the power spectrum by Eq. (5.6) which constrains the

model parameters for the considered model. For some classes of inflation model, this process will be quite straightforward, such as the sum-separable class where $p_{,X\varphi} = 0$ and the product-separable class where $p_{,X\varphi}\varphi'/p_{,X} = -2/u$.

For DBI inflation models with different potentials, we adopted different approaches due to their individual complexities. The DBI inflation with a quadratic potential, if not immediately using limiting cases of c_s, is the least tractable model in the current paper. However we still found predictions for this case, though we have only presented in detail the non-relativistic predictions for this potential. Additionally, in the relativistic case we have obtained predictions matching those derived in the conventional manner using the field speed limit $c_s = 0$ (Alishahiha et al., 2004). Due to the irreversible relation for $\epsilon = \epsilon(N)$ from the e-folds integration $2/(y^2 - 1) = \mathcal{W}(N)$ we have not presented the details, but they can readily be computed if one is interested in the application of the method. The case of DBI inflation with a quartic potential is examined in both the non-relativistic and relativistic cases. For both models, not only do we recover the same results as conventional treatments, but our analysis gives a novel formula for the power spectrum, Eq. (5.112).

The proposed approach is not only able to address monomial potentials, but can also be applied to models with other potentials. For future applications, reconstruction of the inflation model will be an important direction. For the models we have described in this chapter, we hope the method will be useful in that more general context.

A benefit of considering non-canonical Lagrangians is that model predictions can be in better agreement with current data than the canonical case, where even the quadratic potential is starting to come under pressure. We have affirmed previous results (Li and Liddle, 2012; Unnikrishnan et al., 2012) showing that the non-canonical X^n models give predictions that, for a given potential, are in better agreement with data. In this article we have extended that conclusion to the Tachyon models, most explicitly via the field redefinition approach which shows that under slow-roll they are equivalent to canonical models with reshaped potentials of shallower slope, as favoured by the data. For DBI models the situation is less promising; with a quadratic potential the predictions in the non-relativistic limit, seen in Fig. 5.2, are further from scale-invariance than the canonical case, while in the relativistic limit the cancellation of the leading-order slow-roll correction noted in (Alishahiha et al., 2004) places the model too close to scale-invariance. In the quartic case the situation is even less promising. We conclude therefore that DBI models with simple potentials are in significant tension with current data.

· Chapter 6 ·

Discussion and Conclusions

The main goal in this work was to use the current observational data, the WMAP7 year data at the time of documenting this thesis, to constrain several different cosmological models. By both theoretical calculation and developing a numerical code, KMC, we can formulate the degeneracy relation and constrain parameter spaces for the considered non-canonical inflationary (NCI) models.

Part I outlined the essential knowledge in study of the modern cosmology in Chapter 1 and 2. They presented and evidenced that the observed universe is spatially flat, with small anisotropies which are almost Gaussian distributed. The hot topics at the contemporary research frontier are also listed with basic informative sections.

Part II investigated the two topics of the work. The first is the generation of the primordial density perturbations. Chapter 3 addressed one possible mechanism from the scheme of inhomogeneous reheating with a DBI scalar field.

From Chapter 4 to 5, this work also delivered the observational constraints with WMAP data, as of the writing the WMAP 7 data, for a series of NCI models. Chapter 4 focuses on NCI models whose Lagrangian are of polynomial kinetic energy form, and shows that a higher order of X such as X^2, can benefit the predictions for the power spectrum and its spectral index. Under the investigation by MCMC exploration, the parameter space for this model is not well constrained. This suggests the model with high order of linear kinetic X will possess higher degeneracy between model parameters, which cannot be precisely discriminated in light of WMAP 7 data.

Both the Tachyon models and the DBI inflation models are discussed in Chapter 5 through analytical derivation, by means of combining the proposed two methods. One is the *Field Redefinition* which simplifies the analytic calculations, and the other the recursive derivative of the variable $u = 1/\epsilon$ w.r.t. e-folds N which can finally reveal the relation of the observables in terms of e-folds, As such we can have a better understanding of the

predictions in terms of the e-folds which measures the sufficiency of a viable inflation. By using the *Lambert $\mathcal{W}$ function*, not only is the consistency of the prediction for the scalar power spectrum and its index confirmed, but this novel analysis can give a new form of the power spectrum $\mathcal{P}_\zeta$ for the DBI inflation model when the DBI scalar field rolls along the quadratic potential.

Besides the individual conclusion in each Chapters, we can confidently conclude that the presence of the non-canonical kinetic energy form will likely improve the model predictions, and provide a strong attraction to construct effective inflationary models. In light of the high accuracy of the observational data, the NCI models may play an essential and lasting role in explaining both the origin of the primordial density perturbations and the CMB power spectrum and its index.

Further, we have found that large non-Gaussianity (NG) can be generated only through small sound speed c_s. In this thesis I have not calculated the NG for DBI models. However, according to the Planck team (Ade et al., 2013d), the constraint on $f_{nl} = 11 \pm 69$ at 68% for DBI inflation requires $c_\mathrm{s} \geq 0.07$ at 95% (CL). This implies the possible interest of further investigation of DBI inflation in the relativistic limit.

Bibliography

Adams, F. C. and Freese, K. (1991). Double field inflation. *Phys.Rev.*, D43:353–361. 19

Ade, P. et al. (2013a). Planck 2013 results. XVI. Cosmological parameters. *arXiv:1303.5076*. 17

Ade, P. et al. (2013b). Planck 2013 results. XXII. Constraints on inflation. *arXiv:1303.5082*. 20, 62, 77, 78, 80, 85

Ade, P. et al. (2013c). Planck 2013 results. XXIII. Isotropy and Statistics of the CMB. *arXiv:1303.5083*. 7

Ade, P. et al. (2013d). Planck 2013 Results. XXIV. Constraints on primordial non-Gaussianity. *arXiv:1303.5084*. 20

Adshead, P. and Easther, R. (2008). Constraining Inflation. *JCAP*, 0810:047. 18, 42

Adshead, P., Hu, W., and Miranda, V. (2013). Bispectrum in Single-Field Inflation Beyond Slow-Roll. *Phys.Rev.*, D88:023507. 63

Affleck, I. and Dine, M. (1985). A new mechanism for baryogenesis. *Nuclear Physics B*, 249:361–380. 10

Agarwal, N. and Bean, R. (2009). Cosmological constraints on general, single field inflation. *Phys.Rev.*, D79:023503. 42

Alabidi, L. and Lyth, D. H. (2006). Inflation models and observation. *JCAP*, 0605:016. 42

Alabidi, L., Malik, K., Byrnes, C. T., and Choi, K.-Y. (2010). How the curvaton scenario, modulated reheating and an inhomogeneous end of inflation are related. *JCAP*, 1011:037. 40

Albrecht, A. and Steinhardt, P. J. (1982). Cosmology for Grand Unified Theories with Radiatively Induced Symmetry Breaking. *Phys.Rev.Lett.*, 48:1220–1223. 13

Alishahiha, M., Silverstein, E., and Tong, D. (2004). DBI in the sky. *Phys.Rev.*, D70:123505. 19, 20, 32, 64, 85, 91

Amendola, L. (2000). Coupled quintessence. *Phys.Rev.*, D62:043511. 11

Arkani-Hamed, N., Creminelli, P., Mukohyama, S., and Zaldarriaga, M. (2004). Ghost inflation. *JCAP*, 0404:001. 19

Armendariz-Picon, C., Damour, T., and Mukhanov, V. F. (1999). k - inflation. *Phys.Lett.*, B458:209–218. 17, 18, 20, 43, 63, 65, 66

Armendariz-Picon, C., Mukhanov, V. F., and Steinhardt, P. J. (2001). Essentials of k essence. *Phys.Rev.*, D63:103510. 11

Arroja, F., Mizuno, S., and Koyama, K. (2008). Non-gaussianity from the bispectrum in general multiple field inflation. *JCAP*, 0808:015. 32

Bachas, C. (1996). D-brane dynamics. *Phys.Lett.*, B374:37–42. 20

Barnaby, N., Burgess, C., and Cline, J. M. (2005). Warped reheating in brane-antibrane inflation. *JCAP*, 0504:007. 40

Bartolo, N., Komatsu, E., Matarrese, S., and Riotto, A. (2004). Non-Gaussianity from inflation: Theory and observations. *Phys.Rept.*, 402:103–266. 34, 35

Battefeld, T. (2008). Modulated Perturbations from Instant Preheating after new Ekpyrosis. *Phys.Rev.*, D77:063503. 31, 32

Bean, R., Chen, X., Peiris, H., and Xu, J. (2008). Comparing Infrared Dirac-Born-Infeld Brane Inflation to Observations. *Phys.Rev.*, D77:023527. 64

Becker, M., Leblond, L., and Shandera, S. E. (2007). Inflation from wrapped branes. *Phys.Rev.*, D76:123516. 40

Berera, A. and Fang, L.-Z. (1995). Thermally induced density perturbations in the inflation era. *Phys.Rev.Lett.*, 74:1912–1915. 18

Beringer, J. et al. (Particle Data Group), (2012). Review of particle physics. *Phys. Rev. D*, 86:010001. 13

Bertschinger, E. and Zukin, P. (2008). Distinguishing Modified Gravity from Dark Energy. *Phys.Rev.*, D78:024015. 11

Bonometto, S. Gorini, V. and Moschella, U. (2002). *Modern Cosmology*. Bristol : Institute of Physics. 13

Boubekeur, L. and Lyth, D. (2005). Hilltop inflation. *JCAP*, 0507:010. 19

Boucenna, S. and Morisi, S. (2013). Theories relating baryon asymmetry and dark matter: A mini review. *arXiv:1310.1904*. 10

Brandenberger, R. H. (2006). Moduli stabilization in string gas cosmology. *Prog.Theor.Phys.Suppl.*, 163:358–372. 11

Bridges, M., Lasenby, A., and Hobson, M. (2006). WMAP 3-year primordial power spectrum. *Mon.Not.Roy.Astron.Soc.* 27

Burrage, C., de Rham, C., Seery, D., and Tolley, A. J. (2011a). Galileon inflation. *JCAP*, 1101:014. 19, 63

Burrage, C., Ribeiro, R. H., and Seery, D. (2011b). Large slow-roll corrections to the bispectrum of noncanonical inflation. *JCAP*, 1107:032. 63

Cai, Y.-F., Li, S., and Piao, Y.-S. (2009). DBI-Curvaton. *Phys.Lett.*, B671:423–427. 33, 34, 38, 40

Cai, Y.-F. and Wang, Y. (2010). Large Nonlocal Non-Gaussianity from a Curvaton Brane. *Phys.Rev.*, D82:123501. 35

Cai, Y.-F. and Xia, H.-Y. (2009). Inflation with multiple sound speeds: a model of multiple DBI type actions and non-Gaussianities. *Phys.Lett.*, B677:226–234. 35

Cai, Y.-F. and Xue, W. (2009). N-flation from multiple DBI type actions. *Phys.Lett.*, B680:395–398. 35

Challinor, A. (2012). CMB anisotropy science: a review. *arXiv:1210.6008*. 7

Chen, X. (2005). Inflation from warped space. *JHEP*, 0508:045. 40

Chen, X., Huang, M.-x., Kachru, S., and Shiu, G. (2007). Observational signatures and non-Gaussianities of general single field inflation. *JCAP*, 0701:002. 32

Chialva, D., Shiu, G., and Underwood, B. (2006). Warped reheating in multi-throat brane inflation. *JHEP*, 0601:014. 40

Choe, J., Gong, J.-O., and Stewart, E. D. (2004). Second order general slow-roll power spectrum. *JCAP*, 0407:012. 63

Christensen, N. and Meyer, R. (2000). Bayesian methods for cosmological parameter estimation from cosmic microwave background measurements. *arXiv:astro-ph/0006401*. 27

Christensen, N., Meyer, R., Knox, L., and Luey, B. (2001). II. Bayesian methods for cosmological parameter estimation from cosmic microwave background measurements. *Class.Quant.Grav.*, 18:2677. 27

Dark Energy Survey (2012). http://www.darkenergysurvey.org/. 12

Davis, M., Efstathiou, G., Frenk, C. S., and White, S. D. (1985). The Evolution of Large Scale Structure in a Universe Dominated by Cold Dark Matter. *Astrophys.J.*, 292:371–394. 11

Devi, N. C., Nautiyal, A., and Sen, A. A. (2011). WMAP Constraints On K-Inflation. *Phys.Rev.*, D84:103504. 43, 52, 63, 80

Dimopoulos, K. and Lyth, D. H. (2004). Models of inflation liberated by the curvaton hypothesis. *Phys.Rev.*, D69:123509. 31

Dimopoulos, S., Kachru, S., McGreevy, J., and Wacker, J. G. (2008). N-flation. *JCAP*, 0808:003. 19

Dine, M. and Kusenko, A. (2003). The Origin of the matter - antimatter asymmetry. *Rev.Mod.Phys.*, 76:1. 10

Dodelson, S., Kinney, W. H., and Kolb, E. W. (1997). Cosmic microwave background measurements can discriminate among inflation models. *Phys.Rev.*, D56:3207–3215. 42

Douglas, M. R., Kabat, D. N., Pouliot, P., and Shenker, S. H. (1997). D-branes and short distances in string theory. *Nucl.Phys.*, B485:85–127. 20

Dunkley, J., Bucher, M., Ferreira, P. G., Moodley, K., and Skordis, C. (2005). Fast and reliable mcmc for cosmological parameter estimation. *Mon.Not.Roy.Astron.Soc.*, 356:925–936. 27

Dunkley, J. et al. (2009). Five-Year Wilkinson Microwave Anisotropy Probe (WMAP) Observations: Likelihoods and Parameters from the WMAP data. *Astrophys.J.Suppl.*, 180:306–329. 42

Dvali, G., Gruzinov, A., and Zaldarriaga, M. (2004a). A new mechanism for generating density perturbations from inflation. *Phys.Rev.*, D69:023505. 17, 31, 32, 33, 34, 36, 37

Dvali, G., Gruzinov, A., and Zaldarriaga, M. (2004b). Cosmological perturbations from inhomogeneous reheating, freezeout, and mass domination. *Phys.Rev.*, D69:083505. 17, 31, 32, 34, 35

Easson, D. A., Gregory, R., Mota, D. F., Tasinato, G., and Zavala, I. (2008). Spinflation. *JCAP*, 0802:010. 32

Easson, D. A., Gregory, R., Tasinato, G., and Zavala, I. (2007). Cycling in the Throat. *JHEP*, 0704:026. 32

Easson, D. A. and Powell, B. A. (2011). Optimizing future experimental probes of inflation. *Phys.Rev.*, D83:043502. 26

Easson, D. A. and Powell, B. A. (2013). The Degeneracy Problem in Non-Canonical Inflation. *JCAP*, 1303:028. 26

Easther, R. and Kinney, W. H. (2003). Monte Carlo reconstruction of the inflationary potential. *Phys.Rev.*, D67:043511. 18

Easther, R. and Peiris, H. V. (2012). Bayesian Analysis of Inflation II: Model Selection and Constraints on Reheating. *Phys.Rev.*, D85:103533. 52

Enqvist, K. and Sloth, M. S. (2002). Adiabatic CMB perturbations in pre - big bang string cosmology. *Nucl.Phys.*, B626:395–409. 17, 31

Euclid (2013). Euclid project: `http://sci.esa.int/euclid/`. 12

Exirifard, Q. (2011). Phenomenological covariant approach to gravity. *Gen.Rel.Grav.*, 43:93–106. 11

Fairbairn, M. and Tytgat, M. H. (2002). Inflation from a tachyon fluid? *Phys.Lett.*, B546:1–7. 64

Feroz, F., Hobson, M., and Bridges, M. (2009). MultiNest: an efficient and robust Bayesian inference tool for cosmology and particle physics. *Mon.Not.Roy.Astron.Soc.*, 398:1601–1614. 27

Finelli, F., Hamann, J., Leach, S. M., and Lesgourgues, J. (2010). Single-field inflation constraints from CMB and SDSS data. *JCAP*, 1004:011. 52

Freese, K., Frieman, J. A., and Olinto, A. V. (1990). Natural inflation with pseudo - Nambu-Goldstone bosons. *Phys.Rev.Lett.*, 65:3233–3236. 18

Garcia-Bellido, J. and Wands, D. (1996). Metric perturbations in two field inflation. *Phys.Rev.*, D53:5437–5445. 19

Garriga, J. and Mukhanov, V. F. (1999). Perturbations in k-inflation. *Phys.Lett.*, B458:219–225. 16, 17, 20, 43, 44, 45, 63, 65, 66

Gibbons, G. W. (2002). Cosmological evolution of the rolling tachyon. *Phys.Lett.*, B537:1–4. 64

Gmeiner, F. and White, C. D. (2008). DBI Inflation using a One-Parameter Family of Throat Geometries. *JCAP*, 0802:012. 32

Gong, J.-O. and Stewart, E. D. (2001). The Density perturbation power spectrum to second order corrections in the slow roll expansion. *Phys.Lett.*, B510:1–9. 62

Gong, J.-O. and Stewart, E. D. (2002). The Power spectrum for a multicomponent inflaton to second order corrections in the slow roll expansion. *Phys.Lett.*, B538:213–222. 62

Gordon, C. and Malik, K. A. (2004). WMAP, neutrino degeneracy and non-Gaussianity constraints on isocurvature perturbations in the curvaton model of inflation. *Phys.Rev.*, D69:063508. 26

Gordon, C. and Trotta, R. (2007). Bayesian Calibrated Significance Levels Applied to the Spectral Tilt and Hemispherical Asymmetry. *Mon.Not.Roy.Astron.Soc.*, 382:1859–1863. 27

Greene, B. R. and Levin, J. (2007). Dark Energy and Stabilization of Extra Dimensions. *JHEP*, 0711:096. 11

Grivell, I. J. and Liddle, A. R. (1996). Accurate determination of inflationary perturbations. *Phys.Rev.*, D54:7191–7198. 52

Guo, Z.-K. and Ohta, N. (2008). Cosmological Evolution of Dirac-Born-Infeld Field. *JCAP*, 0804:035. 32

Guo, Z.-K., Piao, Y.-S., Cai, R.-G., and Zhang, Y.-Z. (2003). Inflationary attractor from tachyonic matter. *Phys.Rev.*, D68:043508. 64

Guth, A. H. (1981). The Inflationary Universe: A Possible Solution to the Horizon and Flatness Problems. *Phys.Rev.*, D23:347–356. 13

Hamann, J., Hannestad, S., Sloth, M. S., and Wong, Y. Y. (2007). How robust are inflation model and dark matter constraints from cosmological data? *Phys.Rev.*, D75:023522. 26

Hamann, J., Lesgourgues, J., and Valkenburg, W. (2008). How to constrain inflationary parameter space with minimal priors. *JCAP*, 0804:016. 42

Hansen, S. H. and Kunz, M. (2002). Observational constraints on the inflaton potential. *Mon.Not.Roy.Astron.Soc.*, 336:1007–1010. 18

Hertzberg, M. P. and Karouby, J. (2013). Generating the Observed Baryon Asymmetry from the Inflaton Field. *arXiv:1309.0010*. 10

Hinshaw, G. et al. (2013). Nine-Year Wilkinson Microwave Anisotropy Probe (WMAP) Observations: Cosmological Parameter Results. *Astrophys.J.Suppl.*, 208:19. 7, 9

Hoffman, M. B. and Turner, M. S. (2001). Kinematic constraints to the key inflationary observables. *Phys.Rev.*, D64:023506. 18

Hoorfar, A. and Hassanij, M. (2008). Inequalities on the Lambert W function and hyperpower function. *Inequal. Pure and Appl. Math.*, 9(2). 71

Horndeski, G. W. (1974). Second-order scalar-tensor field equations in a four-dimensional space. *Int.J.Theor.Phys.*, 10:363–384. 60

Hu, W. (2008). Lecture Notes on CMB Theory: From Nucleosynthesis to Recombination. *arXiv:0802.3688*. 7, 8, 9

Hu, W. (2010). CMB introduction: `http://background.uchicago.edu/~whu/intermediate/summary.html`. 9

Hu, W. (2011). Generalized Slow Roll for Non-Canonical Kinetic Terms. *Phys.Rev.*, D84:027303. 63

Hu, W. T. (1995). Wandering in the Background: A CMB Explorer. *arXiv:astro-ph/9508126*. 9

Huang, M.-x., Shiu, G., and Underwood, B. (2008). Multifield DBI Inflation and Non-Gaussianities. *Phys.Rev.*, D77:023511. 32, 37

Huang, Q.-G. (2008a). N-vaton. *JCAP*, 0809:017. 35

Huang, Q.-G. (2008b). Spectral Index in Curvaton Scenario. *Phys.Rev.*, D78:043515. 35

Huey, G. and Lidsey, J. E. (2002). Inflation and brane worlds: Degeneracies and consistencies. *Phys.Rev.*, D66:043514. 26

Huston, I. and Malik, K. A. (2011). Second Order Perturbations During Inflation Beyond Slow-roll. *JCAP*, 1110:029. 63

Ichikawa, K., Suyama, T., Takahashi, T., and Yamaguchi, M. (2008). Primordial Curvature Fluctuation and Its Non-Gaussianity in Models with Modulated Reheating. *Phys.Rev.*, D78:063545. 31, 32, 35, 36

Jungman, G., Kamionkowski, M., Kosowsky, A., and Spergel, D. N. (1996a). Cosmological parameter determination with microwave background maps. *Phys.Rev.*, D54:1332–1344. 25

Jungman, G., Kamionkowski, M., Kosowsky, A., and Spergel, D. N. (1996b). Weighing the universe with the cosmic microwave background. *Phys.Rev.Lett.*, 76:1007–1010. 25

Kachru, S., Kallosh, R., Linde, A. D., Maldacena, J. M., McAllister, L. P., et al. (2003). Towards inflation in string theory. *JCAP*, 0310:013. 19

Kecskemeti, S., Maiden, J., Shiu, G., and Underwood, B. (2006). DBI Inflation in the Tip Region of a Warped Throat. *JHEP*, 0609:076. 40

Kinney, W. H. (2002). Inflation: Flow, fixed points and observables to arbitrary order in slow roll. *Phys.Rev.*, D66:083508. 18, 42

Kinney, W. H., Kolb, E. W., Melchiorri, A., and Riotto, A. (2006). Inflation model constraints from the Wilkinson Microwave Anisotropy Probe three-year data. *Phys.Rev.*, D74:023502. 42

Kinney, W. H., Kolb, E. W., Melchiorri, A., and Riotto, A. (2008). Latest inflation model constraints from cosmic microwave background measurements. *Phys.Rev.*, D78:087302. 42

Kinney, W. H. and Tzirakis, K. (2008). Quantum modes in DBI inflation: exact solutions and constraints from vacuum selection. *Phys.Rev.*, D77:103517. 63

Knox, L. (1995). Determination of inflationary observables by cosmic microwave background anisotropy experiments. *Phys.Rev.*, D52:4307–4318. 25

Knox, L., Christensen, N., and Skordis, C. (2001). The age of the universe and the cosmological constant determined from cosmic microwave background anisotropy measurements. *Astrophys.J.*, 563:L95–L98. 27

Kobayashi, T. and Mukohyama, S. (2009). Curvatons in Warped Throats. *JCAP*, 0907:032. 40

Kobayashi, T., Yamaguchi, M., and Yokoyama, J. (2010). G-inflation: Inflation driven by the Galileon field. *Phys.Rev.Lett.*, 105:231302. 19, 63

Kobayashi, T., Yamaguchi, M., and Yokoyama, J. (2011). Generalized G-inflation: Inflation with the most general second-order field equations. *Prog.Theor.Phys.*, 126:511–529. 19

Kofman, L. (2003). Probing string theory with modulated cosmological fluctuations. *arXiv:astro-ph/0303614*. 17, 31, 32

Kofman, L. and Linde, A. D. (2002). Problems with tachyon inflation. *JHEP*, 0207:004. 64

Kohri, K., Lyth, D. H., and Valenzuela-Toledo, C. A. (2010). Preheating and the non-gaussianity of the curvature perturbation. *JCAP*, 1002:023. 32

Kolb, E. W. and Turner, M. S. (1993). *The Early Universe*. Perseus Publishing, Cambridge, Massachusetts. 31

Komatsu, E. et al. (2009). Five-Year Wilkinson Microwave Anisotropy Probe (WMAP) Observations: Cosmological Interpretation. *Astrophys.J.Suppl.*, 180:330–376. 42

Komatsu, E. et al. (2011). Seven-Year Wilkinson Microwave Anisotropy Probe (WMAP) Observations: Cosmological Interpretation. *Astrophys.J.Suppl.*, 192:18. 31, 35, 36, 42

Komatsu, E. and Spergel, D. N. (2001). Acoustic signatures in the primary microwave background bispectrum. *Phys.Rev.*, D63:063002. 25

Kosowsky, A., Milosavljevic, M., and Jimenez, R. (2002). Efficient cosmological parameter estimation from microwave background anisotropies. *Phys.Rev.*, D66:063007. 27

Kunz, M. and Sapone, D. (2007). Dark Energy versus Modified Gravity. *Phys.Rev.Lett.*, 98:121301. 11

La, D. and Steinhardt, P. J. (1989). Extended Inflationary Cosmology. *Phys.Rev.Lett.*, 62:376. 18

Langlois, D. and Renaux-Petel, S. (2008). Perturbations in generalized multi-field inflation. *JCAP*, 0804:017. 32, 37

Langlois, D., Renaux-Petel, S., Steer, D. A., and Tanaka, T. (2008a). Primordial fluctuations and non-Gaussianities in multi-field DBI inflation. *Phys.Rev.Lett.*, 101:061301. 32

Langlois, D., Renaux-Petel, S., Steer, D. A., and Tanaka, T. (2008b). Primordial perturbations and non-Gaussianities in DBI and general multi-field inflation. *Phys.Rev.*, D78:063523. 32, 38

Larson, D., Dunkley, J., Hinshaw, G., Komatsu, E., Nolta, M., et al. (2011). Seven-Year Wilkinson Microwave Anisotropy Probe (WMAP) Observations: Power Spectra and WMAP-Derived Parameters. *Astrophys.J.Suppl.*, 192:16. 35, 42

Leach, S. M. and Liddle, A. R. (2003). Constraining slow - roll inflation with WMAP and 2dF. *Phys.Rev.*, D68:123508. 42

Lesgourgues, J., Starobinsky, A. A., and Valkenburg, W. (2008). What do WMAP and SDSS really tell about inflation? *JCAP*, 0801:010. 25, 52

Lesgourgues, J. and Valkenburg, W. (2007). New constraints on the observable inflaton potential from WMAP and SDSS. *Phys.Rev.*, D75:123519. 25, 52

Lewis, A. and Bridle, S. (2002). Cosmological parameters from CMB and other data: A Monte Carlo approach. *Phys.Rev.*, D66:103511. 27, 42, 53, 90

Lewis, A., Challinor, A., and Lasenby, A. (2000). Efficient computation of CMB anisotropies in closed FRW models. *Astrophys.J.*, 538:473–476. 27, 42, 53

Li, M. and Lin, C. (2008). Reconstruction of the isocurvaton scenario. *arXiv:0807.4352*. 35

Li, M. and Wang, Y. (2008). Consistency Relations for Non-Gaussianity. *JCAP*, 0809:018. 35

Li, S. (2010). Inhomogeneous Reheating Scenario with DBI fields. *JCAP*, 1008:024. ii, 17

Li, S. and Liddle, A. R. (2012). Observational constraints on K-inflation models. *JCAP*, 1210:011. ii, 28, 63, 64, 69, 91

Li, S. and Liddle, A. R. (2013a). Observational Constraints on Tachyon and DBI inflation — I: Analytical Analysis. *arXiv:1311.4664*. ii

Li, S. and Liddle, A. R. (2013b). Observational constraints on tachyon and DBI inflation — Part II: Numerical exploration and model parameter constraints. *[in preparation]*. 63, 80, 81, 88

Liddle, A. R. (2003). Inflationary flow equations. *Phys.Rev.*, D68:103504. 18

Liddle, A. R. and Leach, S. M. (2003). How long before the end of inflation were observable perturbations produced? *Phys.Rev.*, D68:103503. 72

Liddle, A. R. and Lyth, D. H. (1992). COBE, gravitational waves, inflation and extended inflation. *Phys.Lett.*, B291:391–398. 62, 80

Liddle, A. R., Mazumdar, A., and Schunck, F. E. (1998). Assisted inflation. *Phys.Rev.*, D58:061301. 19

Liddle, A. R., Mukherjee, P., and Parkinson, D. (2006). Cosmological model selection. *arXiv:astro-ph/0608184*. 27

Liddle, A. R., Parsons, P., and Barrow, J. D. (1994). Formalizing the slow roll approximation in inflation. *Phys.Rev.*, D50:7222–7232. 18, 25

Linde, A. D. (1982). A New Inflationary Universe Scenario: A Possible Solution of the Horizon, Flatness, Homogeneity, Isotropy and Primordial Monopole Problems. *Phys.Lett.*, B108:389–393. 13, 43

Linde, A. D. (1983). Chaotic Inflation. *Phys.Lett.*, B129:177–181. 18, 43

Linde, A. D. (1986). Eternally Existing Selfreproducing Chaotic Inflationary Universe. *Phys.Lett.*, B175:395–400. 18

Linde, A. D. (1991). Axions in inflationary cosmology. *Phys.Lett.*, B259:38–47. 18

Lorenz, L., Martin, J., and Ringeval, C. (2008a). Constraints on Kinetically Modified Inflation from WMAP5. *Phys.Rev.*, D78:063543. 43

Lorenz, L., Martin, J., and Ringeval, C. (2008b). K-inflationary Power Spectra in the Uniform Approximation. *Phys.Rev.*, D78:083513. 46

Lyth, D. (2005). Some recent work on the curvaton paradigm. *Nucl.Phys.Proc.Suppl.*, 148:25–35. 31, 32

Lyth, D. and Liddle, A. (2009). *The Primordial Density Perturbation: Cosmology, Inflation and the Origin of Structure*. Cambridge University Press, The Edinburgh Building, Cambridge CB2 8RU, UK. 4, 5, 16

Lyth, D. H. and Rodriguez, Y. (2005). The Inflationary prediction for primordial non-Gaussianity. *Phys.Rev.Lett.*, 95:121302. 31, 32, 35

Lyth, D. H., Ungarelli, C., and Wands, D. (2003). The Primordial density perturbation in the curvaton scenario. *Phys.Rev.*, D67:023503. 31, 32

Lyth, D. H. and Wands, D. (2002). Generating the curvature perturbation without an inflaton. *Phys.Lett.*, B524:5–14. 17, 31

Maldacena, J. M. (2003). Non-Gaussian features of primordial fluctuations in single field inflationary models. *JHEP*, 0305:013. 34, 35

Martin, J. and Ringeval, C. (2006). Inflation after WMAP3: Confronting the Slow-Roll and Exact Power Spectra to CMB Data. *JCAP*, 0608:009. 52

Martin, J., Ringeval, C., and Trotta, R. (2011). Hunting Down the Best Model of Inflation with Bayesian Evidence. *Phys.Rev.*, D83:063524. 52

Matarrese, S. and Riotto, A. (2003). Large - scale curvature perturbations with spatial and time variations of the inflaton decay rate. *JCAP*, 0308:007. 17, 31, 32

Mizuno, S. and Koyama, K. (2010). Primordial non-Gaussianity from the DBI Galileons. *Phys.Rev.*, D82:103518. 63

Moroi, T. and Takahashi, T. (2001). Effects of cosmological moduli fields on cosmic microwave background. *Phys.Lett.*, B522:215–221. 17, 31

Mortonson, M. J., Peiris, H. V., and Easther, R. (2011). Bayesian Analysis of Inflation: Parameter Estimation for Single Field Models. *Phys.Rev.*, D83:043505. 18, 25, 27, 42, 51

Moss, I. (1985). Primordial Inflation With Spontaneous Symmetry Breaking. *Phys.Lett.*, B154:120. 18

Mukhanov, V. F. (1985). Gravitational Instability of the Universe Filled with a Scalar Field. *JETP Lett.*, 41:493–496. 62

Mukhanov, V. F., Feldman, H., and Brandenberger, R. H. (1992). Theory of cosmological perturbations. Part 1. Classical perturbations. Part 2. Quantum theory of perturbations. Part 3. Extensions. *Phys.Rept.*, 215:203–333. 16

Mukhanov, V. F. and Steinhardt, P. J. (1998). Density perturbations in multifield inflationary models. *Phys.Lett.*, B422:52–60. 19

Mukhanov, V. F. and Vikman, A. (2006). Enhancing the tensor-to-scalar ratio in simple inflation. *JCAP*, 0602:004. 64

Mukherjee, A. and Banerjee, N. (2013). A Reconstruction of Quintessence Dark Energy. *arXiv:1311.4024*. 11

Nicolis, A., Rattazzi, R., and Trincherini, E. (2009). The Galileon as a local modification of gravity. *Phys.Rev.*, D79:064036. 60

Norena, J., Wagner, C., Verde, L., Peiris, H. V., and Easther, R. (2012). Bayesian Analysis of Inflation III: Slow Roll Reconstruction Using Model Selection. *Phys.Rev.*, D86:023505. 52

Parkinson, D., Mukherjee, P., and Liddle, A. R. (2006). A Bayesian model selection analysis of WMAP3. *Phys.Rev.*, D73:123523. 27

Peccei, R. and Quinn, H. R. (1977a). Constraints Imposed by CP Conservation in the Presence of Instantons. *Phys.Rev.*, D16:1791–1797. 11

Peccei, R. and Quinn, H. R. (1977b). CP Conservation in the Presence of Instantons. *Phys.Rev.Lett.*, 38:1440–1443. 11

Peiris, H. V. and Easther, R. (2006a). Recovering the Inflationary Potential and Primordial Power Spectrum With a Slow Roll Prior: Methodology and Application to WMAP 3 Year Data. *JCAP*, 0607:002. 18, 42

Peiris, H. V. and Easther, R. (2006b). Slow Roll Reconstruction: Constraints on Inflation from the 3 Year WMAP Dataset. *JCAP*, 0610:017. 18

Peiris, H. V. et al. (2003). First year Wilkinson Microwave Anisotropy Probe (WMAP) observations: Implications for inflation. *Astrophys.J.Suppl.*, 148:213. 42

Peiris, H. V. and Easther, R. (2008). Primordial Black Holes, Eternal Inflation, and the Inflationary Parameter Space after WMAP5. *JCAP*, 0807:024. 18

Perlmutter, S. et al. (1999). Measurements of Omega and Lambda from 42 high redshift supernovae. *Astrophys.J.*, 517:565–586. 11

Piao, Y.-S., Cai, R.-G., Zhang, X.-m., and Zhang, Y.-Z. (2002). Assisted tachyonic inflation. *Phys.Rev.*, D66:121301. 64

Planck (2013a). Planck cmb power spectra, http://sci.esa.int/planck/51555-planck-power-spectrum-of-temperature-fluctuations-in-the-cosmic-microwave-background/. 24

Planck (2013b). Planck new cosmology recipe, http://sci.esa.int/planck/51557-planck-new-cosmic-recipe/. 10

Polyakov, A. M. (1974). Particle Spectrum in the Quantum Field Theory. *JETP Lett.*, 20:194–195. 13

Quevedo, F. (2002). Lectures on string/brane cosmology. *Class.Quant.Grav.*, 19:5721–5779. 19

Regan, D. M. (2011). Measuring CMB non-Gaussianity as a probe of Inflation and Cosmic Strings. *arXiv:1112.5899*. 12

Ribeiro, R. H. (2012). Inflationary signatures of single-field models beyond slow-roll. *JCAP*, 1205:037. 63

Riess, A. G. et al. (1998). Observational evidence from supernovae for an accelerating universe and a cosmological constant. *Astron.J.*, 116:1009–1038. 11

Ringeval, C. (2008). The exact numerical treatment of inflationary models. *Lect.Notes Phys.*, 738:243–273. 42

Ringeval, C. (2010). Dirac-Born-Infeld and k-inflation: the CMB anisotropies from string theory. *J.Phys.Conf.Ser.*, 203:012056. 63

Ryden, B. S. (2002). *Introduction to cosmology*. San Francisco, Calif. ; London : Addison-Wesley. 13

Saltas, I. D. and Kunz, M. (2011). Anisotropic stress and stability in modified gravity models. *Phys.Rev.*, D83:064042. 11

Sasaki, M. and Stewart, E. D. (1996). A General analytic formula for the spectral index of the density perturbations produced during inflation. *Prog.Theor.Phys.*, 95:71–78. 63

Scoccimarro, R., Sefusatti, E., and Zaldarriaga, M. (2004). Probing primordial non-Gaussianity with large - scale structure. *Phys.Rev.*, D69:103513. 34, 35

Sen, A. (2002a). Rolling tachyon. *JHEP*, 0204:048. 19, 20, 43, 52, 64

Sen, A. (2002b). Tachyon matter. *JHEP*, 0207:065. 19, 20, 43, 52, 64

Silk, J. and Turner, M. S. (1987). Double Inflation. *Phys.Rev.*, D35:419. 19

Silverstein, E. and Tong, D. (2004). Scalar speed limits and cosmology: Acceleration from D-cceleration. *Phys.Rev.*, D70:103505. 19, 20, 32, 64

Smoot, G. F., Bennett, C., Kogut, A., Wright, E., Aymon, J., et al. (1992). Structure in the COBE differential microwave radiometer first year maps. *Astrophys.J.*, 396:L1–L5. 7

Spergel, D. et al. (2007). Wilkinson Microwave Anisotropy Probe (WMAP) three year results: implications for cosmology. *Astrophys.J.Suppl.*, 170:377. 31

Steinhardt, P. J., Wang, L.-M., and Zlatev, I. (1999). Cosmological tracking solutions. *Phys.Rev.*, D59:123504. 11

Stewart, E. D. (2002). The Spectrum of density perturbations produced during inflation to leading order in a general slow roll approximation. *Phys.Rev.*, D65:103508. 62

Stewart, E. D. and Lyth, D. H. (1993). A More accurate analytic calculation of the spectrum of cosmological perturbations produced during inflation. *Phys.Lett.*, B302:171–175. 62

Suyama, T. and Yamaguchi, M. (2008). Non-Gaussianity in the modulated reheating scenario. *Phys.Rev.*, D77:023505. 31, 32

't Hooft, G. (1974). Magnetic Monopoles in Unified Gauge Theories. *Nucl.Phys.*, B79:276–284. 13

Tegmark, M., Eisenstein, D. J., and Hu, W. (1998). Cosmic complementarity: Combining CMB and supernova observations. *arXiv:astro-ph/9804168*. 26

Trodden, M. and Carroll, S. M. (2004). TASI lectures: Introduction to cosmology. *astro-ph/0401547*. 3

Unnikrishnan, S., Sahni, V., and Toporensky, A. (2012). Refining inflation using non-canonical scalars. *JCAP*, 1208:018. 63, 64, 91

Urrestilla, J., Mukherjee, P., Liddle, A. R., Bevis, N., Hindmarsh, M., et al. (2008). Degeneracy between primordial tensor modes and cosmic strings in futu re CMB data from the Planck satellite. *Phys.Rev.*, D77:123005. 26

Verde, L. et al. (2003). First year Wilkinson Microwave Anisotropy Probe (WMAP) observations: Parameter estimation methodology. *Astrophys.J.Suppl.*, 148:195. 27

Vernizzi, F. (2004). Cosmological perturbations from varying masses an couplings. *Phys.Rev.*, D69:083526. 17, 32

Vilenkin, A. (1983). The Birth of Inflationary Universes. *Phys.Rev.*, D27:2848. 18

Wands, D. (2010). Local non-Gaussianity from inflation. *Class.Quant.Grav.*, 27:124002. 35

Weinberg, S. (2008). *Cosmology*. Oxford University Press, USA. 3, 14

Wikipedia (2013). Lambert w function: `https://en.wikipedia.org/wiki/Lambert_W_function`. 71

Zaldarriaga, M. (2004). Non-Gaussianities in models with a varying inflaton decay rate. *Phys.Rev.*, D69:043508. 17, 31, 32, 34, 35

Zhang, J., Cai, Y.-F., and Piao, Y.-S. (2010). Rotating a Curvaton Brane in a Warped Throat. *JCAP*, 1005:001. 40

Zlatev, I., Wang, L.-M., and Steinhardt, P. J. (1999). Quintessence, cosmic coincidence, and the cosmological constant. *Phys.Rev.Lett.*, 82:896–899. 11

· APPENDIX A ·

Validity of the Slow-roll Approximation for DBI inflation

Here we present further support for our calculations in Chapter 5, notably the slow-roll approximation made in that chapter, for DBI models with different scalar potentials $V(\varphi)$. For consistency we will only discuss the redefined scalar potential φ that puts the Lagrangian into the form of Eq. (5.40), rather than the original ϕ.

A.1 Preliminaries

We carry out the proofs based on the modified equation of motion for DBI scalar field φ in Eqs. (5.57) to (5.62). When considering the predictions under the slow-roll approximation, according to Eq. (5.60),

$$\frac{\ddot{\varphi}}{c_{\rm s}^2} + 3H\dot{\varphi} + \frac{W'}{W}\frac{1}{\lambda_s}\Big(1 + \frac{m}{4}\lambda_s c_{\rm s}\tilde{V}\Big) = 0\,, \tag{A.1}$$

we assumed that the first term $\ddot{\varphi}/c_{\rm s}^2$ is negligible compared to the other terms, specifically the second term $3H\dot{\varphi}$. We start our proof with the following equations,

$$3H^2 = \frac{1}{\lambda_s c_{\rm s}\varphi^4}\mathbf{P} \quad , \quad \mathbf{P} = 1 + \alpha c_{\rm s}\varphi^{(4-m)}\,, \tag{A.2}$$

$$3H\dot{\varphi} \simeq \frac{4}{\lambda_s\varphi}\mathbf{Q} \quad , \quad \mathbf{Q} = 1 + \frac{m}{4}\alpha c_{\rm s}\varphi^{(4-m)} = 1 + \frac{m}{4}(\mathbf{P}-1)\,, \tag{A.3}$$

$$c_{\rm s}^2 = 1 - \lambda_s\dot{\varphi}^2 \quad , \quad \alpha = A\lambda_s\,, \tag{A.4}$$

where the potential $\tilde{V} = A\varphi^{4-m}$ and warp geometry $W = 1/\varphi^4$ are taken to satisfy the simplified equations above.

A.2 Evaluation of the validity of the slow-roll approximation

We define a quantity E as

$$\mathrm{E} = \frac{\ddot{\varphi}/c_\mathrm{s}^2}{3H\dot{\varphi}}\,. \tag{A.5}$$

We aim to find a relation between E and a limited number, optimally one, of the small parameters such as ϵ defined above in Eq. (A.9), since it can be constrained to $\epsilon \in (0,1)$ by observational data, and to prove whether the slow-roll approximation is sufficiently good for DBI inflation by evaluating whether E/ϵ is sufficiently small.

We need to work out some auxiliary parameters according to Eqs. (A.2), (A.3), and (A.4) as follows:

$$\hat{\mathbf{P}} = \frac{\dot{\mathbf{P}}}{H\mathbf{P}} = \Big(s+(4-m)\delta\Big)\frac{\mathbf{P}-1}{\mathbf{P}}\,, \tag{A.6}$$

$$\hat{\mathbf{Q}} = \frac{\dot{\mathbf{Q}}}{H\mathbf{Q}} = \Big(s+(4-m)\delta\Big)\frac{\mathbf{Q}-1}{\mathbf{Q}}\,, \tag{A.7}$$

$$\delta = \frac{\dot{\varphi}}{H\varphi} = 4c_\mathrm{s}\varphi^2\frac{\mathbf{Q}}{\mathbf{P}}\,, \tag{A.8}$$

$$\epsilon = -\frac{\dot{H}}{H^2} = -\frac{1}{2}\Big(\hat{\mathbf{P}}-s-4\delta\Big)\,, \tag{A.9}$$

$$\tilde{\eta} = \frac{\ddot{\varphi}}{H\dot{\varphi}} = \hat{\mathbf{Q}}+\epsilon-\delta\,, \tag{A.10}$$

$$s = \frac{\dot{c}_\mathrm{s}}{Hc_\mathrm{s}} = -\frac{1-c_\mathrm{s}^2}{c_\mathrm{s}^2}\frac{\ddot{\varphi}}{H\dot{\varphi}} = -\frac{1-c_\mathrm{s}^2}{c_\mathrm{s}^2}\tilde{\eta}\,. \tag{A.11}$$

Combining Eqs. (A.9) and (A.10), and replacing $\hat{\mathbf{P}}$, $\hat{\mathbf{Q}}$ by Eqs. (A.6) and (A.7), we obtain

$$\tilde{\eta} = 3\delta+s-\epsilon+\Big(s+(4-m)\delta\Big)\frac{\mathbf{Q}-\mathbf{P}}{\mathbf{P}\mathbf{Q}} = \mathbf{M}\delta-\epsilon+s\Big(1+\Lambda\Big)\,, \tag{A.12}$$

$$\mathbf{M} = \Big(3+(4-m)\Lambda\Big) \quad , \quad \Lambda = \frac{\mathbf{Q}-\mathbf{P}}{\mathbf{P}\mathbf{Q}}\,. \tag{A.13}$$

According to Eq. (A.9) we can denote δ as,

$$\delta = \frac{2}{\mathbf{N}}\epsilon-\frac{1}{\mathbf{P}\mathbf{N}}s \quad , \quad \mathbf{N} = m+(4-m)\frac{1}{\mathbf{P}}\,, \tag{A.14}$$

and further by replacing parameter s in terms of $\tilde{\eta}$ via Eq. (A.11) we can reach the formula for $\tilde{\eta}$ in terms of ϵ, c_s^2 and $\mathbf{P}$,

$$\frac{\tilde{\eta}}{c_\mathrm{s}^2} = \frac{2\frac{\mathbf{M}}{\mathbf{N}}-1}{1+(1-c_\mathrm{s}^2)(\Lambda-\frac{\mathbf{M}}{\mathbf{N}}\frac{1}{\mathbf{P}})}\epsilon\,. \tag{A.15}$$

Note $\mathbf{N}$ is different from the e-folds number N. Recalling the definition of E we can relate it to the above equation,

$$\frac{\tilde{\eta}}{c_\mathrm{s}^2} \equiv \frac{\ddot{\varphi}/c_\mathrm{s}^2}{H\dot{\varphi}} = 3\mathrm{E}\,, \tag{A.16}$$

and therefore we find it to be

$$\mathrm{E} = \frac{\epsilon}{3}\frac{2\mathbf{M}/\mathbf{N} - 1}{1 + (1 - \mathrm{c_s^2})(\Lambda - \mathbf{M}/\mathbf{NP})}\,. \tag{A.17}$$

We have a relation between ϵ and $1 - c_\mathrm{s}^2$ coming from the definition of ϵ in Eq. (A.9),

$$\epsilon = \frac{3}{2}\frac{1 - c_\mathrm{s}^2}{\mathbf{P}}\,. \tag{A.18}$$

Thanks to this we can simplify our prediction for E to

$$\mathrm{E} = \frac{\epsilon}{3}\frac{2\frac{\mathbf{M}}{\mathbf{N}} - 1}{1 + \frac{2}{3}(\mathbf{P}\Lambda - \frac{\mathbf{M}}{\mathbf{N}})\epsilon} \tag{A.19}$$

Instead of Λ and $\mathbf{M}/\mathbf{N}$ we introduce $\Delta = \mathbf{P}\Lambda$ as well as $\Gamma = \mathbf{M}/\mathbf{N}$. We can obtain the new quantities as

$$\Delta = \frac{\mathbf{Q} - \mathbf{P}}{\mathbf{Q}} = \frac{m - 4}{m + \frac{4}{\mathbf{P}-1}}\,, \tag{A.20}$$

$$\Gamma = \frac{\mathbf{M}}{\mathbf{N}} = \frac{3 + \Delta\frac{(4-m)}{\mathbf{P}}}{m + \frac{(4-m)}{\mathbf{P}}}\,, \tag{A.21}$$

$$\Gamma - \Delta = \frac{3 - m\Delta}{m + \frac{4-m}{\mathbf{P}}}\,. \tag{A.22}$$

and so we can write Eq. (A.19) in a new form,

$$\mathrm{E} = \frac{2\epsilon}{3}\frac{\Gamma - \frac{1}{2}}{1 - \frac{2}{3}(\Gamma - \Delta)\epsilon}\,. \tag{A.23}$$

It is still not easy to interpret E, so we need to simplify this equation. We introduce a new but useful transformation defined by

$$\theta = \frac{2}{\mathbf{P} - 1}\,, \qquad (\theta > 0)\,. \tag{A.24}$$

and then we write the Γ, Δ as,

$$\Delta = \frac{m - 4}{m + 2\theta}\,, \tag{A.25}$$

$$\Gamma = \frac{1}{2}\frac{6\theta^2 - (m^2 - 11m + 4)\theta + 6m}{(m + 2\theta)^2}\,. \tag{A.26}$$

We now introduce two functions,

$$\mathbf{F}(\theta; m) = \Gamma - \frac{1}{2} = \frac{1}{2}\frac{2\theta^2 - (m^2 - 7m + 4)\theta - (m^2 - 6m)}{(m + 2\theta)^2}\,, \tag{A.27}$$

$$\mathbf{G}(\theta; m) = \Gamma - \Delta = \frac{1}{2}\frac{6\theta^2 - (m^2 - 7m - 12)\theta - 2(m^2 - 7m)}{(m + 2\theta)^2}\,. \tag{A.28}$$

so that we can simplify Eq. (A.23) further to

$$\mathrm{E} = \frac{2\epsilon}{3}\frac{\mathbf{F}(\theta; \mathrm{m})}{1 - \frac{2\epsilon}{3}\mathbf{G}(\theta; \mathrm{m})}\,. \tag{A.29}$$

We define a transformation

$$x = \frac{1}{m + 2\theta}\,. \tag{A.30}$$

which is defined either in the domain $(0, 1/m)$ if $m > 0$, or in $(1/m, \infty)$ if $m < 0$.[1] Then we have the following elegant representations

$$\mathbf{F}(x;m) = \frac{m(m-4)^2}{4}x^2 - \frac{(m-1)(m-4)}{4}x + \frac{1}{4}\,, \tag{A.31}$$

$$\mathbf{G}(x;m) = \frac{m(m-4)^2}{4}x^2 - \frac{(m+3)(m-4)}{4}x + \frac{3}{4}\,. \tag{A.32}$$

Therefore we can now reformulate the ratio E in Eq. (A.29) to,

$$\mathrm{E} = \frac{2\epsilon}{3}\frac{\mathbf{F}(\mathrm{x};\mathrm{m})}{1 - \frac{2\epsilon}{3}\mathbf{G}(\mathrm{x};\mathrm{m})}\,, \tag{A.33}$$

The potential need not necessarily have $m > 0$. The relation in Eq. (A.33) is the function which we sought and is needed for evaluating the validity of the slow-roll approximation in DBI inflation models. Now we want to know whether there is any chance of $|\mathrm{E}| \gg 1$. To explore this, we need Eq. (A.33) and the following inequality, due to the fact that the inequality $|\mathbf{F}(x;m)| \leq |\mathbf{G}(x;m)|$ always holds,

$$\mathrm{E} < \frac{\frac{2\epsilon}{3}\mathbf{G}(\mathrm{x};\mathrm{m})}{1 - \frac{2\epsilon}{3}\mathbf{G}(\mathrm{x};\mathrm{m})}\,. \tag{A.34}$$

Then we will have,

$$\mathrm{E}\begin{cases} \ll 1\,, & \left(\left|\frac{2\epsilon}{3}\mathbf{G}(x;m)\right| \ll 1\right)\,, \qquad \text{(A.35)} \\ \simeq -1\,, & \left(\left|\frac{2\epsilon}{3}\mathbf{G}(x;m)\right| \gg 1\right)\,. \qquad \text{(A.36)} \end{cases}$$

Further we need to check if there is any singularity, for example $1 - (2\epsilon/3)\mathbf{G}(x;m) = 0$ in Eq. (A.33). We can investigate the boundary values for the function $\mathbf{G}(x;m)$ by expressing this function $\mathbf{G}(x;m)$ as

$$\mathbf{G}(x;m) = \frac{m}{4}\left((m-4)x - \frac{1}{2}\frac{m+3}{m}\right)^2 - \frac{(m-3)^2}{16m}\,. \tag{A.37}$$

Now we investigate in detail under what condition the function E will be less than, for example $10\times\epsilon \lesssim 0.1$. In other words, under what condition will the slow-roll approximation still be valid if we use the approximation in Eq. (A.3). The conclusion is determined by the potential we choose for a particular DBI inflation model. So we examine the possibilities in view of a potential with $m > 0$ below.

[1] In this case a divergence will happen when $2\theta = -m$ because of $\theta > 0$.

⋆ $0 < m < 4$

Considering the potential $V \propto \phi^m$ where $0 < m < 4$, in turn for the domain $x \in (0, 1/m)$ we will have the relation for the stationary point $x_0 = \frac{1}{m}\frac{m+3}{2(m-4)}$,

$$x_0 < x_{D^-} < x_{D^+}\,, \tag{A.38}$$

where $x_{D^-} = 0$ is the left boundary, while $x_{D^+} = 1/m$ is the right boundary. Therefore the lower bound for this function is $\mathbf{G}(x_{D^-}; m)$. The upper bound is located at $x \to 1/m$ denoted by $\mathbf{G}(1/m; m)$,

$$\mathbf{G}\Big|_{\rm min} = \mathbf{G}(0, m) \equiv \frac{3}{4}\,, \tag{A.39}$$

$$\mathbf{G}\Big|_{\rm max} = \mathbf{G}(\frac{1}{m}, m) = \frac{7}{m} - 1\,. \tag{A.40}$$

As $0 < m < 4$ we can give the boundary values by the inequalities,

$$\mathbf{G}\Big|_{\rm max} \begin{cases} > 6\,, & (0 < m < 1)\ , \\ \in (\frac{3}{4}, 6]\,, & (1 \leq m < 4)\ . \end{cases} \tag{A.41, A.42}$$

Equation (A.41) implies that we will have

$$\mathbf{G}(x; m) = \frac{3}{2\epsilon}\,, \tag{A.43}$$

which gives

$$m = \frac{14\epsilon}{3 + 2\epsilon}\,. \tag{A.44}$$

Assuming $\epsilon \sim 0.01$, this condition tells us the singularity will occur if m is of order $m \ll O(0.05)$, and then the slow-roll approximation will be violated in DBI inflation with a single-term polynomial potential $V = A\phi^m$. In turn, it also suggests that if

$$\frac{1}{20} < m_c < 4\,. \tag{A.45}$$

we can still use the slow-roll approximation.

⋆ $m > 4$

We can just re-use the relation in Eq. (A.38),

$$x_{D^-} < x_0 < x_{D^+}\,, \tag{A.46}$$

so that the lower bound is $\mathbf{G}(x_0; m)$ and the upper bound is $\mathbf{G}(x_{D^-}; m) \equiv 3/4$. Then we check the lower bound for $\mathbf{G}(x_0; m)$,

$$\mathbf{G}(x_0; m) = -\frac{(m-3)^2}{16m} < 0\,. \tag{A.47}$$

and also we need the relation for both functions $\mathbf{F}(x;m)$, $\mathbf{G}(x;m)$ by using Eqs. (A.27) and (A.28),

$$\mathbf{F} = \mathbf{G} + \Delta - \frac{1}{2}\,. \tag{A.48}$$

is roughly around $\mathbf{G}$ since $m > 4$ even $m \ll 4$. The value of $|\mathrm{E}|$ in this case will be in the range of the case Eq. (A.35).

To conclude, we only require $m > 1/20$ for the model to satisfy the slow-roll approximation for DBI inflation. For $m > 4$ we can conclude that the steeper the potential, the more secure the slow-roll approximation.

A.3 Validity for particular scalar potentials

Since we are interested in a few simple models, such as the quadratic potential with $m = 2$ and the quartic potential where $m = 4$, we will discuss the validity for these cases.

A.3.1 Quadratic potential

For the quadratic potential we can write down the range for $\mathbf{F}$ and $\mathbf{G}$ as

$$\mathbf{F}(x;m) = 2x^2 + \frac{x}{2} + \frac{1}{4} \in \left(\frac{1}{4}, 1\right)\,, \tag{A.49}$$

$$\mathbf{G}(x;m) = \mathbf{F}(x;m) + 2x + \frac{1}{2} \in \left(\frac{3}{4}, \frac{5}{2}\right) \qquad x \in \left(0, \frac{1}{2}\right)\,. \tag{A.50}$$

So we can evaluate E according to the Eq. (A.33), as

$$|\mathrm{E}| = \left|\frac{2\epsilon}{3}\frac{\mathbf{F}}{1 - \frac{2\epsilon}{3}\mathbf{G}}\right| < \epsilon\mathbf{F}\,. \tag{A.51}$$

due to $\epsilon \ll 1$ during inflation.

A.3.2 Quartic potential

The quartic potential has $m = 4$ leading to the results

$$\mathbf{F} \equiv \frac{1}{4}\,, \tag{A.52}$$

$$\mathbf{G} \equiv \frac{3}{4} \qquad x \in \left(0, \frac{1}{4}\right)\,. \tag{A.53}$$

So we will have a simple formula for E according to the Eq. (A.33), as

$$\mathrm{E} = \frac{\epsilon}{6}\frac{1}{1-\frac{\epsilon}{2}} \in (\frac{\epsilon}{6}, \frac{\epsilon}{3})\,. \tag{A.54}$$

due to $\epsilon \ll 1$ during inflation.

A.4 Summary

In our consideration of DBI inflation (5.4) with polynomial potential form $V(\varphi) = A\varphi^{4-m}$, corresponding to $V(\phi) = A\phi^m$, both Eq. (A.51) and Eq. (A.54) show that the slow-roll approximation is valid for obtaining results. Also, through the analysis, we have not assumed anything about the sound speed c_s; this suggests that even in the limit of $c_\mathrm{s} \ll 1$, the slow-roll approximation retains its validity in calculating observables such as the power spectrum and its spectral index.

· APPENDIX B ·

$s/2\delta$ FOR DBI INFLATION WITH A QUADRATIC POTENTIAL

In this subsection, we present slow-roll calculations for observables in DBI inflation with the quadratic potential. We start from the slow-roll assumptions

$$3H\dot{\varphi} \simeq \frac{2}{\lambda_s \varphi}(1+y) \quad , \quad 3H^2 = \frac{1}{\lambda_s c_{\rm s} \varphi^4} y \,, \tag{B.1}$$

$$y = 1 + \alpha c_{\rm s} \varphi^2 \quad , \quad c_{\rm s}^2 = 1 - \lambda_s \dot{\varphi}^2 \,, \tag{B.2}$$

$$\alpha = A\lambda_s \,. \tag{B.3}$$

for the quadratic potential in DBI inflation.

First we present some definitions for a list of small parameters (some of which are derived in terms of y in Section 5.5.2), as follows:

$$\delta = \frac{\dot{\varphi}}{H\varphi} = \frac{2}{\alpha}\frac{y^2-1}{y} \,, \tag{B.4}$$

$$\epsilon = -\frac{\dot{H}}{H^2} = \delta \frac{y+1}{y} = \frac{2}{\alpha}\frac{y^2-1}{y}\frac{y+1}{y} \,, \tag{B.5}$$

$$\tilde{\eta} = \frac{\ddot{\varphi}}{H\dot{\varphi}} = \delta - \epsilon + \left(\frac{2y^2}{y^2-1} - 1\right)\xi \,, \tag{B.6}$$

$$s = \frac{\dot{c}_{\rm s}}{Hc_{\rm s}} = -\frac{1-c_{\rm s}^2}{c_{\rm s}^2}\frac{\ddot{\varphi}}{H\dot{\varphi}} = -\frac{1-c_{\rm s}^2}{c_{\rm s}^2}\tilde{\eta} \,, \tag{B.7}$$

$$\xi = \frac{\dot{y}}{Hy} = \frac{\dot{y}}{H(y-1)}\frac{y-1}{y} = (s+2\delta)\frac{y-1}{y} \,, \tag{B.8}$$

$$\epsilon = \frac{3}{2}\frac{1-c_{\rm s}^2}{y} \tag{B.9}$$

The last equation is the general form of ϵ for DBI inflation models, independent of the potential. By substituting Eq. (B.8) into Eq. (B.6) and then into Eq. (B.7), the parameters $\tilde{\eta}$ and s can be written as

$$\tilde{\eta} = \delta - \epsilon + \frac{y^2+1}{y(y+1)}(s+2\delta) \,, \tag{B.10}$$

$$s = -\frac{1-c_{\rm s}^2}{c_{\rm s}^2}\left(\delta - \epsilon + \frac{y^2+1}{y(y+1)}(s+2\delta)\right) \,. \tag{B.11}$$

We define an auxiliary variable $z = |s/2\delta|$. According to Eqs. (B.4), (B.5), (B.7), (B.9), and (B.11), we can write

$$z = \left| -\frac{1}{2} \frac{\frac{2y^2-y+1}{y(y+1)}}{\frac{c_{\rm s}^2}{1-c_{\rm s}^2} + \frac{y^2+1}{y(y+1)}} \right| = \frac{f(y)}{g(c_{\rm s}^2) + h(y)}\,, \tag{B.12}$$

where we have defined the positive functions

$$f(y) = \frac{2y^2 - y + 1}{2y(y+1)}\,,\ h(y) = \frac{y^2+1}{y(y+1)}\,,\ g(c_{\rm s}^2) = \frac{c_{\rm s}^2}{1-c_{\rm s}^2}\,. \tag{B.13}$$

The function $f(y)$ is monotonically increasing as the $y \in (1, \infty)$, and $g(c_{\rm s}^2)$ is also a monotonically increasing function in $c_{\rm s}^2 \in (0, 1]$. Meanwhile $h(y)$ is monotonically decreasing in $y \in (1, 1+\sqrt{2})$ then increasing afterwards in $y \in (1+\sqrt{2}, \infty)$. The extremal values for $f(y)$ and $h(y)$ are

$$f(y)\Big|_{\rm min} = h(y=1) = 0.5\,, \tag{B.14}$$

$$f(y)\Big|_{\rm max} = h(y \to \infty) = 1\,, \tag{B.15}$$

$$h(y)\Big|_{\rm min} = h(y = \sqrt{2}+1) = 2(\sqrt{2}-1) \sim 0.828\,, \tag{B.16}$$

$$h(y)\Big|_{\rm max} = h(y=1) = h(y \to \infty) = 1 \tag{B.17}$$

in the range of $y \in (1, \infty)$. The only singularity which may occur is located in the term $g(c_{\rm s}^2) = c_{\rm s}^2/(1-c_{\rm s}^2)$.

We now study two limits of the sound speed $c_{\rm s}^2$.

⋆ $c_{\rm s}^2 \sim 1$

In this limit, as $g(c_{\rm s}^2) \gg 1 \geq h(y)$ we have,

$$z = \lim_{c_{\rm s}^2 \to 1} \frac{f(y)}{g(c_{\rm s}^2) + h(y)} \ll 1\,. \tag{B.18}$$

We have used that both two functions f, h are bounded in a limited range whatever the value of $y \in (1, \infty)$. Hence we can make the approximation in Eq. (5.100) in Section 5.5.2. Under this approximation, we conclude that

$$z \ll 1\,. \tag{B.19}$$

is always true while $c_{\rm s}^2 \sim O(1)$.

⋆ $c_{\rm s}^2 \ll 1$

In this limit, $g(c_{\rm s}^2)$ is much less than one and can even be zero. As $g(c_{\rm s}^2) < h(y)$ we can approximate z as

$$z \simeq \frac{f(y)}{h(y)} = \frac{2y^2 - y + 1}{2(y^2+1)}\,. \tag{B.20}$$

We find that $z \in (0.5, 1)$ while y ranges from $(1, \infty)$. Therefore in Eq. (5.100) in Section 5.5.2, this ratio is comparable to the assumed leading term 1. To study the model observables in this case, we cannot use the results which have been obtained in Section 5.5.2. Instead we need to include this ratio in Eq. (5.100).